Climatology of Queensland Landfalling Tropical Cyclones:

Evaluating Instrumental, Historical and Prehistorical

Records

Thesis submitted by

Shaun Alexander FLAY

in February 2006

for the degree of Doctor of Philosophy

in the School of Tropical Environmental Studies and Geography

James Cook University

STATEMENT OF SOURCES

DECLARATION

I declare that this thesis is my own work and has not been submitted in any form for another degree of diploma at any university or other institution of tertiary education. Information derived from the published or unpublished work of others has been acknowledged in the text and a list of references is given.

_____   ___1 November 2006___
            Signature   Date

STATEMENT OF ACCESS

I, the undersigned, author of this work, understand that James Cook University will make this thesis available for use within the University Library and, via the Australian Digital Theses network, for use elsewhere.

I understand that, as an unpublished work, a thesis has significant protection under the Copyright Act and;
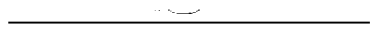
I do not wish to place any further restrictions on access to this work.

_____	___1 November 2006___
Signature	Date

ELECTRONIC COPY

I, the undersigned, the author of this work, declare that the electronic copy of this thesis provided to the James Cook University Library is an accurate copy of the print thesis submitted, within the limits of the technology available.

_____   ___1 November 2006___
             Signature   Date

ABSTRACT

Knowledge of the probability of occurrence of major tropical cyclone events forms an integral part of developing hazard mitigation strategies in regions prone to their impact. Queensland landfalling tropical cyclones are analysed in this study in order to provide a climatology of event frequency and magnitude. The adopted modelling approach differs from previous studies in the region in that it focuses specifically on the incorporation of historical and prehistorical information. The availability of such records offers a means to test whether the satellite-based instrumental record, which encompasses only the last few decades, provides a representative sample with which to characterise extremes of the process.

A methodology based on Bayesian statistical techniques is presented and applied to facilitate the incorporation of historical information. Through this approach, historical observations are specified as prior information for models of seasonal activity and intensity. When combined with reliable information from the instrumental record, subsequent inferences on the landfall climatology can be made with greater precision and confidence. Among the statistical models considered is a Poisson distribution for seasonal counts, a Generalised Linear Model that incorporates an index of ENSO as a predictor for seasonal activity, and a Generalised Pareto Distribution for tropical cyclone minimum central pressures.

The inclusion of historical information is shown to lead to increased certainty in parameter estimates for these models. Furthermore, the incorporation of historical information on storm intensities leads to predictions of the frequency of major

landfall events that are higher than what would be expected from an analysis using only the instrumental record. A further outcome of implementing a Bayesian strategy is the development of predictive distributions showing the probability of specific levels being reached in future periods.

A trend analysis identified the presence of decadal to multi-decadal variability in seasonal storm numbers and in the strength of the relationship between ENSO and tropical cyclone activity. A statistically significant downward trend in landfalling storm intensities over the 20th century was also detected. For Coral Sea region tropical cyclones, there is also evidence of decadal variability in storm numbers. Interestingly, a marginally significant upward trend in peak intensities is found for the Coral Sea region over the period 1960/61-2004/05, which is in contrast to the general downward trend in landfall intensities. No evidence is found to suggest that ENSO has a direct effect on either regional or landfall storm intensities.

A simulation model was then derived from the Coral Sea region satellite record and subsequently applied to generate a series of landfall events. Comparison of the observed landfall record with this simulated series showed close agreement. A further comparison of observed and simulated records with prehistoric data, previously reconstructed from storm ridge sequences found throughout the Great Barrier Reef region, showed some discrepancy. In particular, estimates based on observed and simulated data were tending to underestimate the frequency of major events. Uncertainties inherent in reconstructing storm intensities from the geological record complicate the utility of this comparison, however, suggesting further work is needed to address the use of prehistoric records as an independent data source.

ACKNOWLEDGEMENTS

TABLE OF CONTENTS

LIST OF TABLES

LIST OF FIGURES

CHAPTER 1

INTRODUCTION

Tropical cyclones pose an increasing risk to communities in Queensland because of the proliferation of development along its coastal margin over recent decades. The growing exposure of these communities to the impact of tropical cyclones has recently prompted several studies aimed at quantifying that level of risk (e.g. Harper 1999; McInnes et al. 2000; Harper et al. 2001; Hardy et al. 2004). The extent of this threat is not easily assessed however, due to the relatively short length of reliable observational data and the complex nature of tropical cyclone behaviour. In particular, at-site records of extreme winds and storm tide levels associated with these storms are typically available for periods of only a few decades. These records alone are of limited practical use to directly infer design levels that form the basis of most hazard mitigation strategies.

As a result, the use of simulation-based techniques has become a standard tool for assessing tropical cyclone risk in several countries including Australia (Harper 1999). Fundamental to this approach is that a climatology be derived from available meteorological observations to describe the characteristics of tropical cyclones in the region of interest. In its simplest form this climatology represents a statistical analysis of parameters describing tropical cyclone numbers, tracks, sizes and

intensities. This climatology then provides a means to simulate a large number of storm events from which to assess long-term event probabilities at a site of interest.

The construction of a climatology is a largely empirical approach though, and as such, relies on the assumption that the observed history acts as a useful guide to the future. Given that climate is a dynamic system that varies over several time scales, the typically limited duration of this observed history represents an obstacle to obtaining a representative climatology.

This is especially relevant for the Australian region where tropical cyclone observations are generally considered to be only reliable since the 1960s (Holland 1981). Hence, most previous studies in the Queensland region aim at quantifying risk have sought to limit their analyses to the post-1960s period (e.g. Harper 1999; Harper et al. 2001; Hardy et al. 2004; James and Mason 2005). Any attempt to derive this climatology must, however, be acutely aware of the uncertainties inherent in analysing observational series of limited temporal coverage. Failure to recognise and accommodate such uncertainty can ultimately lead to misguided inferences on the nature of risk.

The acquisition and use of additional data is therefore imperative to establish how representative the recent past may be in terms of assessing future risk. In the Queensland region compelling evidence of past cyclone activity contained in historical and geological records has, however, largely been overlooked in previous studies for the region. Given that such data sources generally comprise a less complete and less precise record of events, the reluctance among many investigators

to utilise this information is understandable. However, this raises an important question as to whether such concerns should immediately outweigh any relevant information that may be obtained from these records. Hence, the question of the utility of incorporating historical and prehistorical information into a baseline climatology for Queensland landfalling tropical cyclones is the main catalyst for this study.

The main objective of this thesis is to develop this climatology by maximising the use of all available data sources. This includes observations from the post-1960s satellite era as well as historical records from the pre-1960s period. Furthermore, a prehistorical record of major storm events in the Queensland region reconstructed from geological evidence (Nott and Hayne 2001) is also incorporated. To achieve this objective the study has been focused towards addressing several aims. Specifically, these are:

- To provide and implement a framework for the inclusion of historical information in analysing statistics of landfalling storm counts and intensities in the Queensland region;

- To address the issue of the identification of trends in the time series of these variables;

- To examination the influence of climate variability, particularly that related to ENSO, on seasonal landfall activity; and,

- To test the representativeness of the recent instrumental record against historical and prehistorical information sources.

The structure of this thesis is tailored to investigate each of these aims. Firstly, in Chapter 2 relevant background information on the nature of the tropical cyclone threat from a Queensland perspective is presented. This chapter provides a brief introduction to the physical characteristics of tropical cyclones in the Queensland region as well as an overview of the tropical cyclone wind and storm tide hazards. This chapter also provides a discussion on the available sources of tropical cyclone observations in the region.

Chapter 3 reviews pertinent literature regarding the development of tropical cyclone climatologies from observational records. This chapter introduces the various sampling strategies that have been employed in previous studies to statistically analyse tropical cyclone characteristics. A discussion on the various factors that are likely to have influence on the representativeness of the modern record is then raised. This discussion is placed in the context of previous studies conducted for the Queensland region. The potential limitations of applying short observational records are also highlighted with reference to several studies showing evidence of temporal variability in storm activity and subsequent risk levels. Lastly, this chapter introduces the principles and previous uses of a Bayesian statistical approach as a means to include historical information in the analysis of observed time series.

Chapter 4 presents the first stage of a climatology of Queensland landfalling tropical cyclones derived from observations in the best track database for the Australian

region. This details the implementation of a Bayesian statistical approach to combine historical counts from the pre-1960s historical era with reliable records from the post-1960s satellite period. This chapter primarily focuses on the development of statistical models for seasonal activity from the combined record of landfall events. Included is a regression model that examines the effect of ENSO on seasonal activity. Moreover, the detection of trends in the time series is also addressed.

Chapter 5 presents the second stage of the analysis on Queensland landfall events with emphasis on the observed series of storm intensities. This follows along similar lines as Chapter 4 with a Bayesian approach again used to combine historical observations with information from the modern instrumental record. The main objective of the chapter is the development of a model describing the frequency distribution of seasonal storm intensities through the implementation of extreme value techniques. Furthermore, an analysis into identifying trends and investigating the effect of ENSO on storm intensities is also conducted.

The development of a regional climatology for the Coral Sea region from instrumental records for the period 1960/61-2004/05 is addressed in Chapter 6. This regional climatology serves as a basis to further assess the representativeness of the instrumental record by later comparison to statistics of observed landfall events. This chapter begins with an analysis of trends and climate influences on the regional record of counts and peak intensities. A modelling approach is then adopted to simulate landfalling storms by combining a relatively simple empirical model for generating Coral Sea tropical cyclone tracks with a model for storm intensities

conditioned on observed spatial and temporal characteristics of the process. Diagnostic procedures used to verify the adequacy of the derived models for these variables are also presented.

Chapter 7 is devoted to evaluating recent work conducted on the geological record of past storm events. This chapter initially overviews some of the recent developments in the study of prehistoric tropical cyclones. A comprehensive review of several sites in the east Queensland region where records of major events have been reconstructed is provided. An overview of the methodology for reconstructing storm intensities from geological evidence is presented and an evaluation of the robustness of this methodology then undertaken. This is achieved by modelling the water level responses to several recent tropical cyclones at a case study site. Lastly, a discussion on both the potential merits and limitations of the prehistorical record is given.

Chapter 8 compares climatologies for landfalling tropical cyclones derived from analyses of instrumental, historical and prehistorical records presented in previous chapters. This is accomplished by firstly generating a time series of landfall events from the Coral Sea regional simulation model described in Chapter 6. The results of these simulations are then compared with statistics of storm intensities developed from historical and instrumental records as outlined in Chapter 5. Further comparison of these results with the prehistorical record reviewed in Chapter 7 is then undertaken.

Chapter 9 summarises major findings, discusses implications, and provides recommendations from this research, including avenues for further extensions to the

analysis. Results are cast in the context of previous studies aimed at analysing the statistical properties of tropical cyclones in the Queensland region. The implications of the results for the prediction of tropical cyclone risk are then discussed. In light of this research, directions for future study are given including a proposed methodology for further incorporation of the prehistoric record.

CHAPTER 2

QUEENSLAND PERSPECTIVE

2.1 Introduction

Being the most developed region of tropical Australia, the east coast of Queensland is particularly vulnerable to the impacts of tropical cyclones. This chapter provides a brief introduction to the nature of the tropical cyclone threat in this region. A review of the general characteristics of tropical cyclones in the region is firstly presented. An overview of two major components of the hazard that have received considerable attention in recent studies, namely extreme winds and storm tides, is then provided. Finally, a review of available sources of tropical cyclone information in the Queensland region is summarised with particular reference to the best-track database.

2.2 Queensland Tropical Cyclones

Tropical cyclone activity in the Queensland region is highly seasonal, typically extending from November to May and peaking over the period January to March. Figure 2.1 shows a histogram of the intraseasonal distribution of tropical cyclone occurrences for the Coral Sea region. This highlights a peak in occurrence at around the middle of February. McBride and Keenan (1982) found that the majority of

tropical cyclones in the Australian region develop in the Southern Hemisphere monsoon trough that extends across northern Australia for much of the cyclone season. There are two key regions of tropical cyclone formation near Queensland, the Coral Sea and Gulf of Carpentaria (Figure 2.2). Storms that originate in the Gulf region generally pose a reduced threat of significant impact to the east coast, at least in terms of generating extreme winds and high sea levels, as they rapidly weaken after landfall tracking across the continental landmass. Overland these systems may decay to tropical depressions, although when conditions are favourable they can re-intensify after moving back over water into the Coral Sea (McBride and Keenan 1982).
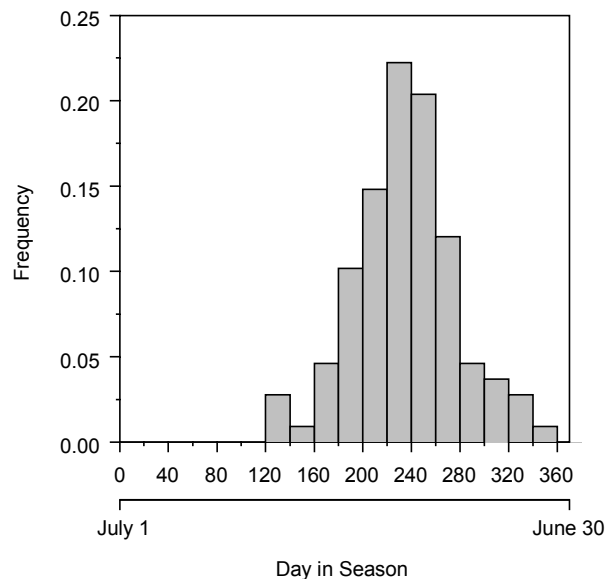
Figure 2.1 Histogram of Coral Sea tropical cyclones occurrence given by day in season for events over the period 1960/61-2004/05. The season covers from the beginning of July to the end of June in the following year.

9
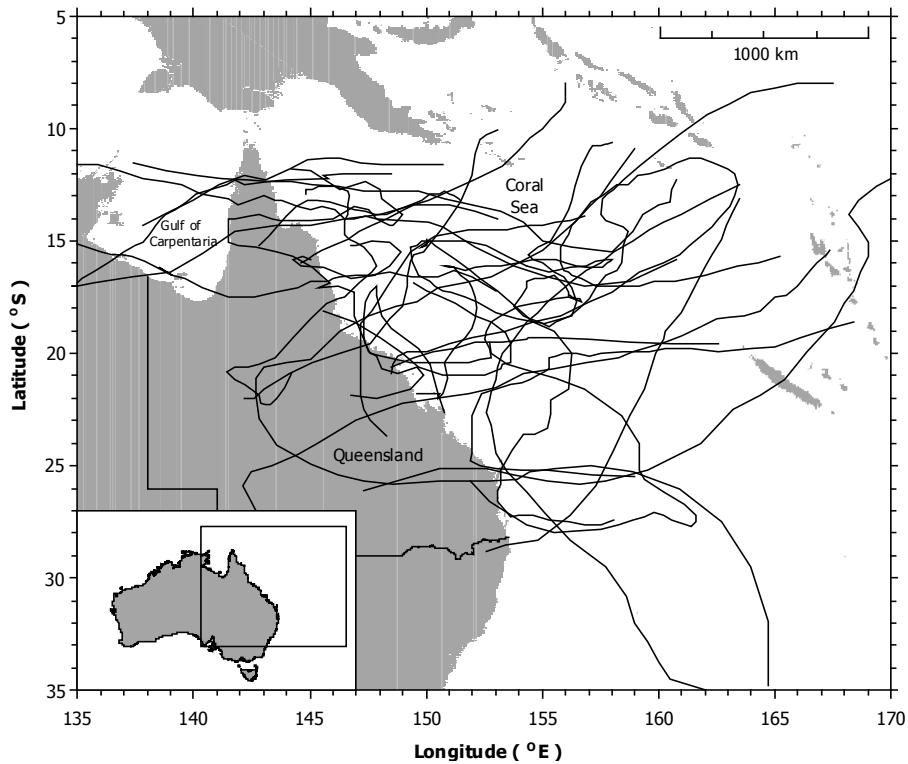
Figure 2.2 Map showing tracks of Queensland landfalling tropical cyclones of Coral Sea origin over the period 1960/61-2004/05. Note that only events that attained a minimum central pressure of at least 990 hPa at some stage are plotted.

The majority of storms that impact directly on Queensland's east coast originate in the Coral Sea region of the southwest Pacific. Although tropical cyclone paths often exhibit erratic behaviour in this region (Holland 1984; Dare and Davidson 2004), the most usual track is for the low latitude intensifying system to initially move westwards and polewards towards the Queensland coast. Interactions with mid-latitude trough and ridge systems that develop in regions to south of the monsoon trough have a strong influence on the subsequent motion and intensification patterns of tropical cyclones in this region (Dare and Davidson 2004).

Many tropical cyclones exhibit a tendency to following recurving tracks from west to east at higher latitudes (Holland 1984). Polewards of about 14-15^{0}S this strong tendency for eastwards motion, which is unique to the southwest Pacific basin, becomes increasingly apparent. Given the northwest to southeast orientation of the Queensland coast (Figure 2.2), this often results in a number of coastal tropical cyclone paths being directed either offshore or approximately parallel to the coast at some stage.

Typically, only those tropical cyclones that retain a strong westward component of motion make landfall on the Queensland coast. Landfalling storms usually decay rapidly after crossing the coast, although a number re-intensify by either re-entering the Coral Sea after recurving or continuing westwards to the Gulf region. At subtropical latitudes, decaying and transitional systems tend to predominant due to encountering strongly sheared, middle-upper tropospheric westerlies as well as lower sea surface temperatures (Holland 1984). As a result, few Coral Sea tropical cyclones reach their maximum intensity polewards of 22^{0}S. In the case of those systems tracking near to the coast, funnelling of low-level winds along the Great Dividing Range also acts to weaken many systems as very dry continental air is advected into the cyclone, which limits their tropical moisture supply (Holland 1984).

The Bureau of Meteorology (BoM) classifies tropical cyclone intensity in the Australian region according to a five-tier scale shown in Table 2.1. This classification scheme differs form the conventional Saffir-Simpson scale used in the Atlantic Basin. Events reaching category three status on this scale are commonly

referred to as severe tropical cyclones. The most intense events tend to originate around 8-12^{0}S in the Coral Sea region (Holland 1984, Figure 6, p. 36). These systems also tend to intensify at a faster rate and take longer to reach their maximum intensity than do weaker systems. Another notable feature is the apparent frequent occurrence of 'midget' storms, comprising a class of small, rapidly intensifying systems with recent examples being tropical cyclones *Rona* (1998/99), *Steve* (1999/00) and *Tessi* (1999/00).

Table 2.1   Australian scale for ranking tropical cyclone intensity

Category	Peak Wind Gust (km/h)[1]	Central Pressure (hPa)
1	<125	>985
2	125-170	970-985
3	170-225	945-970
4	225-280	920-945
5	>280	<920

[1] 3-second peak gust.

While globally an average of about 80 tropical cyclones are observed to form each year (Emanuel 2003), the likelihood of a severe tropical cyclone reaching any one location along the east Queensland coast is relatively low. For instance, over the period 1960/61-2004/05 (45 tropical cyclone seasons) a total of 37 tropical cyclones

that formed in the Coral Sea region, and reached minimum central pressures of at least 990 hPa at some stage, made landfall along the Queensland coast (Figure 2.2). Of these, only ten were severe tropical cyclones at the time of landfall, classed as having minimum central pressures ≤970 hPa. The lowest central pressure was recorded during tropical cyclone *Dinah's* landfall (945 hPa) in the 1966/67 season. Other notable events have included *Ada* (961 hPa) in 1969/70, *Althea* (950 hPa) in 1971/72, *Simon* (950 hPa) in 1979/80, *Winifred* (957 hPa) in 1985/86, *Aivu* (955 hPa) in 1988/89, and more recently *Ingrid* (955 hPa) in 2004/05. The rarity of major tropical cyclone events (category 4 and 5) since 1960/61 serves to highlight that little information is available in the recent history to characterise the frequency of extremes in the region. Several decades prior to this, however, major tropical cyclones events including *Mahina* in 1898/99 (914 hPa) and two storms recorded during the 1917/18 season and impacting Mackay (930 hPa) and Innisfail (926 hPa) respectively, caused substantial impacts.

Historically, tropical cyclone activity in the Coral Sea has also shown a strong dependence on large-scale climate fluctuations. In particular, the interannual (or interseasonal) variation in storm activity associated with the El Niño-Southern Oscillation (ENSO) phenomenon has a marked bearing on the number of tropical cyclones that form in the entire Australian region from season to season (Solow & Nicholls 1990; Nicholls 1992). This has lead to the development of several forecast schemes for seasonal tropical cyclone activity that incorporate an index of ENSO. In the Coral Sea region the reduced (increased) incidence of storm activity during El Niño (La Niña) phases appears to be primarily related to localised sea surface temperature (SST) variability (Nicholls 1984; Basher and Zheng 1995).

During El Niño phases, positive SST anomalies occur further eastwards causing tropical cyclone genesis to in turn shift eastwards. During La Niña phases, positive SST anomalies occur closer to the Queensland coast, which generally results in an increased likelihood in the incidence of tropical cyclones nearer Queensland. There is also some indication that tropical cyclone tracks extend further south during La Niña seasons. Grant and Walsh (2001) recently suggested that variability in east Queensland storm activity is also linked to the influence of low-frequency Pacific SST anomalies associated with the Interdecadal Pacific Oscillation (IPO). They subsequently attributed this as being related to changes in vertical wind shear associated with the pattern of decadal SST variability.

2.3 Tropical Cyclone Hazards

In regions prone to their impact, tropical cyclones represent a hazardous event because of their capability to generate a range of responses. These include extreme winds, intense rainfall, terrestrial flooding, and coastal flooding from the combined effects of the storm surge and wind-generated ocean waves. Tropical cyclones accounted for an estimated average cost of $266 million annually and almost one-third of all known building damage from natural hazards in Australia over the last century (Blong 2004). Historically, the greatest loss of life associated with these events in Queensland has been due to heavy seas and river flooding associated with heavy rainfall. With an expanding base of industry, infrastructure and residential housing along this coast, however, exposure to both severe winds and coastal flooding is of increasing concern.

2.3.1 Severe Winds

Tropical cyclone *Tracy*, which caused around $837 million (2003 dollars) in insured losses and destroyed 65% of Darwin's residential buildings in 1974 (Blong 2004), serves to highlight the destructive and costly nature of tropical cyclone winds. Due to the large spatial extent of the tropical cyclone's circulation the scale of its impact can be geographically widespread. Variation in the size of individual storms of similar intensity can also produce markedly different scales of impact along the coast. Callaghan (1996) highlights several cases in which variations in the size of individual tropical cyclones of similar intensity produced markedly different responses along the Queensland coast.

As exemplified with tropical cyclone *Tracy*, which was a small storm with a radius of maximum winds of only 7 km (Holland 1980), the more devastating impacts are generally confined to the eyewall region surrounding the storm's centre. This is where the strongest winds are often experienced. Highest wind speeds are also generated on the side of the vortex where an asymmetry in the wind field is produced by the storm's forward motion (Emanuel 2003). This forward motion asymmetry often results in stronger winds being produced to the left of the direction of motion in southern hemisphere tropical cyclones.

Tropical cyclones generally weaken overland due to the loss of their latent heat supply that is derived through the transfer of heat from the ocean to the atmosphere. The increase in surface friction at landfall is accompanied by increased turbulence though, which acts to generate strong, short-duration wind gusts. These gust

deviations contribute substantially to the destructive nature of tropical cyclone winds overland. For several United States hurricanes, Krayer and Marshall (1992) found that 2-second wind gust speeds were on average 55% higher than the 10-minute mean wind speed at locations of open terrain. Spatial variations in the pattern of wind damage may also arise due to the modification of wind flow by topography. Damage surveys conducted by Walker and Reardon (1986) after tropical cyclone *Winifred's* landfall in 1986 indicated that sheltering and channelling of the wind flow brought about significant variation in impacts at locations along the northeast Queensland coast.

Another potentially important factor on the severity of tropical cyclone impacts is the influence that improved building standards, introduced shortly after the impact of tropical cyclone *Tracy* in 1974, have had in reducing the vulnerability of Queensland coastal communities to the severe wind hazard. Walker and Reardon (1986) attributed the relatively low levels of damage to structures during tropical cyclone *Winifred*, which generated peak wind gusts of the order of 180 to 200 km/h, as largely due to post-*Tracy* building regulations.

2.3.2 Coastal Flooding

A storm surge is a trapped, long wave motion that is forced by the low surface pressure and sustained high winds acting on the ocean surface associated with severe weather systems like tropical cyclones. Together with the nearshore wind-wave effects of set-up and run-up this can result in an extensive incursion of seawaters into low-lying coastal areas. An historical example is the severe category 4 tropical

cyclone (930 hPa) that struck Mackay in January 1918. It produced a 5.4 m storm tide that inundated most of the township and resulted in 30 lives lost and some $2 million (1918 dollars) in damages (Davidson et al. 1993). Smith and Greenaway (1994) showed that an occurrence of a similar event today would inundate a large proportion of residential buildings in Mackay by over one metre with a significant associated cost. This highlights the problem faced by the growing exposure of Queensland coastal communities to tropical cyclones.

The magnitude of the storm surge depends on a number of factors including the intensity, speed, size and path of the storm as well as coastal bathymetry and topography. Initially an 'inverse barometer effect', which mirrors the storm's surface pressure profile, raises the sea level about 0.1 m for every 10 hPa drop in the ambient or peripheral pressure. As the storm nears the coast the wind-generated surface current will often greatly increase the surge height by forcing waters over the continental shelf. The degree to which this 'wind set-up' of onshore flow elevates sea levels is determined largely by the depth, extent and gradient of the continental shelf.

The state of the astronomical tide at the time of the storm's arrival at the coast will also influence the total water level and the extent of any coastal flooding. Tropical cyclone *Althea*, which generated a storm surge of nearly 3 m at Townsville, caused only minor damage as its landfall occurred shortly after a low tide such that total water levels were only slightly above the highest astronomical tide (HAT). The critical level at which the storm tide (i.e. the combined surge and tide) generally becomes hazardous is that which exceeds the local HAT, above which most coastal

development is located. Short-period wind-waves superimposed on the storm tide create an additional increase in water levels within the nearshore zone through the effects of wave set-up and run-up.

2.4 Available Data Sources

The limited availability and accuracy of tropical cyclone information sources has long remained an obstacle to providing a statistically robust description of the tropical cyclone climate. In the Queensland region documented sources of tropical cyclone information are available from the mid-1800s (Callaghan, 2004). The actual best-track database for the Australian region contains observations dating back to the early 1900s. In addition, there exists a long-term record of extremes for the region based on events reconstructed from geological evidence. In the following sections a review of these information sources is given.

2.4.1 Best-Track Database

In the Australian region a tropical cyclone is defined as a nonfrontal, synoptic-scale system that has developed over tropical waters and has a 10-minute mean surface wind speed of at least 63 km/h (17.5 m/s) near the centre of the organised wind circulation (Dare and Davidson 2004). The best-track database archived by the BoM compiles observations of these events in the Australian region (90^0E - 160^0E). This dataset provides the bulk of the data used in this study and is available in electronic format at http://www.bom.gov.au/climate/how/. To ensure greatest

accuracy, observations within this database were cross-referenced with information from the Queensland region (approximately 135^0E - 165^0E) tropical cyclone database, which was obtained from the Severe Weather Section of the BoM in Brisbane. The Queensland region database represents a subset of the Australian best-track database and contains observations for the Coral Sea and Gulf of Carpentaria regions. In cases where there was a discrepancy in corresponding observation between the two datasets, the Queensland region database was used as the preferred record.

The observations within the best-track databases are quite variable in terms of their accuracy, completeness and temporal resolution. The overall record prior to about 1960 is generally acknowledged to be of poorer quality (Holland 1981; Harper et al. 2001). For the post-1960 period, records of individual events are typically given as six-hourly fixes of location (longitude and latitude) and intensity (minimum central pressure) for the time intervals 0000, 0600, 1200, and 1800 UTC. In some instances central pressure estimates are not always available at every six-hourly fix, while in other cases estimates are given at hourly or three-hourly intervals. In contrast, for events prior to the 1960s observations are in the main less complete and only available at 12 or 24-hourly intervals.

A comprehensive review of the Australian region dataset was originally undertaken by Holland (1981) who summarised the evolution of the observational network and provided an informative assessment of the accuracy of several key parameters (Table 2.2). The main point emphasised by Holland (1981) is that the quality of this

database is largely a reflection of available observation platforms, which have improved over time in association with several factors. Namely;

- The commencement of the Second World War in 1939 led to an escalation in sea and air traffic in the Coral Sea region that was paralleled by a large increase in surface observations.

- During the mid-1950s weather watch radars were installed at several locations providing almost continuous nearshore coverage of the Queensland coast.

- During the 1960s satellite-based analysis techniques became formalised and have since provided the bulk of positional and intensity fixes.

At present, due to the relatively sparse distribution of the Australian surface recording network over the ocean and the absence of any regular aircraft reconnaissance of tropical cyclones, sampling is largely conducted by analysis of remotely sensed imagery. The principal means by which storm intensity is estimated has been the *Dvorak* satellite analysis technique (Bureau of Meteorology 1978). Put simply, this method indirectly derives tropical cyclone intensity (minimum central pressure or maximum wind speed) on the basis of interpretation of various cloud patterns observed in satellite imagery. On occasions such estimates are supplemented with direct recordings from several offshore and coastal automatic weather stations (AWS).

Table 2.2 Accuracy of key parameters for eastern Australian cyclones that approached to within 500 km of the coast (adapted from Holland 1981).

Parameter	1909-39	1939-59	1959-69	1969-79
Occurrence (undetected)	15-30%	5-15%	<5%	<5%
Landfalling (undetected)	5-15%	<5%	<5%	<5%
Locational Errors	<250 km	<150 km	<100 km	<50 km
Intensity [a]	<15 hPa	<15 hPa	<15 hPa	<10 hPa
Intensity [b]	unknown	unknown	<30 hPa	<20 hPa

[a] observations made within 100 km and 12 hrs of the time of maximum intensity
[b] all other observations

While the *Dvora*k technique generally allows for complete and consistent intensity estimates (Martin and Gray 1993), it is important to note that no extensive calibration of the technique has been undertaken in Australia due to the lack of independent data (e.g. from aircraft reconnaissance). Moreover, this technique, (i) incorporates a strong empirical component, which is derived entirely from observations in the northwest Pacific and Atlantic basins, and (ii) relies on analysis techniques adopted by local meteorological authorities (e.g. wind-pressure relationships). Hence, there does exist a potential for error in estimating storm intensities using the method. Holland (1981; 1984) for instance, notes a systematic underestimate of 10-15 hPa in earlier satellite estimates of intensity in the Coral Sea region. In comparing satellite-based intensity estimates with more reliable measurements obtained from aircraft reconnaissance in the northwest Pacific, Martin and Gray (1993) found average differences of 10 hPa between the two platforms.

Prior to the advent of satellite technology, intensity estimates were only obtainable from surface measurements from ships and land stations. Consequently, much of the database is incomplete in the earlier half of last century. During this period a number of tropical cyclones, particularly those that remained well out to sea for their duration, were likely to have been undetected. Conversely, it is also likely that some weather systems were mis-classified as tropical cyclones due to inadequate surface information. Overall, estimates of storm intensities during this period are sparse and in many cases are not likely to be an accurate reflection of the actual intensities. Holland (1981) demonstrated that central pressures were consistently underestimated in the absence of adequate surface measurements from the tropical cyclone's inner core.

It has been recommended on this basis that any statistical analysis of the Queensland sample be limited to only the period post-1960 or later (Harper et al. 2001; James and Mason 2005). In recent years though, improvements and extensions, particular to the landfall record prior to the 1960s, have progressed (e.g. Davidson and Dargie 1996; Callaghan 2004). Furthermore, Holland's (1981) analysis indicates that most landfalling events would likely have been identified (see Table 2.2) due to a dense network of coastal stations. In fact, there is a clear indication of a greater quantity and quality of observations during the early half of last century when tropical cyclones made landfall. This is a consequence of a greater concentration of population in coastal areas. As such, there was an increased likelihood of obtaining a direct surface measurement for landfalling storms. This means that a greater level of reliability can be attached to the landfalling record than for the basin as a whole in the era prior to satellite observations.

A distinction is made throughout this thesis between an instrumental era (post-1959/60) and an historical era (pre-1960/61) in the best-track observations. The former represents the beginning of a formal structure in the tracking and recording of tropical cyclones, whereas the later represents a period in which sampling was largely *ad-hoc*. This separation into two periods is consistent with the results of Buckley et al. (2003) who identified a major discontinuity in a subset of the best-track database during the mid-1950s, which was attributed to improvements in the observational network. The period post-1960 has been used in a number of recent studies (e.g. Harper et al. 2001; McDonnell and Holbrook 2004) as the period for which reliable data on tropical cyclones in the Australian region is available.

Even over the post-1960 period Nicholls et al. (1998) point out that further improvements in observational technologies and greater scientific understanding have had an effect on tropical cyclone classification. Buckley et al. (2003) also noted the presence of a shift in tropical cyclone frequency in the late 1970s that was attributed to an increased ability to discriminate between tropical cyclones and other low-pressure systems. The effect of this on the observational database would be an artificial bias towards a greater number of tropical cyclone events than was actually present.

2.4.2 Prehistorical Records

Recent research focused towards reconstructing past, unobserved storm events on the basis of evidence preserved in the geological record (e.g. Nott and Hayne 2001; Liu and Fearn 2000), has emerged as a promising means to gain a better insight into the

long-term behaviour of tropical cyclones. It extends the current historical and instrumental records to periods well beyond that of human observation. In some cases this prehistoric record can be extended back over the last 5,000-6,000 years, which coincides with the termination of the mid-Holocene marine transgression (Nott 2004).

At several locations along the Queensland coast the presence of coral shingle ridges has been inferred to be the product of elevated water levels associated with major tropical cyclone events (Chappell et al. 1983; Chivas et al. 1986). Nott and Hayne (2001) recently developed a methodology to reconstruct a history of past events at sites where long sequences of storm ridges have been preserved. This record is reviewed in greater detail in Chapter 7 including a discussion on its potential advantages and possible limitations. Given the rarity of major storm events observed along the Queensland coast over the last century, this prehistoric record is complementary in providing an additional and independent source of information on extremes.

2.5 Summary

Landfalling tropical cyclones remain amongst the greatest natural threats to life and property in Queensland. As a result of increasing coastal population and development in the region, vulnerability to extreme winds and storm tides generated by tropical cyclones has increased. While tropical cyclone information in the Queensland region is available for over 100 years, prior to the 1960s observations are

generally less reliable. However, since the introduction of satellite monitoring and analysis of tropical cyclones in the Australian region during the 1960s, only a few major storm events have made landfall along the Queensland coast. This situation represents a barrier to providing an informed assessment of risk and highlights a need to consider additional sources of information such as historical and prehistorical records.

CHAPTER 3

LITERATURE REVIEW

3.1 Introduction

Considerable effort has been dedicated to researching both the physical and statistical characteristics of tropical cyclones in the Australian region. This has included investigations into the basic mechanisms governing track movements, spatial distribution of genesis, and rates of intensification (e.g. McBride and Keenan 1982; Holland 1984; Dare and Davidson 2004). Other studies have focused on the effects of climate variability, particularly that related to ENSO, on seasonal activity (e.g. Nicholls 1992; Nicholls et al. 1998; Grant and Walsh 2001; McDonnell and Holbrook 2004). Moreover, the projected effects of global climate change on tropical cyclone behaviour have also received considerable attention in recent years (e.g. Henderson-Sellers et al. 1998; Walsh and Ryan 2000).

Similarly, studies of tropical cyclone risk in Australia have been numerous. These have been based on the application of Monte Carlo simulation techniques using parametric and numerical models of the tropical cyclone wind field, storm tides and wind-waves to generate site responses. The output from these simulated responses are then used to determine the likelihood of extreme levels being reached. These design level estimates have subsequently been employed to assess physical and

economic risks to structures for the purposes of hazard mitigation (Smith and Greenaway 1994; Granger et al. 1999; Stewart 2003).

Over the past few decades a concerted effort has been made to develop and improve models for the simulation of tropical cyclone responses for risk assessment. Some recent examples are the inclusion of overland coastal inundation in a numerical model for storm surges (Hubbert and McInnes 1999) and the representation of secondary eyewalls in a tropical cyclone wind field model (McConochie et al. 1999). In contrast, relatively little progress has been achieved in improving climatological models necessary to characterise the underlying stochastic process. This is somewhat surprising given that this aspect represents perhaps the most vital component of the simulation-based methodology, which chiefly aims to describe this process within a statistical framework. The approach is fundamentally probabilistic, seeking to ascertain the likelihood with which various tropical cyclone events are likely to occur.

The intention of this chapter is to outline the general framework for obtaining this probabilistic description as well as examine potential limitations in the Queensland context. Firstly, a brief theoretical background to the estimation of event probabilities is summarised. A review of the various sampling strategies that have been employed in the literature to define the statistical properties of tropical cyclones is then provided. Of key importance to the veracity of a statistical approach is the issue of representativeness. For natural hazards, this relates mainly to the capacity of available records to model the stochastic behaviour of extreme values of the process. This is discussed with respect to the importance of fully describing uncertainty as

well as with reference to various studies highlighting temporal variability in tropical cyclone behaviour. The final part of the review describes methodologies that have been applied in recent years, specifically Bayesian statistical techniques, as a means to incorporate less reliable sources of historical information.

3.2 Risk Prediction Concepts

As a starting point, the prevailing methodology in assessing the risks of natural hazards seeks to define the likelihood of an extreme event occurring in a given future period. This gives rise to concepts such as the 100-year design level, which is loosely defined as the magnitude of an event expected to occur, on average, once every 100 years. Such concepts are more conveniently expressed as an odds-ratio, where for example, the 100-year event would be referred to as the magnitude of an event with a 1 in 100 chance of being exceeded in a given year. The widespread use of design events in hazard mitigation is generally seen as adopting a compromise between providing a sufficient level of protection from a particular hazard, while not overly restricting development and other human activity in areas potentially vulnerable to the hazard. Whether such an approach offers a rational and justifiable means of reducing risk has been subject to much debate (see e.g. Baker 1994).

The basis of the approach generally relies on using established statistical methods to estimate the probability of an extreme event occurring, based on the past record of such events. According to Hosking and Wallis (1997) a statistical approach is often preferable given the various sources of uncertainty inherent in physical processes that

give rise to observed events. While this notion is open to some criticism, because of its assumptions and neglect of important physical processes responsible for generating the hazard, it nevertheless provides a means to analyse risk from complex phenomena whose dynamics are not fully understood.

The principle objective of conducting a statistical analysis in this context is to quantify the behaviour of the process at high levels that correspond to hazardous events. This involves deriving a probabilistic structure for the process from the observed data so as to make inferences on anticipating extremes in a future period. In doing so it is assumed that the sequence of observed values $x = (x_1, \ldots, x_m)$ comprise realisations of a random variable X. For discrete random variables the probability mass function:

$$f(x) = \Pr(X = x),\tag{3.1}$$

gives the probability that the random variable X takes the value x. For a continuous random variable, its cumulative probability distribution function, defined as:

$$F(x) = \Pr(X \leq x),\tag{3.2}$$

assigns probability to the range of values that the random variable X may take.

Estimation of the probability distribution is achieved using either nonparametric or parametric methods. In the latter case, the variable X is assumed to follow a particular distribution with parameters that are estimated from the data

$x = (x_1, \ldots, x_m)$ using techniques such as that based on the principle of maximum likelihood. As an example of the discrete case, it is commonly assumed that the distribution of tropical cyclone counts follows a Poisson distribution (Solow and Nicholls 1990; Elsner and Bossak 2001). In the continuous case, it is often assumed on the basis of mathematical argument that annual maximum observations of some environmental variables follow certain limiting distributions of the extreme value type (Coles 2001; Katz et al. 2002).

The advantage of parametric methods for assigning probability to events is that they provide a convenient framework to model processes at high levels for which few data are available. This also applies to the case of extrapolation to unobserved levels. One disadvantage concerns the assumption of a particular probability distribution for the underlying process, which if incorrectly specified can result in a poor representation of the process at high levels. Alternative procedures based on nonparametric methods do not make this assumption, however, they also have limitations in describing the process at high levels because of their reliance on local estimation of the empirical probability distribution. In either case it is important to show that the adopted model at least describes the observed data well using various diagnostic techniques.

3.3 A Review of Sampling Strategies

By far the most common approach to assessing long-term tropical cyclone risks consists of generating a series of storm responses. This is motivated by the fact that

the rarity of storm events affecting any one site is such that direct estimation of long-term probabilities of their responses (e.g. winds and storm tide levels) is rarely possible. In an attempt to overcome this, simulation-based methods have become an accepted way to generate a viable at-site dataset of storm responses (Harper 1999). This typically involves a statistical analysis of the regional tropical cyclone meteorology in order to derive a climatology. This climatology then serves as the basis for simulating a full array of possible storm scenarios to characterise the local response climate. Thus, by generating an artificial series of storm events, whose statistical characteristics are consistent with those observed, this dataset of responses can feasibly be enlarged.

In order to apply this technique the selection of an appropriate sampling strategy is required. By analysing the statistical properties of observed storms over a broad geographical region a more robust description of the tropical cyclone climate is achievable. In effect this can be viewed as an attempt to overcome the sparsity of local tropical cyclone events by a 'substitution of space for time' principle that considers a wider area to develop the climatology. In some respects such an approach is necessary due to the fact that tropical cyclones are translating systems whose core characteristics are not sampled at fixed sites, but rather at points defined by the storm's path.

3.3.1 Fixed Subregion Approach

The traditional sampling strategy considers a fixed region around the target site and draws upon only storms that entered this area to define the regional climatology.

This supposes that the climatology is relatively uniform or homogenous across that region. McInnes et al. (2000) presents a typical example of the application of this approach for estimating storm tide design levels at Cairns in north Queensland. This sampling strategy has also been used in other studies conducted in the region (e.g. Hardy et al. 1987; Harper 1999). The approach has also formed the basis of several studies on hurricane wind risk conducted in the United States including Vickery and Twisdale (1995) and Huang et al. (2001). Chu and Wang (1998) also applied this technique in the central North Pacific.

A potential shortcoming in the application of this strategy regards the choice of sampling region. This is often selected as a compromise between obtaining a large enough sample size, while not being overly biased by the inclusion of tropical cyclones that are physically unrepresentative of those likely to impact the target site. For instance, Harper (1999) selected a 500 km radius around sites along the Queensland coast to serve as a 'control volume', although presents no formal test to justify this selection. Vickery and Twisdale (1995) undertook an investigation into the effects of sample region size and noted difficulties in choosing an optimal region, highlighting the difficulties in identifying heterogeneity at small spatial scales with limited data.

3.3.2 Basin-wide Approach

Several alternative sampling methods have been proposed in recent years, which endeavour to obtain more of a 'basin-wide climatology' and then simulate the entire lifespan of a tropical cyclone event. Casson and Coles (2000) accomplish this by

generating hurricane events in the Atlantic basin from a probability model that describes the spatial and temporal patterns of the process. Their approach combines a model for generating storm tracks with a model for minimum central pressures with parameters that vary according to the location in space and time of each point along the simulated track. These relationships were derived from the United States best-track database over the period 1886-1994.

James and Mason (2005) present a method to simulate the track movements and intensities of tropical cyclones across the Coral Sea region that makes use of a series of first-order autoregressive models. Underlying this approach is the assumption that after initialisation, future changes in a storm's location and intensity are governed by changes at the previous time step. The parameters for this model were derived from 128 tropical cyclone events in the Coral Sea region over the period 1968/69-2000/01. This simulation model forms the basis of the most recent attempts to estimate design levels for storm tide risk in Queensland (Hardy et al. 2004) as well as tropical cyclone wind-wave statistics in the Great Barrier Reef (Hardy et al. 2003). Vickery et al. (2000) simulate hurricane events in the United States using a somewhat similar approach, although their model attempts to account more for the spatial variation in these relationships and makes use of a substantially larger database of events.

The application of these basin-wide sampling approaches has largely superseded the simpler alternative of using a fixed subregion, although the latter is not without its merits. Unlike the Atlantic basin, the lack of reliable basin-wide records in the Coral Sea region prior to the advent of satellite monitoring restricts the time period available for analysis. The availability of a long period of record provides a way to

not only develop a more robust statistical model, but also a more solid basis with which to verify simulated event characteristics. For instance, Vickery et al. (2000) describe a comparison of simulated landfalling intensities of major United States hurricanes from an Atlantic basin climatology with the observed record of such events.

The utility of such an approach in the Queensland region would clearly be restricted if such a comparison were limited to only the past few decades of recorded events. James and Mason (2005) present a comparative analysis of simulated event characteristics with observed values for three subregions along the Queensland coast. Given that James and Mason (2005) utilised only tropical cyclone observations over the period 1968/69-2000/01, the sample size for each of their subregions ranged from between 20-38 events. Furthermore, there were relatively few observed extremes in the samples derived from these subregions so it is unclear how well hazardous events are modelled.

3.4 The Issue of Representativeness

The successful implementation of any scheme aimed at defining the statistical properties of a hazard process is foremost dependent on the observed record being a representative sample of the population. This is especially relevant for an analysis concentrating on the occurrence of extremes. It is widely recognised that for many environmental variables the typical length of observational records makes the

estimation of extreme events probabilities a difficult undertaking (Hosking and Wallis 1997).

Furthermore, as pointed out in the seminal paper of Baker (1994) on the role of statistics in the prediction of extreme flood events, most analyses have tended to concentrate on datasets comprising predominantly small events to model the properties of unobserved high magnitude events. Clearly, the use of such techniques alone does not guarantee that the prediction of risk is ultimately improved. As argued by Baker (1994) the need to obtain greater information on past large magnitude events fundamentally represents the most important avenue to achieving better estimates of risk.

There are several important factors relating to this issue of representativeness that highlight potential shortcomings with past approaches taken in the Queensland region. It is especially important to recognise that the availability of further data may lead to vastly different estimates of the statistical properties of the process. Here aspects pertaining to the assessment of uncertainty in tropical cyclone simulation techniques as well as the presence of temporal variability in tropical cyclone records are reviewed in this context of representativeness.

3.4.1 Representation of Uncertainty

In any form of statistical inference there exists two main types of uncertainty, sampling uncertainty and model uncertainty. Both forms of uncertainty are influenced by the amount of data available for model fitting. An important

component of the application of tropical cyclone simulation-based techniques is the representation of uncertainty associated with generated event characteristics. Uncertainty in this process is introduced in a number of ways. Primarily, these are related to the length of the simulated response series and the climatological model from which events are randomly selected and subsequently simulated.

While it is common to assess uncertainty based solely on the simulated event series, this can lead to unrealistically small measures of uncertainty. By generating a series corresponding to a long simulation period the level of uncertainty in this component of the process is arbitrarily reduced. Harper (1999) for instance recommends the simulation of a 10,000-year duration to adequately determine design levels up to return periods of 1,000 years. The contribution of this to the overall level of uncertainty is thus likely to characterise only a small fraction of the total amount. Furthermore, up to the point where a suitable model can be reliably fit to the simulated observations, there is little to be gained by conducting further simulations as a means to reduce uncertainty.

According to Coles and Simiu (2003) a greater amount of uncertainty arises from the climatological model employed to simulate the event series. For this reason it is pertinent to also assess uncertainty on the basis of the length of the available tropical cyclone record used to derive this model component. There are however, relatively few examples in the literature that have adequately dealt with this issue. Ideally this should be approached by taking into account uncertainty in the various statistical models that comprise the climatological model, which includes variables describing tropical cyclone frequencies, intensities, paths and sizes.

For the simulation of United States hurricane events Casson & Coles (2000) accomplish this by assuming parameter estimates for each model variable to be asymptotically normally distributed. They then repeated a Monte Carlo simulation of hurricane events a number of times by randomly generating parameter values from each variable's sampling distribution. An alternative approach proposed by Coles and Simiu (2003) involves employing bootstrap resampling techniques on the simulated event series. In this approach, the size of each bootstrap sample is selected to correspond to the size of the observed series of tropical cyclone events, rather than be a function of the size of the simulated event series.

The importance of addressing these uncertainties centres on recognizing that simulation techniques are used to generate an increased, but nevertheless, artificial series of events. For previous studies conducted in the Queensland region there has been an evident lack of consideration of this aspect. For instance, in the most recent estimates of design-level for wind speeds (Harper 1999) and storm tides (Hardy et al. 2004) obtained through the application of simulation techniques, no formal assessment of uncertainty in these levels is given. This essentially highlights a failure to test the representativeness of the observed sample by not adequately characterising the variability inherent in the process.

3.4.2 Temporal Variability

The reluctance among many investigators to seek and use past sources of information in the Queensland region must be placed in the contexts of criticisms like those of Baker (1994) for river flood hazard assessments. In this region concerns over the

representative nature of the modern tropical cyclone record have recently been raised in light of the interpretation of long-term geological evidence. This reconstructed record appears to show that periods existed in the past where the frequency of major tropical cyclone events was dissimilar to that directly observed in recent times (Nott and Hayne 2001; Nott 2003). The implications of this information for tropical cyclone risk have yet to be fully considered.

These concerns must also be placed in the context of the dynamic nature of the climate system and its subsequent effect on the recorded time series of natural events. Evidence of this is apparent from growing recognition that interannual to interdecadal forms of climate variability have the effect of reducing or elevating the level of risk from natural hazards like floods and tropical cyclones over time (e.g. Kiem et al. 2003; Jagger et al. 2001). For instance, Jagger et al. (2001) demonstrated the variation in annual hurricane wind risk in the United States conditional on the influence of climate factors like ENSO.

In addition to this, it is now known that the effect of ENSO on climate is not constant through time, but varies over decadal time scales (e.g. Power et al. 1999). Elsner et al. (2001) found that the strength of the relationship between U.S. hurricanes and ENSO varied on decadal scales over the 20th century. A full understanding of the consequences of this, and other forms of variability, for tropical cyclone risk in the Queensland region is difficult to discern from the short period of satellite observation.

Where longer-term instrumental records are available, such as in the Atlantic basin, evidence for the presence of shifts to active or inactive regimes in major hurricane activity has also been identified (e.g. Gray 1990; Goldenberg et al. 2001). Gray (1990) found that multidecadal variability in United States major hurricane landfalls were closely linked to multidecadal variations in West African summer rainfall. Goldenberg et al. (2001) attributed a recent shift to an active period of major hurricane activity in the United States to simultaneous increases in North Atlantic SSTs and decreases in vertical wind shear. In the central north Pacific region, Chu and Zhao (2004) applied a change-point analysis to show that a shift to a more active period of tropical cyclone activity occurred during the early 1980s.

Little attention has traditionally been given in the analysis of tropical cyclone risk to directly addressing the implication of these regimes, which may encompass periods of increased or reduced risk (Nott 2004). Clearly, the availability of longer-term historical and geological records allows much greater scope for better understanding such features. For instance, Liu and Fearn (2000) hypothesised that the existence of millennial-scale regimes in major hurricane landfalls in Florida, reconstructed from geological evidence, was linked to large-scale shifts in the position of the Bermuda High.

The lack of a long-term, high-resolution record of tropical cyclones in the Australian region obviously represents an obstacle to fully resolving some of these issues. Nevertheless, the incorporation of available sources of historical and prehistorical information that have been largely overlooked in recent studies conducted in Queensland, offers an opportunity to assess the representativeness of recent records.

In the United States, prehistorical information has recently proven to be a useful tool for independently assessing design levels (Murnane et al. 2000). Murnane et al. (2000) compared predictions of hurricane wind speed exceedance probabilities estimated from a model using the 20th record against sedimentary evidence documenting the frequency of major hurricane events over millennial time scales.

The role of such information has assumed a greater importance in the field of natural hazards risk assessment over recent decades, yet there do remain several impediments to its ultimate incorporation. These stem largely from the inherent uncertainties associated with past information sources. Addressing any ambiguities that may arise in the interpretation of such evidence and making account for the likely lower level of precision should thus also be given priority.

3.5 Incorporation of Historical Information

As discussed in Chapter 2, prior to introduction of satellite reconnaissance the capability to detect and monitor tropical cyclones in the Australian region was limited. Given the range of issues raised in the previous section, however, it is important to determine if the period of satellite observation offers a sufficiently representative sample to characterise the process at high levels. In this context, the recent works of Solow and Nicholls (1990), Elsner and Bossak (2001), Solow and Moore (2000), Chu and Zhao (2004) and Elsner and Jagger (2004) are particularly relevant. These studies have focused on the development and application of

40

methodologies that enable the incorporation of historical data in analysing the statistical aspects of tropical cyclone behaviour.

Adopting a novel approach, Elsner and Bossak (2001) recently highlighted the advantages of Bayesian statistical methods as ideally suited for combining reliable sources of instrumental hurricane records with less precise historical data. In recent years the Bayesian statistical approach has been employed by a number of investigators examining times series of environmental variables. Examples include the use of expert opinion in predicting the frequency of intense rainfall events (Coles and Tawn 1996), the use of regional information to improve predictions of high wind speeds (Coles and Powell 1996), the incorporation of historical flood information to improve estimates of flood frequency (Kuczera 1999), and accounting for error reporting in a regression model for tornado counts (Wikle and Anderson 2003).

3.5.1 Bayesian Approach

As demonstrated in the aforementioned studies, Bayesian techniques offer an alternative to classical statistical approaches by providing a rational framework for incorporating prior information. This is especially important for an analysis of extremes, which by definition are rare events and often poorly represented in observed time series. Such prior information can be either informative or non-informative, wherein the former is derived from various sources including expert opinion, spatial information and historical observations. In the context of modelling tropical cyclones, the Bayesian approach offers a framework to incorporate informative knowledge about the process, in the form of historical data, with more

reliable information contained in instrumental records (Elsner and Bossak 2001). This allows the period of record to be extended. To date, no studies have implemented this methodology in the Queensland region.

As a starting point, consider a sequence of observations $x = (x_1,...,x_m)$ that are independent realizations of a continuous random variable whose density falls within the parametric family $\{f(x|\theta):\theta \in \Theta\}$, where θ are the model parameters. In the conventional statistical approach, θ is assumed fixed and its estimate is typically obtained as that most likely to have generated the sample observations by maximizing the likelihood function, $L(\theta|x)$, of $f(x|\theta)$. Fundamental to the Bayesian philosophy is that θ is treated as a random variable and assigned a prior density $\pi(\theta)$, about which information is expressed without reference to the data x. Inference concerning θ is then based on the posterior distribution, which is obtained by Bayes' Theorem as:

$$\pi(\theta|x) = \frac{\pi(\theta)L(\theta|x)}{\int_\Theta \pi(\theta)L(\theta|x)\mathrm{d}\theta} \propto \pi(\theta)L(\theta|x), \tag{3.3}$$

where Θ denotes the parameter space of θ. The posterior distribution thus involves a contribution from the observed data through $L(\theta|x)$ and prior information through $\pi(\theta)$. The output of a Bayesian analysis is not a single point estimate of θ, but rather a posterior distribution that summarises all information about θ. This has several advantages over classical techniques, particularly in terms of representing uncertainty, which can lead to improved predictive inference.

Predictions of future values of the process are computed with the posterior predictive density. Given a future observation z with density function $f(z|\theta)$, the posterior predictive density of z, given the data x, is:

$$f(z|x) = \int_{\Theta} f(z|\theta)\,\pi(\theta|x)\,d\theta. \tag{3.4}$$

The predictive density averages the distribution across the uncertainty in θ, as measured by the posterior distribution (Coles and Powell 1996). Thus, it summarises the uncertainties in both the model parameters and that in the future value of z.

3.5.2 Other Approaches

There are several alternative approaches outlined in the literature to facilitate the inclusion of historical observations, particularly in the case relating to incomplete records. For instance, working under the assumption that the record of landfalling United States hurricanes is complete dating back to 1930, Solow and Moore (2000) used this information to extend backwards the incomplete record of hurricane activity in the North Atlantic Basin and then tested for a trend in the extended basin-wide record. Similarly, in fitting a regression model to tropical counts in the Australian region with an index of ENSO as a predictor, Solow and Nicholls (1990) treated counts prior to 1965 as incomplete. They then proposed a model for estimating the likelihood that an event was observed during the pre-1965 period as a means to reconstruct the incomplete portion of the record.

In the field of flood frequency analysis another approach based on the concept of censoring has gained considerable popularity for dealing with incomplete historical information (e.g. Martins and Stedinger 2001; Kuczera 1999). This methodology arose as an approach to deal with circumstances where, in addition, to a continuously gauged record of flood flows, there may also exist a partial record of extreme events based on documentary accounts or physical evidence of palaeoflood events.

In such cases, the historical or prehistorical record may be complete in terms of recording all major events above some local threshold. Standard statistical techniques based on treating the combined record as a censored dataset can then be implemented, wherein unobserved, pre-gauged events are classified as censored observations. In the context of historical tropical cyclone accounts, such an approach may also prove a feasible technique. This is because with certain major historical storms, particularly those landfalling events causing substantial impacts, there is likely to exist reasonable estimates of their magnitude. A central pressure estimate of 914 hPa recorded during the landfall of tropical cyclone *Mahina* in Queensland in 1899, which is known to have caused over 300 fatalities (Callaghan 2004), is one notable example.

3.6 Summary

As is the case in any attempt to define the statistical properties of a hazard process, the short period of time for which data has been sampled presents perhaps the greatest limitation to better understanding and managing risk. Most recent studies of

tropical cyclone risk in Queensland have opted to limit their analyses to observations collected in the post-1960s satellite period. As demonstrated in this chapter though, there are several important issues associated with this decision that amounts to an assumption that this record is a representative sample. To date, no investigation has been conducted to test whether such an assumption is justifiable. Given that several methodologies are described in the literature for extending the analysis to include past sources of historical information, it is apparent that similar techniques can readily be applied in the Queensland context.

The presence of temporal variability in storm behaviour due to natural climate variability emphasises a dynamic component to risk that also warrants attention from a Queensland perspective. Furthermore, an in-depth investigation into uncertainty levels in simulated event characteristics is needed to address issues of representativeness. Also, recent studies based on examining geological evidence of past major storm events have reported results that are at odds with the observed history of the process. This further highlights a need to formally conduct a comparative analysis to further evaluate the representativeness of the observed record.

CHAPTER 4

QUEENSLAND LANDFALLING TROPICAL

CYCLONES: COUNTS

4.1 Introduction

To date, no comprehensive analysis of the frequency and intensity of landfalling tropical cyclones in Queensland has been undertaken. In this chapter Queensland landfalling tropical cyclone counts over the period 1910/11-2004/05 are studied. The analysis is largely based on a Bayesian statistical approach. The best-track record is separated into historical (1910/11-1959/60) and instrumental (1960/61-2004/05) eras. Through the Bayesian approach historical counts are combined with instrumental observations to fit a model for seasonal activity. This is then extended to a regression model incorporating an index of ENSO as a covariate term. A trend analysis is also conducted on the time series to examine for variation in seasonal activity over time and in its relationship to ENSO.

The main aim of the analysis is to investigate ways of using earlier historical counts to improve inference on the frequency of landfall events. As mentioned in previous chapters, as a consequence of improvements in the observational network in the latter half of last century, tropical cyclone observations in the Australian region are generally less reliable prior to the 1960s. The analysis presented here is based on the

assumption that landfall events are relatively well represented in the pre-1960s record. Indeed, Holland (1981) noted that most coastal crossing events in the eastern Australian region dating back to 1910 would likely have been identified. Furthermore, Grant & Walsh (2001) considered data back to 1920 as sufficiently reliable for the purposes of investigating the effects of ENSO on Queensland storm activity. Thus, the assumption that an analysis of tropical cyclone landfall characteristics in the Queensland region need not be restricted to the post-1960s period would appear to be reasonable.

4.2 Data

Landfalling events for the period 1910/11-2004/05 were extracted from the BoM Australian and Queensland region best-track databases. Prior to conducting the analysis, tropical cyclones that did not attain a minimum central pressure of ≤990 hPa at some stage during their lifetime were removed. This follows the approach taken by Nicholls et al. (1998) in minimising any potential contamination of the record due to observational bias. Both Nicholls et al. (1998) and Buckley et al. (2003) attributed an apparent shift to a lower frequency of events at sometime between the late 1970s and mid-1980s to an increased ability to discriminate between tropical cyclones and other low-pressure systems. Thus, the 990 hPa threshold is used here to remove weak events that may in fact be other forms of low-pressure systems.

A landfall was defined here as a tropical cyclone originating in the Coral Sea and crossing the mainland east Queensland coast (Figure 2.2). This definition also includes major near-coast islands. Note also that multiple landfalls of the same tropical cyclone were counted only as a single event. Figure 4.1 shows the time series of landfall counts for the period 1910/11 to 2004/05. Table 4.1 provides summary statistics for the series separated into historical and instrumental eras. The 90% confidence intervals for the mean listed in Table 4.1 were obtained using a bias-corrected and accelerated percentile bootstrap method (Efron and Tibshirani 1993) employing 1,000 bootstrap samples. The overlap in confidence intervals for the historical and instrumental eras shown in Table 4.1 indicates no significant difference, although the mean is somewhat higher during the instrumental era.
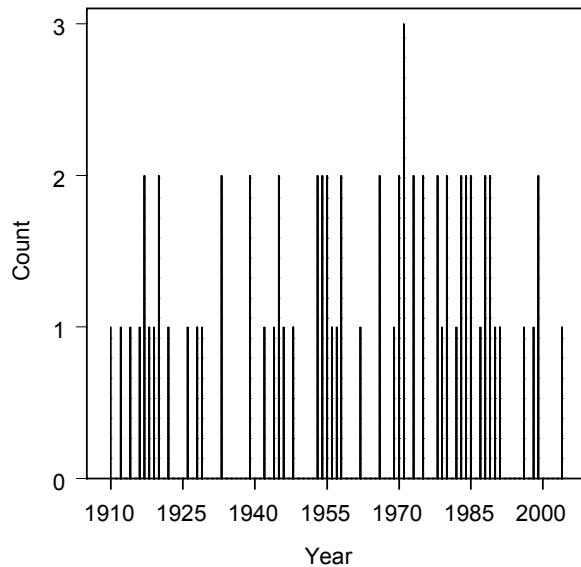
Figure 4.1 Time series of Queensland tropical cyclone landfall numbers over the period 1910/11-2004/05. Note that only tropical cyclones that attained a central pressure of 990 hPa or lower at some stage are counted.

Table 4.1 Summary statistics of Queensland landfalling tropical cyclone counts separated into historical and instrumental eras.

Period	Mean	Variance	Quantiles of Mean	
			5%	95%
1910/11-1959/60	0.68	0.59	0.46	0.90
1960/61-2004/05	0.82	0.83	0.56	1.07

4.3 Model for Seasonal Activity

Given the time series of seasonal counts, the first step in the development of the landfall climatology is a model for seasonal activity. This section describes the adopted model for this variable as well as a methodology for including historical observations in the fitting process. The distribution of counts was taken to follow a Poisson process (Solow and Nicholls 1990; Elsner and Bossak 2001; Chu and Zhao 2004). The Poisson distribution is a probability model for the frequency of discrete random events. The distribution is characterised by single parameter, λ, specifying the mean rate of event occurrence. Under this model, the probability of $\hat{n}$ events occurring in T seasons is given by (Elsner and Bossak 2001):

$$\Pr(\hat{n}|\lambda,T) = \exp(-\lambda T)\frac{(\lambda T)^n}{n!},$$

for $n = 0,1,2,...,$ (4.1)

where $\lambda > 0$ and $T > 0$.

The mean and variance of the Poisson distribution are both given as the product of λT. The maximum likelihood estimate of λ can be determined from the number of events n recorded in the sample interval T.

Keim and Cruise (1998) proposed a formal goodness-of-fit test for the Poisson distribution. Specifically, the ratio $\hat{R}$ of the sample variance to the sample mean is compared against a critical value R_C of the chi-squared distribution with m-1 degrees of freedom, where m is the sample size. The value of R_C is obtained from $[\chi^2_{m-1,\alpha}/(m-1)]$, where the one-tailed $\alpha = 0.10$ significance level is used. If $\hat{R} < R_{C,1-\alpha}$ or $\hat{R} > R_{C,\alpha}$, depending on whether $\hat{R}$ is less than or greater than 1, the Poisson hypothesis is rejected (Keim and Cruise 1998).

Table 4.2   Summary of Poisson hypothesis test for observed seasonal counts.

Period	$\hat{R}$	Reject Region	Decision
1910/11-1959/60	0.87	<0.75	Do Not Reject
1960/61-2004/05	1.01	>1.28	Do Not Reject

Applying this test to the record indicated that the Poisson distribution was an acceptable candidate for the series (Table 4.2). Keim and Cruise (1998)

recommended using the $\alpha = 0.10$ significance level in preference to the standard $\alpha = 0.05$ level for the Poisson hypothesis test, as this favours an easier rejection of the null hypothesis and thus greater confidence in the distribution should it be accepted. An alternative to the Poisson distribution, in the case where the Poisson hypothesis is rejected, would be the binomial (negative binomial) distribution when the variance is significantly smaller (larger) than the mean.

4.3.1 Combining Historical and Instrumental Counts

Historical counts naturally contain a greater degree of uncertainty due to sampling limitations. Prior to the introduction of remote sensing technologies this may be because some tropical cyclones went undetected, or because some systems were misclassified as tropical cyclones. Elsner and Bossak (2001) describe the use of a Bayesian approach to deal with this circumstance. They combine historical counts for the period 1851-1899 with reliable observations for the period 1900-2000 to make inferences on United States hurricane activity. The approach supposes that instead of disregarding historical counts due to their likely lower level of precision, such data can still provide useful information in estimating the seasonal rate of event occurrence.

To effect a Bayesian analysis the Poisson rate parameter λ is firstly assigned a prior distribution. A natural candidate is the gamma distribution:

$$f(\lambda \mid n', T') = \frac{T'^{n'} \lambda^{n'-1}}{\Gamma(n')} \exp(-\lambda T') ,$$
(4.2)

which is the conjugate prior for the Poisson rate parameter with conditional expectation $E(\lambda) = n'/T'$. In this formulation n' and T' are prior parameters and $\Gamma(.)$ denotes the gamma function. Since the gamma distribution is the conjugate prior for λ, it can be shown that the posterior distribution for λ belongs to the same distributional family and is also a gamma distribution (Elsner and Bossak 2001; Chu and Zhao 2004). It then follows, given prior parameters n' and T' and the sample statistics n and T, the posterior parameters for λ are given as $n'' = n' + n$ and $T'' = T' + T$.

The prior parameters (n', T') here represent the contribution of historical information, while the sample statistics (n, T) summarise the reliable instrumental observations. For the instrumental record there were 37 landfall events in 45 seasons (1960/61-2004/05), so $n = 37$ and $T = 45$. Since the earlier historical counts are observed with less certainty it is necessary to incorporate this into the estimation process through the specification of prior parameters that reflect this lower level of precision. Elsner & Bossak (2001) approach this using bootstrap resampling to obtain 90% bootstrap confidence intervals for the historical rate. These confidence intervals allocate a likely range of uncertainty in estimating λ from historical observations. This effectively acknowledges that while any estimate of λ from historical counts is less precise due to sampling limitations, there are sufficient data to conclude that it is falls within the range given by the bootstrap confidence intervals (Table 4.1). The prior parameters obtained here by taking a similar approach to that detailed by Elsner and Bossak (2001) were $n' = 24.5$ and $T' = 36.9$, which gives posterior parameters of $n'' = 61.5$ and $T'' = 81.9$.

Figure 4.2 shows gamma distributions on λ based on prior, likelihood and posterior parameters. It is apparent from this figure that there is only a small difference in the location of the densities, although the inclusion of historical data as prior information results in a more 'peaked' posterior density for λ than that based on only the instrumental counts. Hence, the use of historical data advantages the analysis by reducing uncertainty.

As discussed in Chapter 3, a further advantage of the Bayesian approach is the scope it provides for predictive inference on future values of the process. In this framework, uncertainty in both parameter estimates and that due to randomness in future observations is conveniently handled. Specifically, inference on future values of the process is made possible with the posterior predictive density. The predictive density under the Poisson-Gamma model structure is a negative binomial distribution (Elsner and Bossak 2001; Chu and Zhao 2004). Thus, the number $\hat{n}$ of events expected in future period $\hat{T}$, given values for n'' and T'', can be estimated with:

$$\Pr(\hat{n}\,|\,n'', T'', \hat{T}) = \frac{\Gamma(\hat{n}+n'')}{\Gamma(n'')\,\hat{n}!}\left(\frac{T''}{\hat{T}+T''}\right)^{n''}\left(\frac{\hat{T}}{\hat{T}+T''}\right)^{\hat{n}}, \tag{4.3}$$

with mean $\hat{T}\,n''/T''$ and variance $\hat{T}\,n''/T''\,[(\hat{T}+T'')/T'']$.

Figure 4.2 shows a predictive distribution for a $\hat{T}$ = 20-season prediction period. This indicates that there is about a 85% probability of observing at least 10 landfalling tropical cyclones (conditional on their attaining a central pressures of

≤990 hPa at some stage) over the next 20 years, while there is only about a 10% probability of there being at least 20 landfalls.
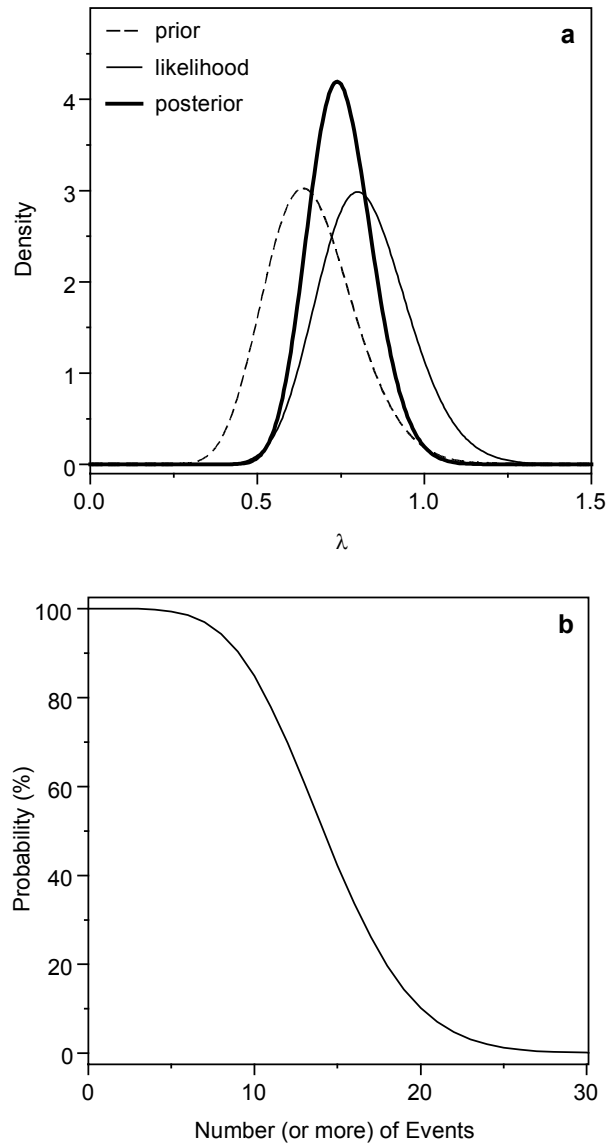
Figure 4.2 Bayesian analysis of landfall counts. (a) Gamma densities on the Poisson rate parameter based on prior, likelihood and posterior parameters, and (b) predictive distribution for the number of tropical cyclone events expected over a 20-year period.

4.4 Relationship to ENSO

It is well recognized that tropical cyclone activity in the Australian region exhibits marked interannual variability in association with the El Niño Southern Oscillation (ENSO) (Solow and Nicholls 1990; Nicholls 1992; Nicholls et al. 1998). ENSO is a coupled atmospheric-oceanic cycle that occurs quasi-periodically in the tropical Pacific Ocean on a time scale of 2-7 years. The importance of this relationship has also been established for Coral Sea and Queensland region tropical cyclones (Basher and Zheng 1995; Grant and Walsh 2001; McDonnell and Holbrook 2004). Here it is proposed to examine the significance of ENSO as a predictor of seasonal tropical cyclone landfall numbers with a regression analysis.

4.4.1 Regression Analysis

Nicholls et al. (1998) employed a linear regression on the August lead SOI and storm counts in the entire Australian region as a means to forecast seasonal activity. Both Solow and Nicholls (1990) and McDonnell and Holbrook (2004) adopted a Poisson regression model in a similar context using the September SOI. Poisson regression is a special case of the generalised linear model (GLM), which is an extension to the classical linear models to include response variables that follow distributions in the exponential family (e.g. Poisson, Gamma, Negative Binomial). The generalisation allows a function $g(.)$ to link the random component of the model, which is the probability distribution for the mean of the response variable (u), to a systematic component that describes the predictor variables or covariates $(x_1,...,x_p)$ (McCullagh and Nelder, 1989):

$$g(u) = \beta_0 + \sum_{j=1}^{p} \beta_j x_j \,.$$

(4.4)

The GLM is typically fit by way of a maximum likelihood procedure to estimate the parameter vector $\boldsymbol{\beta} = (\beta_0, ..., \beta_p)$ using iterative reweighted least squares (McCullagh and Nelder, 1989).

Use of a Poisson regression is preferable here due to the relatively small number of seasonal counts, and particularly because the series contains multiple zero counts. The seasonal ENSO index used in the analysis was obtained from a four-month average of the Southern Oscillation Index (SOI), the normalised surface pressure difference between Darwin and Tahiti, for the period August to November. This pressure difference is a measure of the strength of the trade winds from regions of high pressure in the eastern Pacific to regions of low pressure in the western Pacific. Monthly values of the SOI used in the regression model were obtained from the BoM (http://www.bom.gov.au/climate/current/soihtm1.shtml). A four-month SOI average is used in preference to a single monthly value because the SOI is known to contain significant variability that is unrelated to the ENSO phenomena itself (Trenberth 1997). Use of the four-month average filters out some of this noise. The SOI time series is shown in Figure 4.3.

Due to the relatively short length of the instrumental record available for fitting a Poisson GLM it is again important to adopt a suitable methodology that uses historical records. In fitting a similar model to tropical cyclone counts in the entire Australian region, Solow and Nicholls (1990) adopted an approach to reconstructing

the incomplete record of basin-wide counts. An alternative approach that is employed here follows Elsner and Jagger (2004) in adopting a Bayesian strategy to fitting the GLM with historical counts used to obtained informative prior distributions on the regression parameters.
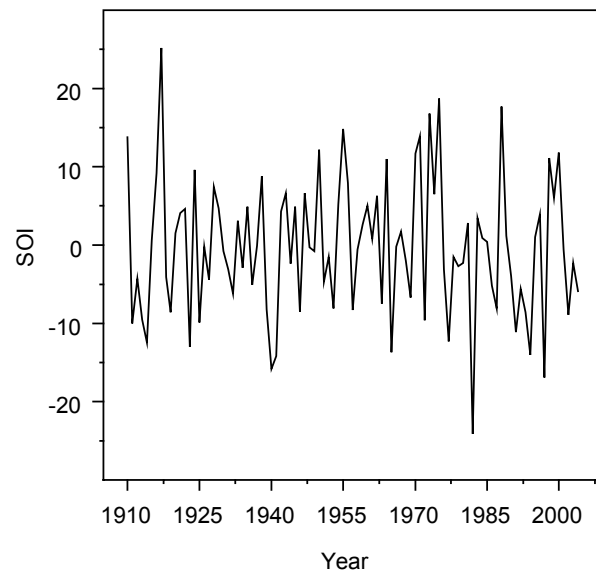
Figure 4.3 SOI time series for the period 1910/11-2004/05, derived from an average of August-November monthly values.

The model structure for seasonal counts conditional on ENSO takes the form:

$$x_i \sim \text{Poisson}(\lambda_i)$$
$$\ln(\lambda_i) = \beta_0 + \beta_1 \text{SOI} \qquad (4.5)$$
$$\boldsymbol{\beta} \sim \text{MVN}(\phi, \Sigma).$$

This particular structure represents a three-stage hierarchical Bayesian model (see e.g. Wikle and Anderson 2003). At the first stage a Poisson process with rate parameter λ is specified for the data x. At the second stage a GLM is used to relate the log-transformed rate parameter to an index of ENSO, with parameters $\boldsymbol{\beta} = (\beta_0, \beta_1)$ describing the strength of the association. Note that the natural logarithm is the canonical link function for the Poisson GLM (McCullagh and Nelder 1989). Finally, at the third stage a multivariate normal prior distribution with mean vector ϕ and covariance matrix Σ is assigned to the model parameters. In fitting this particular model the seasonal SOI values were divided by a factor of 10 to allow for a more convenient representation of results.

Following Elsner and Jagger (2004) a bootstrap resampling procedure is used to estimate the values for ϕ and Σ from historical counts. This is accomplished by fitting a GLM of the form, $\ln(\lambda) = \beta_0 + \beta_1 \text{SOI}$, individually to 1,000 bootstrap samples of the historical counts. Fitting is done through maximum likelihood. The purpose of using the bootstrap resampling procedure is again to allocate a likely range of uncertainty to estimating model parameters from historical records. For each bootstrap sample the parameter estimates $\boldsymbol{\beta}^* = (\beta_0^*, \beta_1^*)$ are retained, allowing ϕ and Σ to be calculated from the series $\boldsymbol{\beta}_1^*, ..., \boldsymbol{\beta}_{1000}^*$.

Bayesian inference for this model is fairly straightforward with the use of Markov chain Monte Carlo (MCMC) techniques such as the Gibbs sampler (Gelfand and Smith 1990). MCMC techniques offer an efficient way of obtaining an empirical estimate of the Bayesian posterior distribution, avoiding the need for direct

numerical integration in cases where the posterior has no analytical solution. The basic principle of MCMC methods is to produce a Markov chain whose state space is the parameter space and whose limiting distribution is the target posterior distribution $\pi(\theta \,|\, x)$.

A Markov chain refers to a model for a system which moves randomly between various states in such a way that the transition to the next value in the sequence depends only on the current value. Starting with values to initialise the sampling algorithm, the chain is run for a specified length of time, referred to as 'burn in', after which it will be approximately distributed as $\pi(\theta \,|\, x)$. Features of the posterior distribution are then summarised with reference to the sequence after convergence has been reached. Determining the appropriate length of 'burn-in' is a particularly important component of this process.

The MCMC scheme used here is based on a Gibbs sampler, which successively updates the individual parameters of the model conditionally on the current values of the other parameters (Gelfand and Smith 1990). Elsner and Jagger (2004) provide an overview of its application to fitting Bayesian GLM's. The sampling scheme here utilised a 5,000 iteration burn-in period with 10,000 subsequent updates used to summarise posterior distributions of the GLM parameters. Convergence was verified by visual inspection of the simulated chains for apparent stability and by repeating the process with several different initial values. Further, autocorrelation functions for each chain showed negligible correlations for lags greater than 3 iterations.
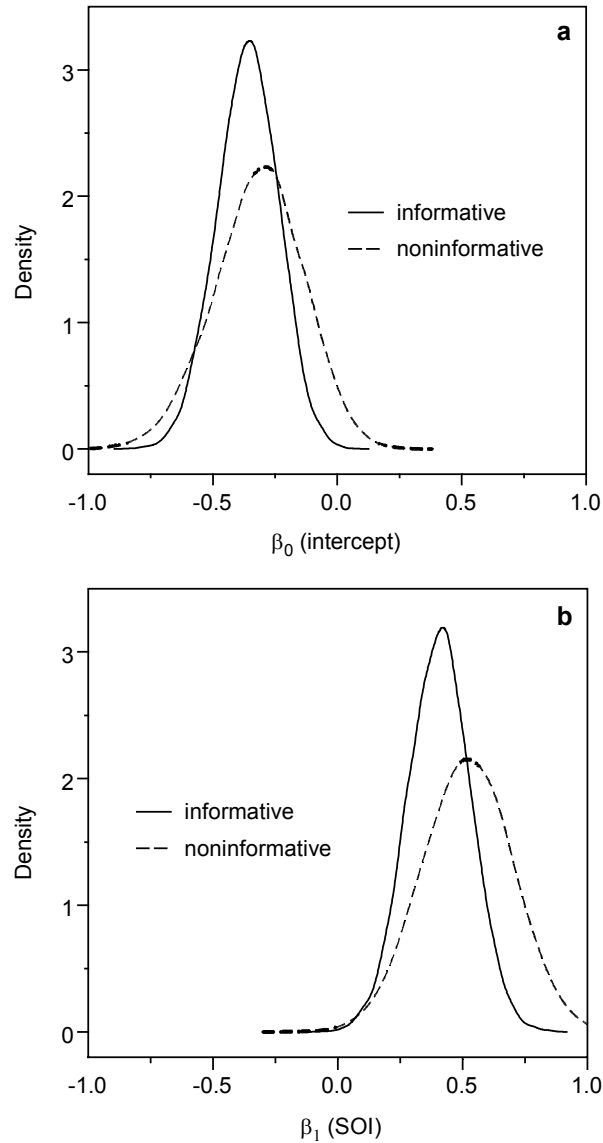
Figure 4.4 Posterior densities of the GLM parameters using noninformative and informative priors. (a) intercept term, and (b) SOI term. Note that the SOI was divided by a factor of 10 in model fitting to approximately scale it with the intercept term.

Posterior density estimates for the regression parameters are plotted in Figure 4.4. These were obtained by applying a standard normal kernel density estimator to the post-convergence MCMC samples using the Gaussian reference bandwidth of

Silverman (1986). The posterior density for β_1, representing the influence of the SOI, is seen to have a mass largely greater than zero.

To check the sensitivity of the results to the prior specification, the Bayesian GLM was also fit with a noninformative prior, thus placing emphasis on the reliable sample information (i.e. instrumental record) in the estimation process. The resulting posterior distributions obtained using this noninformative prior are also plotted in Figure 4.4. They indicate that inclusion of historical data as prior information shifts the posterior density for β_1 slightly towards zero, suggesting the role of ENSO was possibly weaker during the historical era. The posterior mean for β_1 with the historical prior is 0.4059, while for the noninformative prior case the mean is 0.5191. Again it can be seen that posterior distributions are less diffuse after inclusion of historical information, suggesting that uncertainty in parameter estimates is reduced.

In order to examine the model's predictive capacity two scenarios representing extremes of ENSO were considered. Predictive distributions for the model are readily computed using the post-convergence sequence of the MCMC output. Figure 4.5 gives predictive distributions showing the probability of observing a certain number of events in a given season conditional on SOI values of –20 and 20. These correspond respectively to a major El Niño and a major La Niña event. As expected these show a marked increase in the probability of observing one or more events during a major La Niña event than during a major El Niño event. For instance, the probability of observing two or more landfalls in a season when the SOI = 20 is about 43% higher than when the SOI = -20.
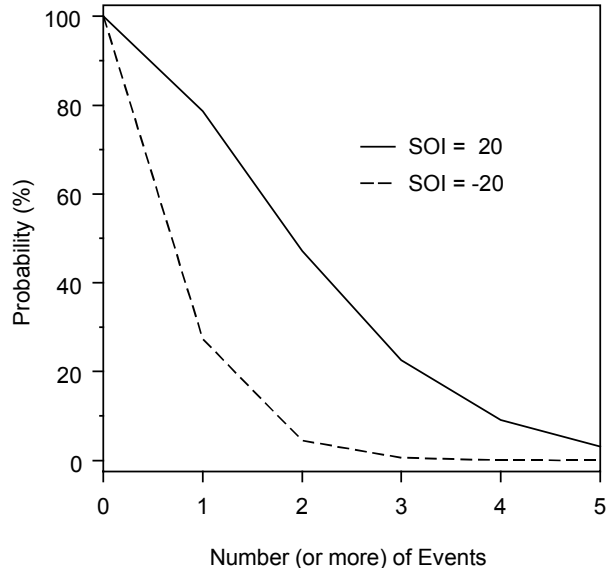
Figure 4.5 Predictive distributions showing the probability of observing tropical cyclone landfalls under two ENSO states as defined by extremes of the SOI.

4.5 Trend Analysis

Traditionally, the simulation of tropical cyclones for the purposes of generating an event series is undertaken without regard to possible temporal changes in the observed time series of storm events. In this section landfall counts are analysed to detect the presence of trends. At the outset it is important to acknowledge the limitations of the trend analysis due to the less reliable nature of historical counts. Nevertheless, it is instructive to identify any trends even if they are the result of

artificial causes. Firstly, an examination of serial correlation in the record is provided. Then, a methodology for the identification of both linear and nonlinear trends in the series is presented. Finally, an investigation into possible temporal variability in the relationship between tropical cyclone activity and ENSO is addressed.

4.5.1 Trends in Storm Counts

Independence of the seasonal counts was first examined by calculating sample autocorrelations for the time series. The autocorrelation function is a commonly used tool for describing the temporal dependence structure of a time series. It graphically highlights how much correlation is present between successive observations by plotting correlation coefficients for consecutive lags.

Figure 4.6 shows autocorrelation functions (ACF) and partial autocorrelation functions (PACF) for time series of storm counts. The partial autocorrelation function filters out the effect of correlation at shorter lags from the correlation estimates at longer lags. Also shown on these plots are confidence bands for white noise or randomness. These bands give ranges of two standard errors based on the sample size. Inspection of the plots shows insignificant correlations for lags of 1-10 seasons, suggesting independence in counts from season to season. This is consistent with other tropical cyclone basins (see e.g. Parisi and Lund 2000; Chu and Zhao 2004), and is not surprising here given the high interannual variability in storm numbers that results from the influence of ENSO.
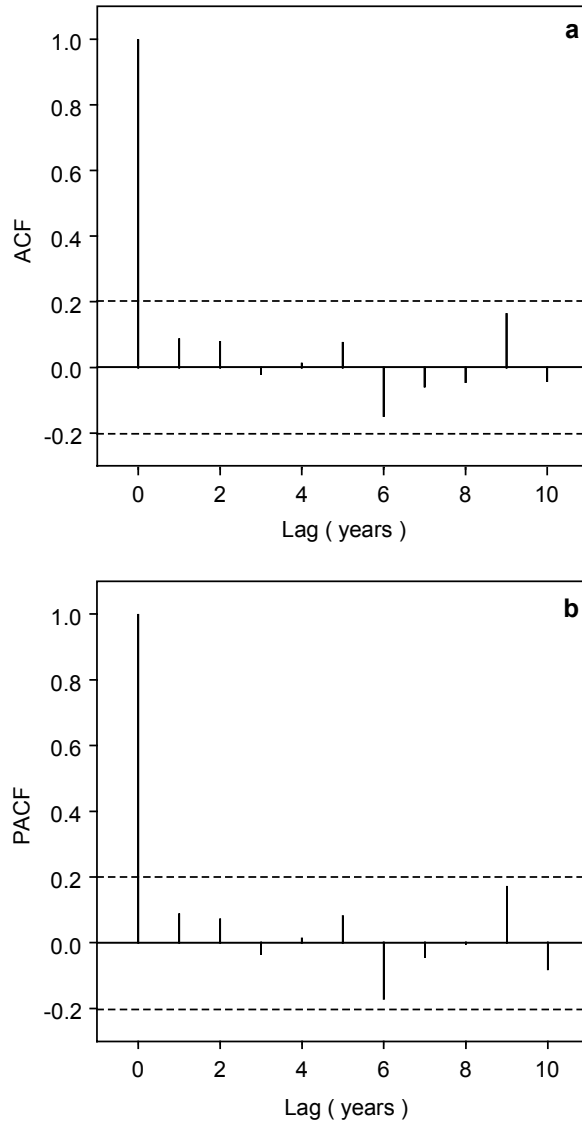
Figure 4.6   Serial correlation in storm counts. (a) autocorrelation function for seasonal counts, and (b) partial autocorrelation function. Both plots show pointwise 95% confidence bands.

In order to then test for the possibility of a trend over time in seasonal counts, a

linear trend in the Poisson rate parameter was firstly considered:

$$\lambda_t = \exp(a_0 + a_1 t), \tag{4.6}$$

where λ_t is the rate in season $t = 1,...,m$, with $t = 1$ corresponding to the 1910/11 season, and a_0 and a_1 are unknown coefficients. The exponential function ensures λ is nonnegative. In fitting this model, interest centres on testing the hypothesis that $a_1 = 0$ (i.e. constant rate over time) against the hypothesis $a_1 \neq 0$ (i.e. nonconstant rate). The maximum likelihood estimates of a_0 and a_1 are determined with the trend λ_t plotted in Figure 4.7. The form of this particular trend shows that storm activity has apparently increased over time. This is consistent with results summarised in Table 1 where the historical rate is seen to be lower than the instrumental rate. However, the *p*-value for this fit, as measured by the likelihood ratio statistic, is 0.390, which implies the null hypothesis $a_1 = 0$ cannot be rejected and thus the trend is not statistically significant.

An alternative approach that is perhaps more suitable for examining any underlying trend in storm activity is local likelihood estimation (Solow 1989). Local likelihood estimation is a semi-parametric regression technique that offers greater flexibility by supposing that the Poisson rate parameter λ varies smoothly with time, rather than being constrained to a specific parametric form such as that given in equation 4.6. Fitting involves estimating the function λ_t at each value of t, using observations that fall within the neighbourhood of each point. The value of λ_t is then obtained by fitting a low-order polynomial to these neighbouring observations, which are also weighted by their proximity to the estimation point. A local linear model is assumed

here with the number of neighbouring observations and their weights determined using a bandwidth and a symmetric weight function.

Choice of bandwidth is obviously crucial to this process as too small a bandwidth may result in an overly variable fit and too large a bandwidth may give a biased fit. Due to the difficulties associated with bandwidth selection in such applications, it was decided here to use a range of bandwidths and examine the resulting fits for any major differences. Figure 4.7 shows an estimate of λ_t obtained using nearest neighbour bandwidths of 0.25 and 0.40. These give window widths covering 25% and 40% of the data respectively. The underlying pattern was fairly similar for these bandwidths, with an underlying trend of decadal to multi-decadal variability in evidence.

A notable feature from the local fits is the rather abrupt increase in the rate at around the late 1960s that extends into the late 1980s. This follows a period of lower activity in the 1920s through 1940s. Given the point at which the increase occurs, a possible explanation is one of observational bias. As the trend is only indicative of storms with intensities below ≤990 hPa, there is the possibility of a bias in the record caused by the general underestimation of storm intensities in the pre-satellite era. If this were indeed the case, then a number of tropical cyclones in this era would actually have attained a maximum intensity of ≤990 hPa, however their recorded intensity was given as >990 hPa due to insufficient information. Holland (1981) demonstrated that in the absence of surface observations from the tropical cyclone core, storm intensities in the Australian region were likely to be consistently underestimated during the pre-satellite era. Thus, the possibility that the observed

66

drop in activity over the 1920-1940 period is simply an artefact of removing observational bias in the series cannot be ruled out.
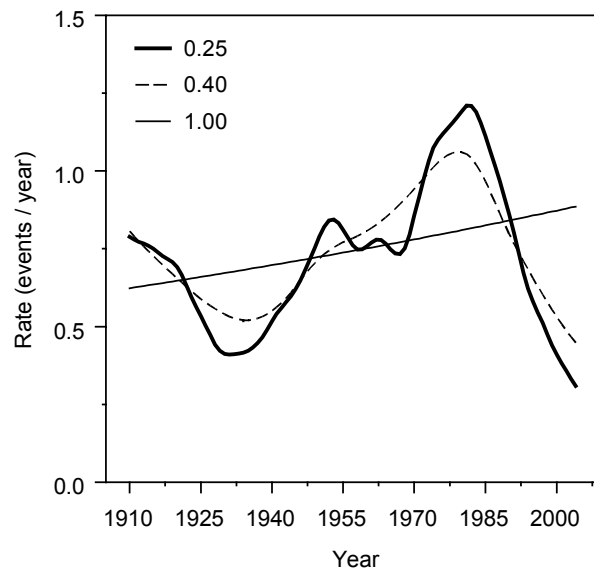
Figure 4.7   Trend in the Poisson rate parameter over the period 1910/11-2004/05. Plot shows local linear fits with nearest neighbour bandwidths of 0.25 and 0.40 as well as global linear fit.

An alternative explanation to the observed pattern is one of natural climate variability. In this case the 1920-1940 period would be characterised as a period of reduced tropical cyclone activity along the Queensland coast. This is in contrast to the period 1970/71-1990/91 where activity was evidently much higher.   Activity

during the post-1990/91 period was comparatively lower than during the 1970/71-1990/91 period. Figure 4.7 also shows that the first decade of the record was fairly active in comparison to the following two decades. Ultimately, it is likely that the observed trend reflects the influence of both natural and artificial factors, although the degree to which either has influence is difficult to ascertain.

4.5.2 Temporal Variability in the ENSO Relationship

The results of the regression analysis in section 4.4.1 indicated that the relationship between ENSO and tropical cyclone activity was possibly weaker during the historical era than during the instrumental era. This raises the possibility of variation in the ENSO relationship with tropical cyclone landfalls over time. A relatively simple approach adopted here to examine this was to fit the Bayesian GLM to a moving window of the tropical cyclone counts.

Figure 4.4 shows that the mass of the posterior distribution of the regression parameter β_1 is greater than zero in both informative and noninformative prior cases. A suitable test of significance can therefore be established by requiring 95% of the posterior samples generated from the MCMC scheme to be greater than zero for β_1 to be a significant term at the $\alpha = 0.05$ level of significance. By applying this criterion to the GLM fit to a moving window of the record, variation in the strength of the relationship over time can be examined. This approach is similar to Elsner et al. (2001) who used maximum likelihood fitting of a Poisson GLM to United States hurricane counts and ENSO over a 50-year moving window to examine secular variability in the relationship over the 20th century.

Figure 4.8 shows the application of this approach with a 40-year moving window of the tropical cyclone record from 1910/11 to 2004/05. The p-values on the y-axis measure the significance of β_1 as a term in the model, with values greater than 0.05 indicating that the SOI term is not significant. This amounts to implying that the inclusion of an index of ENSO offers no improvement over a null model (i.e. the climatological mean rate).
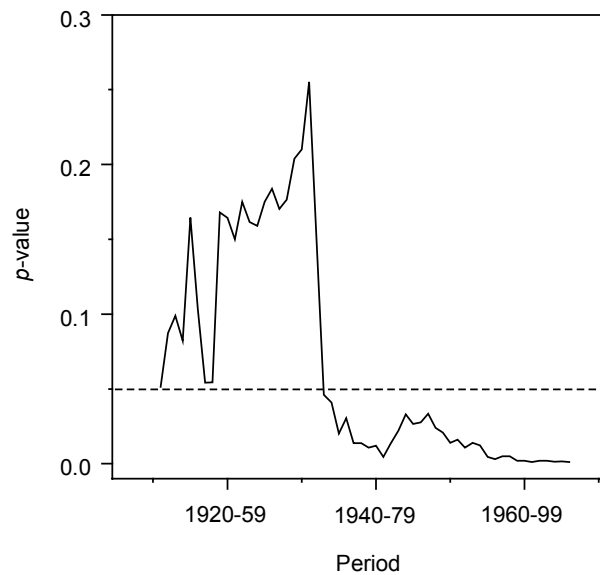
Figure 4.8 Strength of the association between tropical cyclone landfalls and ENSO over a 40-year moving window of the record. Significance is established when the curve falls below the dashed line.

Each p-value in Figure 4.8 corresponds to a successive fit of the model in equation 4.5 using a noninformative prior. The first point plotted in the figure gives the p-

value for the fit to the period 1910/11-1949/50, the second for the period 1911/12-1950/51, and so on up to 1965/66-2004/05. Interestingly, the plot highlights a pattern whereby there is an absence of a significant association between the SOI and Queensland landfall activity over much of the early half of last century.

4.6 Summary

The analysis presented in this chapter has demonstrated that the Bayesian methodology provides a useful framework for incorporating historical information when analysing the frequency of tropical cyclone landfalls in Queensland. Results show that inclusion of historical counts led to parameter estimates for a model of seasonal activity that has a lower level of statistical uncertainty than a model based on only the instrumental record. Similar conclusions apply for a regression model incorporating an index of ENSO as a predictor for seasonal activity. The regression analysis confirmed the importance of ENSO's influence on tropical cyclone landfalls in the region. The Bayesian approach also facilitates predictive inferences on future landfall activity within a probabilistic framework. Example predictions are plotted in Figures 4.2 and 4.5.

A trend analysis highlighted no evidence of temporal dependence in storm counts as well as no indication of a significant upward or downward trend in activity over time. A Poisson local likelihood fit to the time series did indicate the presence of decadal variability in storm activity. It should be noted though that because of the relatively small number of observed landfalls, sampling variability is likely to influence the

results of the trend analysis. Random fluctuations in small samples may either mask the presence of a trend, or alternatively, result in mistakenly interpreting the presence of a trend. This combined with both the assumptions of the analysis and the uncertain nature of historical records makes trend identification difficult. For these reasons it is not possible to conclusively state whether the observed pattern of decadal variability solely reflects natural causes.

The results of an analysis into temporal variability in the relationship between ENSO and tropical cyclone counts shows the lack of a significant association between these variables during the early half of last century. Whether this reflects an actual trend of decadal variability in the relationship, or is simply indicative of the less precise nature of storm counts in the historical era is again difficult to decipher. It is known, however, that the strength of ENSO teleconnections with climate patterns in the northeast Australian region are modulated on decadal time scales (Power et al. 1999).

CHAPTER 5

QUEENSLAND LANDFALLING TROPICAL

CYCLONES: INTENSITIES

5.1 Introduction

While knowledge of the frequency with which landfalling tropical cyclones occur is an essential component of the climatology, it is also important to have an understanding of the frequency with which extreme events occur. Clearly though, the relatively short time period over which reliable observations are available in the region combined with the rarity of major landfalling events over recent decades complicates any analysis of the statistical properties of extremes. The historical record of landfalling events again provides a useful source of information on such events for the period before the era of satellite monitoring. Furthermore, during this era there were several storms with landfall intensities greater than that observed in the recent satellite record.

This chapter constitutes an analysis of Queensland landfalling tropical cyclone intensities and follows along similar lines as that presented in the previous chapter. It focuses primarily on approaches for incorporating historical observations. After a description of the data, the first part of the chapter deals with the application of a Bayesian approach to make use of historical observations obtained before 1960/61 as

prior information in fitting an extreme value model to a time series of minimum central pressures. The emphasis here is on examining the ways that historical information can assist predictions of the probability of major landfall events. An alternative methodology based on a censoring procedure is then presented as means to verify results obtained from the Bayesian analysis. An investigation into detecting trends in storm intensities over the 20th century is then conducted by fitting simple trend functions in the extreme value model. This approach is also employed to examine any possible effect of ENSO on storm intensities.

5.2 Data

The best-track database of tropical cyclone observations in the Australian region again forms the basis of the data used in this analysis. Following the approach taken in the previous chapter storms that did not attain a minimum central pressure of 990 hPa or lower at some stage were firstly removed. A separation of the record into an instrumental era (1960/61-2004/05) and an historical era (pre-1960/61) was again adopted. In addition, the historical record was extended to include events dating back to the 1898/99 season so as to make use of all major recorded landfall events. Historical records of storm intensities extracted from the best-track database were also supplemented with accounts of major tropical cyclones impacting Queensland documented by Callaghan (2004), which includes information on landfall central pressures not recorded in the best-track database.

In the main, observations of storm intensity in the historical era would be expected to be less reliable than for storms sampled in the instrumental era. An examination of the quality of the Australian best-track database by Holland (1981) indicates that the chief cause of this lower reliability was a lack of surface measurements from the inner region of the tropical cyclone. This often resulted in minimum central pressures for a number of storms being overestimated (i.e. storm intensities being underestimated).
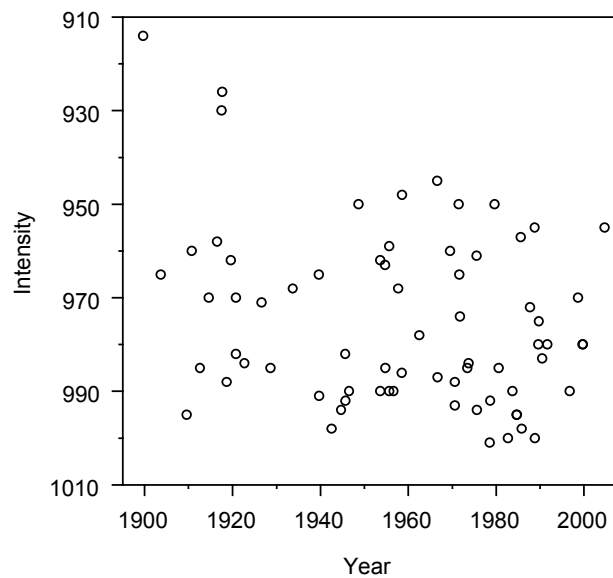
Figure 5.1 Time series of minimum central pressures for Queensland landfalling tropical cyclones over the period 1898/99-2004/05.

As with the previous chapter, it is assumed here that historical landfall observations are more reliable than observations for the Coral Sea region as a whole due to the

increased likelihood of obtaining a direct surface measurement at coastal locations. The time series of minimum central pressures used in the analysis is shown in Figure 5.1. Note that a few landfall storms during the historical era did not have central pressure measurements at or near the time of landfall and hence were not used in the subsequent analysis.

5.3 Distribution of Storm Intensity

Tropical cyclone intensity is typically characterised by either the lowest central pressure or maximum wind speed. Measurements of maximum wind speeds in tropical cyclones are far less complete in the best-track database, and as such minimum central pressures are more commonly used as an indicator of severity (Holland 1981). The analysis conducted here is based on fitting a probability distribution to the lowest observed central pressure series shown in Figure 5.1.

5.3.1 Extreme Value Analysis

When interest is in modelling the extremes of a given process, classical extreme value theory offers a suitable framework for estimating event probabilities including those beyond the range of the observed sample. The fundamental basis of the theory is that for a sufficiently long sequence of independent and identically distributed random variables, their maxima (or minima) are described by one of three basic families; Gumbel, Fréchet or Weibull types. As these extreme values distributions are formally justified as limiting distributions for the maxima (or minima) of random

variables they have theoretical motivation for examining the statistical properties of physical processes at high levels. The three types are more conveniently combined into a single family, known as the Generalised Extreme Value (GEV) distribution (Coles 2001):

$$F(x|\xi,\sigma,\kappa) = \exp\left\{-\left[1+\kappa\left(\frac{x-\xi}{\sigma}\right)\right]^{-1/\kappa}\right\},$$

$$\text{defined on} \quad [\,x : 1+\kappa(x-\xi)/\sigma > 0\,], \tag{5.1}$$

$$\text{where} \quad \sigma > 0.$$

In this model ξ, σ and κ are location, scale and shape parameters respectively. Importantly, the value of the shape parameter determines the nature of the upper tail of the distribution. Specifically, the case $\kappa > 0$ corresponds to the heavy-tailed Fréchet type, $\kappa < 0$ to the Weibull type with bounded upper tail, and in the limit as $\kappa \to 0$ the Gumbel distribution is obtained. Note that the model given in equation 5.1 applies to the distribution of maxima. To fit the model to sample minima (e.g. minimum central pressures) requires a transformation of the observed values $(x_1,...,x_m)$ to their negatives $(-x_1,...,-x_m)$.

In practical applications the GEV distribution has been widely used to model the extremes of various processes like floods, sea levels, rainfall, wave heights and wind speeds (see e.g. Coles 2001; Martins and Stedinger 2001; Katz et al. 2002). The model is particularly suitable for most environmental time series because of its asymptotic basis and flexible range of tail behaviours.

The GEV distribution provides a model for the behaviour of block maxima, wherein a block refers to a fixed period of time (e.g. year, season) for which the maximum observed value is used in the analysis. This is particularly important when results are interpreted in terms of return periods that are typically presented on an annual scale. Due to both the infrequent nature and high interannual variability of tropical cyclone landfalls, however, use of a seasonal block consisting of the lowest central pressure value for each season results here in a series containing missing values. Over the period of record there were several seasons in which no tropical cyclones, that reached central pressures of at least 990 hPa at some stage, crossed the Queensland coast. One strategy that could be implemented in this instance is to increase the block size and use the largest value from, for instance, every two consecutive seasons. However, this approach leads to the loss of valuable information in an already data scarce series.

Another potential drawback of the block maxima approach is that only the largest value from each block (in this case each season) is utilised and other large events in the season are discarded regardless of their magnitude. In the present case, the occurrence of more than one extreme landfall event in a particular season is not common, although there have been several active seasons (e.g. 1917/18, 1970/71) in which multiple severe tropical cyclones made landfall.

For these reasons the use of an alternative extreme value model based on exceedances over high thresholds is preferred here. The primary motivation for implementing a threshold approach is that it does not require a value for each season to conduct the analysis and also because it makes use of all available data on

extremes.   In its most common form the threshold exceedances approach incorporates two components:

- The number of exceedances of a given threshold (u) follows a Poisson distribution with rate parameter λ, and;
- The excesses follow a Generalised Pareto Distribution (GPD).

The GPD is the asymptotic distribution used to describe the behaviour of independent events exceeding a sufficiently high threshold. With a Poisson process describing the annual exceedance rate, the Poisson-GPD model is closely related to the GEV distribution for annual maxima (Davison and Smith 1990; Coles 2001). Defining a threshold exceedance as $y_i = x_i - u, x_i > u$, the GPD with shape (κ) and scale (σ) parameters is given by:

$$F\left(y\,|\,\sigma,\kappa\right) = 1 - \left(1 + \kappa\frac{y}{\sigma}\right)^{-1/\kappa}$$

(5.2)

where $\sigma > 0$ and $1 + \kappa\, y/\sigma > 0$.

As with the GEV distribution the shape parameter in equation 5.2 gives 3 cases; when $\kappa > 0$ the distribution of excesses is unbounded, when $\kappa < 0$ the distribution has an upper bound at $u - \sigma/\kappa$, and in the limit as $\kappa \rightarrow 0$ the exponential distribution is obtained. The motivation for equation 5.2 as a model for extremes is that it arises as a limiting distribution for the excesses over high thresholds if the parent distribution is in the domain of attraction of the GEV distribution. As such,

the GPD shape parameter κ is equivalent to that of the corresponding GEV distribution (Coles 2001).

Common methods of the parameter estimation for the GPD, for known threshold, include those based on maximum likelihood (ML), moments and L-moments. Due to its asymptotic properties and general flexibility, the maximum likelihood approach is initially employed here. Given the sequence of independent observations of a random variable $x = (x_1,...,x_m)$, which is assumed to belong to a specific parametric family $f(x|\theta)$ with the parameter vector θ, the maximum likelihood estimator of θ, given x, is obtained by maximizing the likelihood (or log-likelihood) function:

$$L(\theta|x) = \prod_{i=1}^{m} f(x|\theta).$$
(5.3)

The maximum likelihood procedure for the GPD requires an iterative solution for $\theta = (\sigma, \kappa)$ by maximising the log-likelihood of equation 5.2. Given the sequence of m excesses (i.e. $y_1,..., y_m$), this is given by (Coles 2001):

$$\ell(\sigma, \kappa|y) = -m\ln(\sigma) - \left(1 + \frac{1}{\kappa}\right)\sum_{i=1}^{m}\ln\left(1 + \frac{\kappa y_i}{\sigma}\right).$$
(5.4)

In this case estimation of the threshold crossing rate component can be separated from estimation of the GPD parameters. An estimate of the T-year return level is then given by:

$$z_T = u + \frac{\sigma}{\kappa} [(\lambda T)^{\kappa} - 1],$$ (5.5)

where u, σ, κ and λ are substituted by their sample estimates.

Also crucial to the application of this Poisson-GPD model is the estimation of the threshold level (u). Ultimately, there is a need to compromise between selecting a sufficiently high threshold so as to conform to the asymptotic basis of the model, yet at the same time obtain a sufficiently large sample to minimise sampling error. A useful property of the GPD is that of 'threshold stability', where if the GPD assumption is valid for the threshold u_0, it should equally be valid for all thresholds $u > u_0$ (Coles 2001). It also follows that for $u > u_0$ the expectation of the excesses, $E(x - u \,|\, x > u)$, is a linear function of u. Thus, a common method of threshold selection is the mean excess plot, comprising a plot of a range of thresholds against their mean observed excess to identify approximate linearity (Davison and Smith 1990; Coles 2001).

In Figure 5.2 a mean excess plot for the instrumental portion (1960/61-2004/05) of the time series of minimum central pressures is given. This shows approximate linearity across the threshold range. The downward trend evident in the plot is consistent with a distribution bounded from above (i.e. $\kappa < 0$). Hence, the GPD was fit to this series with a threshold of 1002 hPa so as to include all events, conditional on them having obtained a minimum central pressure of 990 hPa or lower at some stage. Parisi and Lund (2000) also used this threshold when fitting the GPD to United States landfalling hurricane central pressures. Subsequent maximum

likelihood estimates of the GPD parameters are $\hat{\sigma} = 39.9$, $\hat{\kappa} = -0.679$, and for the

threshold exceedance rate, $\hat{\lambda} = 0.822$ (37 events in 45 seasons).
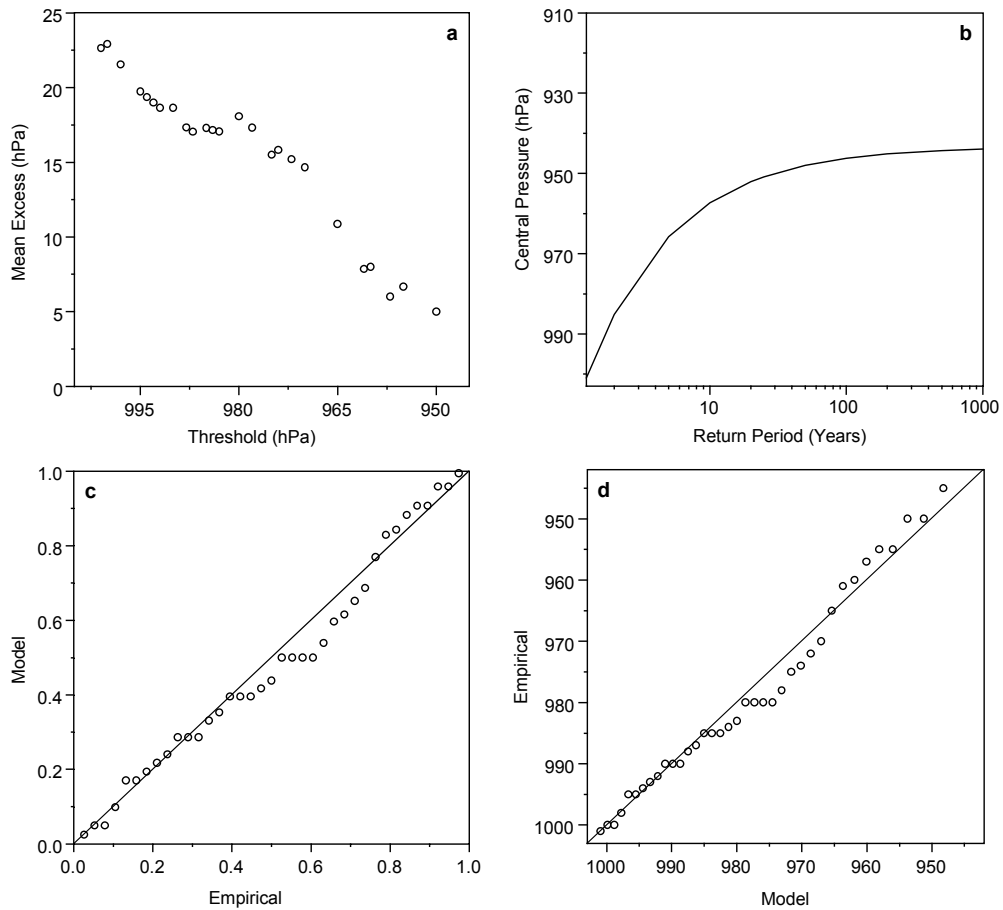
Figure 5.2   Plots of GPD fit to landfalling central pressures for the period 1960/61-2004/05 (a) Mean excess plot, (b) return period plot, (c) probability plot, and (d) quantile plot.

Figure 5.2 also shows a return period curve for the fitted model as well as probability

and quantile plots. As detailed by Coles (2001), the probability and quantile plots

are diagnostic tools for assessing the goodness-of-fit between the model and raw observations. These plot exceedance probabilities and quantiles for the model against a 'distribution-free' empirical estimate of these quantities. The empirical distribution function $\hat{F}(x)$ used to estimate these quantities is defined by the rank mean plotting positions, $i/(m+1)$, where i is a rank for each ordered observation and m is the sample size. This is an unbiased, nonparametric estimate with no assumption made regarding the distribution type. The plots shown in Figure 5.2 highlight that a reasonable fit is obtained with the adopted threshold.

5.3.2 Incorporation of Historical Information

Given the utility of the Bayesian approach for incorporating historical observations of storm counts, it seems natural to extend this approach to the case of modelling landfall intensities. The ability to incorporate prior information sources is recognised to offer an advantage over conventional techniques in estimating extreme value distributions from small samples (Coles and Powell 1996). The approach adopted here is analogous to that presented in the previous chapter, whereby historical observations are incorporated through the specification of prior distributions for the model parameters.

With a fixed threshold, estimation of the GPD parameters (σ, κ) can be assumed independent from estimation of the threshold exceedance rate, which is governed by a Poisson process with rate parameter λ. As the analysis here uses the entire series of landfall events, the threshold crossing rate is equivalent to the seasonal rate of

tropical cyclone occurrence, estimation of which was discussed in the previous chapter.

In the Bayesian context, the GPD parameters are considered random variables with prior distributions assigned. The choice of prior structure is an important step in a Bayesian analysis, although there are relatively few examples in the literature for the GPD case. Coles and Powell (1996) adopted a multivariate normal distribution as a prior for parameters of the GEV distribution fit to wind speed data in the United States. In their study wind speed records from multiple sites were aggregated to construct an informative prior. Adopting a similar prior distribution, the model structure used here is summarised as follows:

$$
\begin{aligned}
y_i &\sim \text{GPD}\{\log(\sigma), \kappa\} \\
\{\ln(\sigma), \kappa\} &\sim \text{MVN}(\phi, \Sigma),
\end{aligned}
\tag{5.6}
$$

where ϕ and Σ are respectively a vector of means and covariance matrix for the multivariate normal distribution. Log-transformation of the scale parameter σ, constrains it to positive values in the estimation process. Like the analysis presented in the previous chapter, the values of ϕ and Σ are determined empirically by using the maximum likelihood procedure to estimate $\{\ln(\sigma), \kappa\}$ from 1,000 bootstrap samples of the historical series (1898/99-1959/60) of minimum central pressures.

Histograms of the GPD shape and scale parameters based on the bootstrap samples are shown in Figure 5.3. Also shown are bootstrap sampling distributions obtained from applying the same procedure to the instrumental series. Of note is the tendency

for estimates of the shape parameter from the historical series to be less negative than

for instrumental series, indicative of a longer-tailed distribution.
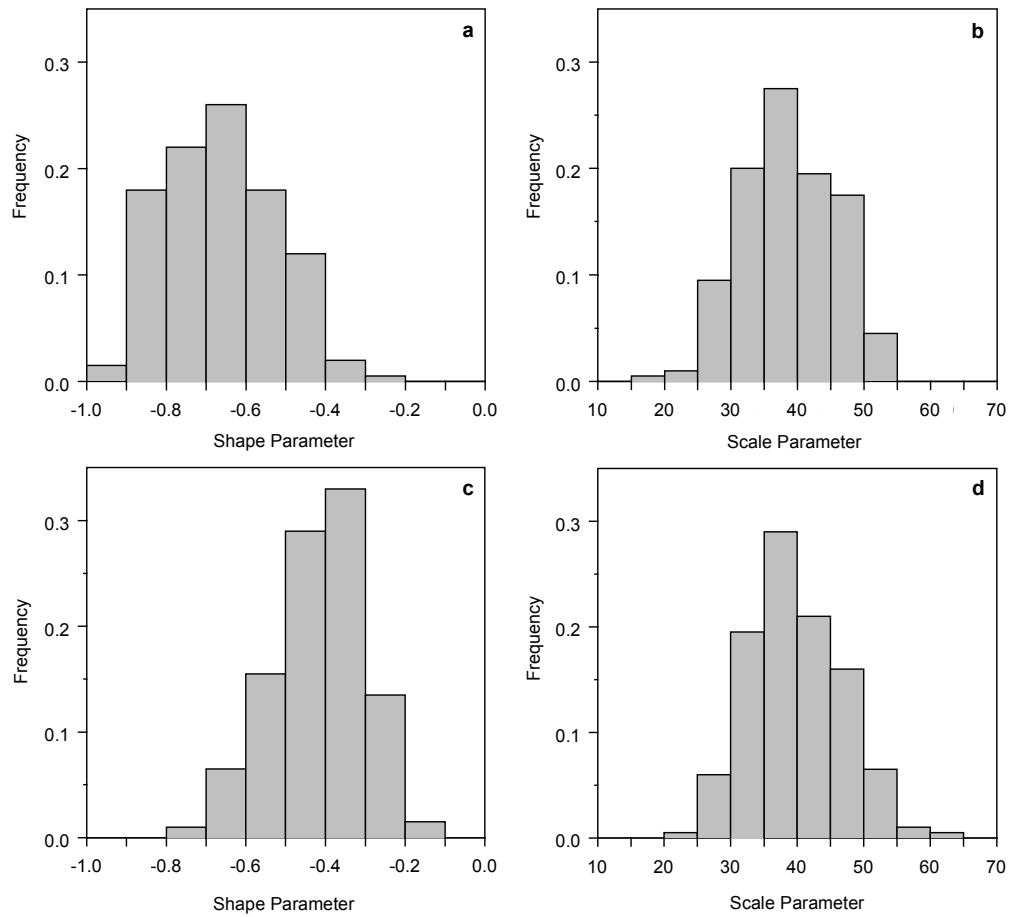
Figure 5.3 Bootstrap sampling distributions of GPD parameters. (a) shape parameter for instrumental series, (b) scale parameter for instrumental series, (c) shape parameter for historical series, and (d) scale parameter for historical series.

Bayesian inference for the model given in equation 5.6 is made possible with the use

of Markov chain Monte Carlo (MCMC) methods. As outlined in the previous

chapter, this involves simulation from a Markov chain whose equilibrium distribution is the target posterior distribution. The adopted procedure employs a Gibbs sampler, which successively updates individual parameters conditional on the current values of the other parameters (Gelfand and Smith 1990). An additional step in the Gibbs sampling algorithm is further necessary to account for the conditional distributions not being of standard form, and hence not directly available for sampling. This can be overcome by including a Metropolis-Hastings step with random-walk proposals at each parameter update of the Gibbs sampler (see e.g. Coles and Tawn 1996).

A 100,000 burn-in period was used with 200,000 subsequent updates of the MCMC algorithm used to summarise posterior distributions. The sampling process incorporated a thinning interval of 10 iterations to reduce dependence between successive parameter updates. Visual inspection of the chains and the use of multiple starting values indicated stability was reached and that the chains were exploring parameter space sufficiently. The resulting posterior densities for (σ, κ) are plotted in Figure 5.4. The posterior distribution for κ gives convincing evidence for this parameter to be negative $\{\Pr(\kappa > 0) < 0.001)$ and thus for the distribution of excesses to have an upper bound. Combining the posterior distributions for (σ, κ) with an estimate of the threshold exceedance rate gives posterior densities of return periods under the Poisson-GPD model. Figure 5.5 shows examples for 50 and 100-year return periods.

When interest is in predictive inference, the Bayesian approach also allows an estimate of the probability of future events reaching extreme levels through the

posterior predictive density. Specifically, the probability of the level z not being exceeded during a year (season) is given by:

$$\Pr(z\,|\,\theta) = \exp\left\{ -\lambda\left[1 + \kappa\left(\frac{z - u}{\sigma} \right) \right]^{-1/\kappa} \right\}.$$

(5.7)
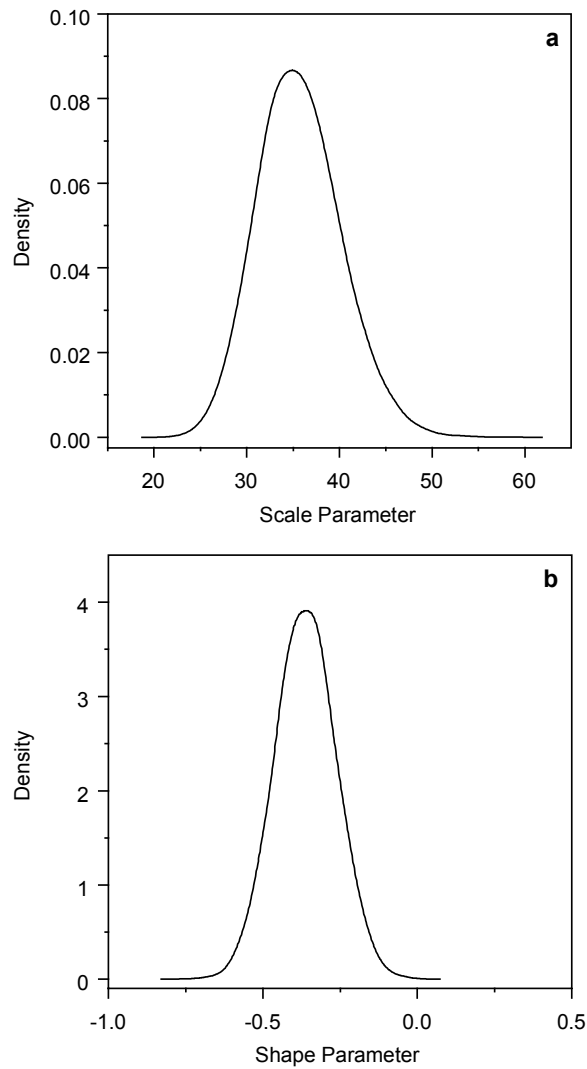
Figure 5.4 Posterior distributions of GPD parameters as estimated using Bayesian statistical approach. (a) scale parameter, and (b) shape parameter.

Substitution of the parameter values $\theta_i = (\sigma_i, \kappa_i)$ at each update from the MCMC output (post-convergence) into equation 5.7, and subsequent averaging across the sequence allows a predictive distribution to be obtained. Figure 5.6 shows predictions for the probability of observing landfalling tropical cyclones covering a range of intensities over 5 and 10-year periods. Taking the cases of tropical cyclone *Mahina* (914 hPa) and the 1918 Innisfail (926 hPa) and Mackay (930 hPa) events as the three most intense in the record, this plot shows that there is respectively a 3.7%, 13.6% and 19.5% chance of a future landfalling event reaching similar intensities in the next 10-years. These events could be expected to occur on average once within a period of around 254-years (914 hPa), 66-years (926 hPa), and 44-years (930 hPa).
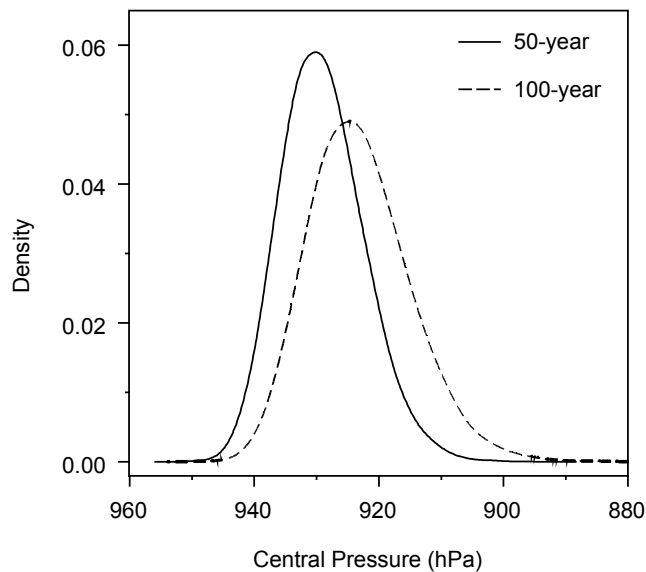
Figure 5.5 Posterior distributions of 50-year and 100-year return periods under Poisson-GPD model fit to landfall minimum central pressures.
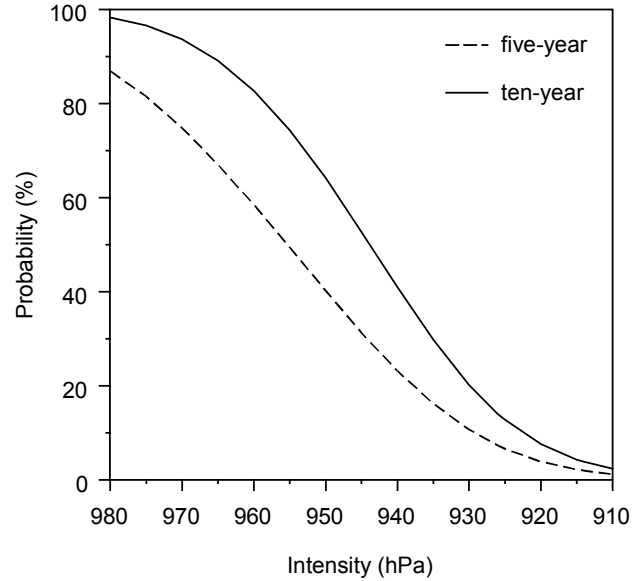
Figure 5.6 Predictive distributions showing probability of tropical cyclones of various intensities occurring in five and ten-year periods.

5.3.3 Validation

In order to investigate the suitability of the Bayesian model for incorporating historical observations an alternative approach is considered in this section for the purposes of verification. This approach is based on treating the combined historical and instrumental record as a censored dataset. As discussed in Chapter 3, application of this approach has been extensive in the field of flood frequency analysis where the value of historical and palaeoflood information has long been recognised (see e.g. Kuczera 1999; Martins and Stedinger 2001). This procedure relies on the definition of a fixed magnitude threshold u_M, above which historical data on event magnitudes are available, but below which historical data are unknown. As shown in Figure 5.7

this case is commonly referred to as type I censoring, whereby the unobserved

historical values below u_M are censored.
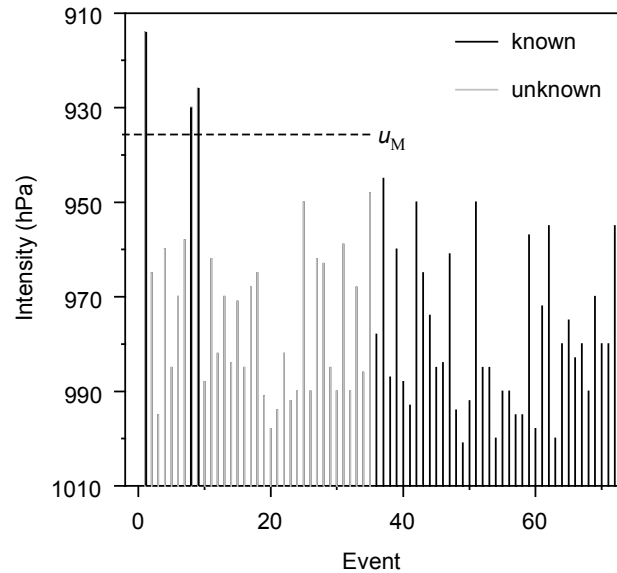
Figure 5.7 Outline of type I censoring for fitting threshold exceedances to instrumental and historical records.

In the context of this analysis, events that fall below u_M are treated as unknown in

the context that they do not necessarily have reliable measures of intensity. Thus, in

addition to having a complete series of reliable sample values (i.e. the instrumental

series), there is also an historical record that is complete only in the sense that it

contains all sample values above some fixed magnitude threshold. The historical

storms of particular relevance here are tropical cyclone *Mahina* (914 hPa) and the two tropical cyclones of 1918 that struck Innisfail (926 hPa) and Mackay (930 hPa). It is likely due to both the severity and impact of these storms that their recorded intensities are relatively accurate measures of their magnitudes. The censoring procedure used here is based on the assumption the historical record is complete in its recording of major events above u_M.

Based on the situation depicted in Figure 5.7, an historical period of 62-seasons (1898/99-1959/60) was assumed, in which three tropical cyclones with known intensities exceeded a value of u_M equal to 935 hPa. The value of u_M was selected arbitrarily, although was set high so as to minimise the possibility that a greater number of historical storms could have exceeded this threshold. This amounts to treating the historical record as complete for tropical cyclones with central pressures lower than 935 hPa. Martins and Stedinger (2001) give the maximum likelihood procedure for estimating a Poisson-GPD model that implements the type I censoring approach.

Figure 5.8 compares the fitted Poisson-GPD models using the Bayesian and censoring approaches considered in this study. The return period curve for the Bayesian analysis is seen to compare relatively well with that based on the censoring approach. The curve for the Bayesian analysis plots the posterior predictive distribution for a 1-year period, which has the advantage of implicitly accounting for parameter uncertainty. Maximum likelihood estimates are $\hat{\sigma} = 32.3$ and $\hat{\kappa} = -0.307$ for the censoring approach, which compares favourably with the Bayesian posterior mean estimates of $\hat{\sigma} = 35.4$ and $\hat{\kappa} = -0.362$.

Figure 5.8 also plots the return period curve for the model fit to only the instrumental record. Both Bayesian and censoring approaches indicate the importance of using historical information in the analysis as a means to predict the frequency of extreme events. Both approaches also show how model estimation is most sensitive to the largest events in the series. Thus, an analysis that only makes use of the information available in the instrumental record would lead to comparatively lower predictions on the frequency of major tropical cyclone events making landfall in the Queensland region.
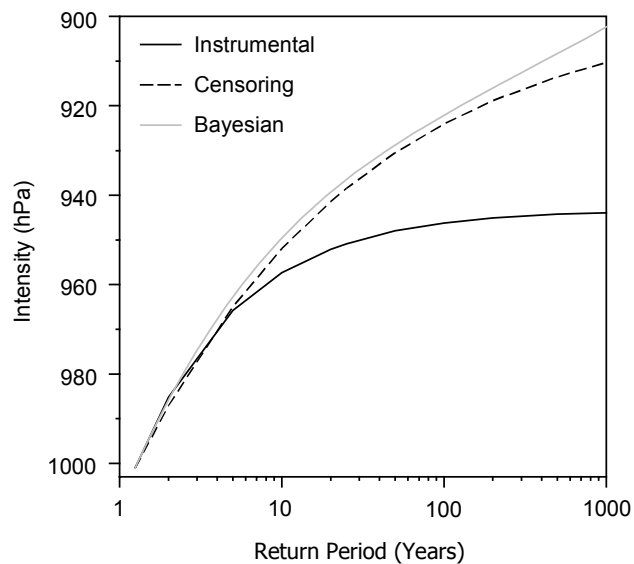
Figure 5.8 Comparison of return period curves based on fitting GPD to tropical cyclone intensities.

5.4 Trends and the Effect of ENSO

The identification of trends in the frequency of extremes is problematical given the limited amount of data on such events. A cursory examination of the time series of minimum central pressures (Figure 5.1) highlights periods of both heightened and reduced activity in intense storm occurrences. A peak in the incidence of severe tropical cyclones occurred early in the time series with a secondary peak around the early 1970s. Notable inactive periods are apparent over the 1920-1940 period and in the more recent post-1990/91 period.

Serial correlation in the time series of minimum central pressures was firstly examined in this section using autocorrelation plots similar to those presented in the previous chapter. The analysis proceeds by then fitting a linear trend in the probability model for minimum central pressures to investigate the presence and significance of any underlying temporal pattern. Finally, an investigation into the effect of ENSO on extremes is conducted.

Figure 5.9 shows autocorrelation and partial autocorrelation functions for the raw time series plotted in Figure 5.1. The autocorrelation and partial autocorrelation plots provide a graphical indication of the temporal dependence structure of the series by highlighting correlation between successive observations at various lags. Inspection of the plots highlights no indication of temporal dependence in the series with correlations for lags of 1-10 observations falling within the 95% confidence bands for randomness.
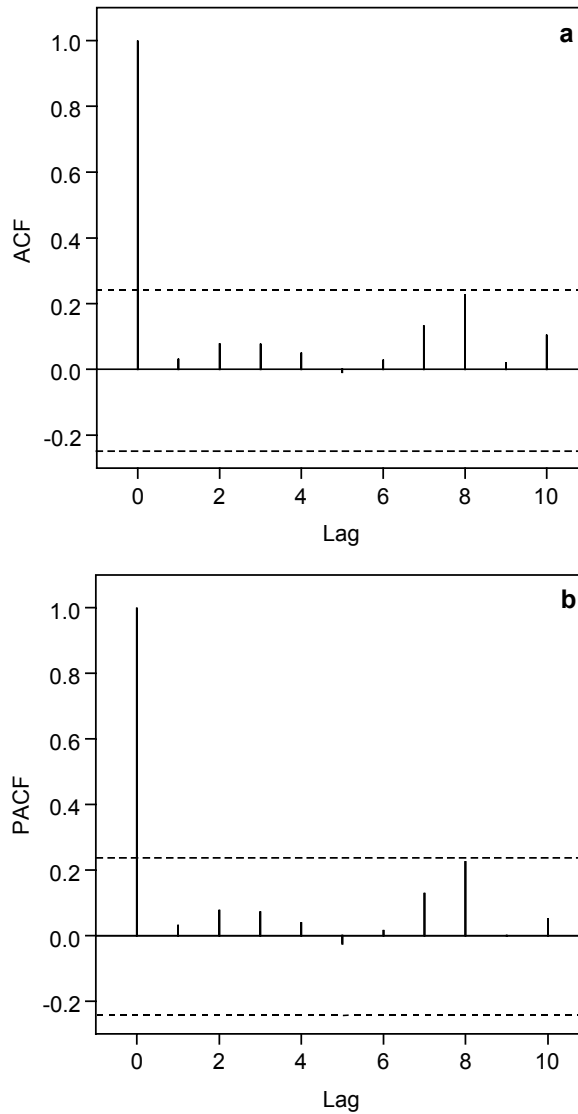
Figure 5.9 Serial correlation in storm intensities. (a) Autocorrelation function for seasonal intensities, and (b) partial autocorrelation function for the series. Both plots also show 95% confidence bands.

5.4.1 Time Trends

One common approach to modelling a trend in extremes is to allow the parameters of

the model to vary with time according to a specific parametric function. Both Coles

(2001) and Katz et al. (2002) give examples of fitting such trend functions to parameters of extreme value distributions. Here a linear trend in the log-transformed scale parameter (σ) of the GPD distribution for minimum central pressures is considered:

$$\ln(\sigma) = a_0 + a_1 t \ , \tag{5.8}$$

where t is an index for time. Estimating the parameters of this model by maximum likelihood leads to a log-likelihood of -295.9. The log-likelihood for the standard model without a trend (i.e. $a_1 = 0$) is -303.2. Comparison of the models is possible using the deviance statistic (D), defined by Coles (2001) as:

$$D = 2\{\ell_1(\theta|x) - \ell_0(\theta|x)\}, \tag{5.9}$$

where $\ell_0(\theta|x)$ and $\ell_1(\theta|x)$ are respectively the maximised log-likelihood of the standard model with no trend and the maximised log-likelihood of the model with a trend. This statistic is used to compare nested models to determine if there is strong evidence for favouring the more complex model structure. A large value of D would imply that the trend model explains significantly more variation in the data than a model in which parameters are fixed. Formally, the standard model $\ell_0(\theta|x)$ is rejected by a test at the α-level of significance if $D > C_\alpha$, where C_α is the $(1-\alpha)$ quantile of the χ^2 distribution (Coles 2001).

The value of D obtained by testing the linear trend model against the standard model is 14.6. The critical value of C_α for the test of significance is 3.84, which indicates strong evidence (p-value < 0.01) for a linear trend in extremes. The form of this particular trend indicates that storm intensities have decreased over time. Figure 5.10 shows the median of the fitted GPD with the trend in the scale parameter given by equation 5.8. This shows minimum landfall central pressures increasing from about 967 hPa to about 984 hPa over the period of record. The possibility of a quadratic trend in the scale parameter was investigated and also found to be significant (p-value < 0.01), although offered no real advantage over the linear trend model.

While there is statistical evidence to suggest that the trend is significant, it is apparent from Figure 5.10 that there is considerable scatter in the series. Ultimately there is no physical reason here to suppose that a linear trend will describe the underlying process well. Moreover, given both the relatively small number of sample exceedances available and the less reliable nature of the historical observations it is difficult to draw conclusions on the practical significance of the trend. It is likely though that the downward trend in storm intensities over time is not an artificial feature given that the largest three events occurred in the first portion of the series and have relatively accurate estimates of their intensities.

5.4.2 ENSO Effects

Chapter 4 showed that the El Niño Southern Oscillation (ENSO) has a dramatic effect on year-to-year landfall numbers in Queensland. These results are consistent

with previous studies demonstrating a significant relationship between ENSO and tropical cyclone activity in Australia (e.g. Nicholls et al. 1998) and in Queensland (e.g. Grant and Walsh 2001). The effect of ENSO on storm intensities has, however, not been quantified in previous studies.
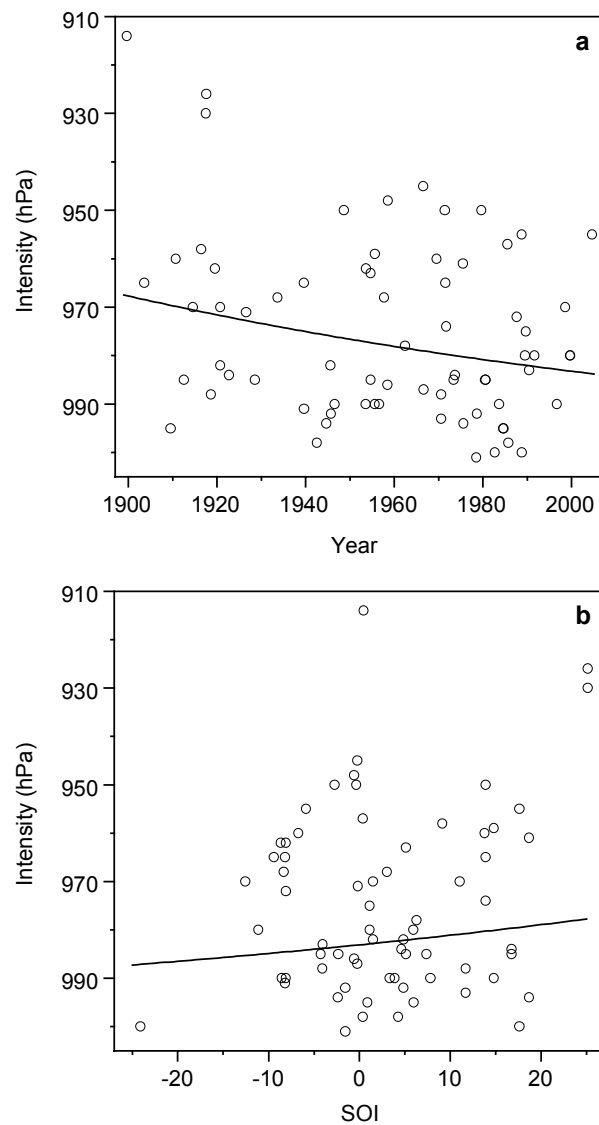
Figure 5.10 Estimate of median of the fitted GPD for storm intensities incorporating a linear trend in scale parameter for (a) time, and (b) the SOI.

In order to investigate the influence of ENSO on landfalling intensities the following model was considered:

$$\ln(\sigma) = b_0 + b_1 \, \text{SOI} \qquad\qquad (5.10)$$

where SOI is the Southern Oscillation Index averaged over the period August to November (Figure 4.3) for the season in which each event occurred. This amounts to replacing time (t) as a covariate term in equation 5.8 by an index of ENSO in the trend function for the log-transformed GPD scale parameter. Using the significance test described in the previous section, the value of the deviance statistic obtained for this model is 1.6 (p-value = 0.211), which indicates that a model without the SOI trend (i.e. b_1 = 0) is acceptable. Figure 5.10 shows the effect of the SOI on the median of the fitted GPD distribution, and indicates that any such effect is very weak.

5.5 Summary

There is a clear indication from the analysis presented in this chapter, as well as in the previous chapter, that there are advantages to considering historical information when investigating the frequency and intensity of Queensland landfalling tropical cyclones. The results show that combining historical and instrumental records leads to a greater level of certainty in describing the statistical properties of landfalling storms. The inclusion of historical observations of storm intensities through the Bayesian approach is also seen to result in markedly different predictions on the

frequency of extremes than would be expected from an analysis based solely on the instrumental record. This was subsequently confirmed with the application of a censoring-based methodology to incorporate major historical events. This difference appears to reflect predominantly the influence of the largest few events occurring prior to the beginning of satellite detection and monitoring techniques. The location of these events at the beginning of the time series is also suggestive of a significant downward (upward) trend in storm intensities (minimum central pressures) over time.

The results of the trend analysis indicated that ENSO appears not to have a significant effect on the intensity of landfalling tropical cyclones. It is likely that the slight tendency for more extreme events to occur under La Nina conditions (see Figure 5.10) simply reflects the influence of ENSO on tropical cyclone activity. This is consistent with Nicholls et al. (1998), who regarded the role of ENSO as important in dictating the broad environmental conditions leading to tropical cyclone genesis in the Australian region, but as having little or no influence on the intensity of a storm once developed.

It is important to note that the results obtained here apply to landfalls along the entire Queensland coast. Spatial variability in landfall event characteristics due to environmental conditions is likely to be an important factor. For instance, the northern-most latitudes of the Queensland coast appear less likely to experience a major landfall event due to the inherent polewards movement of tropical cyclones combined with few having origins within $5\text{-}10^0$ of the equator. Similarly, at subtropical latitudes a combination of lower sea surface temperatures and an

increasingly sheared environment means that most events crossing the coast here are naturally weaker than those crossing the tropical coast. It should also be noted that a tropical cyclone's central pressure does not alone necessarily provide a good indicator of potential impacts, with other factors such as the tropical cyclone's spatial scale and forward speed also being important (Callaghan and Smith 1998).

CHAPTER 6

A SIMULATION MODEL DERIVED FROM CORAL

SEA REGION TROPICAL CYCLONES

6.1 Introduction

Through the combination of historical and instrumental records a greater insight into the statistical properties of Queensland landfalling tropical cyclones has been gained. The intent of this chapter is to provide a basis for testing the representativeness of the regional Coral Sea record over the period 1960/61-2004/05 against this landfall climatology. This is approached through the development of a simulation scheme from the Coral Sea record that can be employed to generate a series of landfalling events and thus serve as a means to facilitate a comparison with the observed record.

By considering a wider geographical region for which to develop a climatology an attempt is made to overcome the limited amount of data directly available in the landfall record. This, however, comes at a cost of having to shorten the time period for analysis, because historical observations from the pre-satellite era are far less reliable over the entire Coral Sea region than for landfall events. For this reason it is essential to assess the representativeness of this shortened temporal record to ensure it provides a reasonable basis for simulating events. This chapter outlines details of a simulation model that was developed for this purpose. This analysis makes use of

only Coral Sea observations from the instrumental era covering the period 1960/61-2004/05.

The chapter begins with an overview of available data for Coral Sea tropical cyclones. The identification of trends and the effects of ENSO on tropical cyclone frequency and intensity are then addressed. Details of a simulation model for generating tropical cyclone tracks and central pressures from this record is then described. The simulation model described herein attempts to capture the observed spatial and temporal characteristics of Coral Sea events by combining a relatively simple model for simulating track paths with an extreme value model for minimum central pressures with parameters that depend on the simulated track.

6.2 Data

The analysis again utilises the best-track database of tropical cyclone observations in the Australian region. From this database all tropical cyclones originating in the Coral Sea region and reaching their maximum intensity while tracking west of 165^0E were extracted. Only events recorded during the instrumental period 1960/61-2004/05 were included in the model development. Furthermore, to be consistent with the analysis in previous chapters only tropical cyclones that reached a minimum central pressure of at least 990 hPa at some stage during their lifetime were retained. The data takes the form of locational fixes of the storm's track (longitude and latitude) at six-hourly intervals along with the corresponding central pressure. The dataset comprises 108 tropical cyclones with 37 landfalling events and 71

nonlandfalling events. The maximum number of tropical cyclones in a season was nine, with three seasons recording no events. Figure 6.1 shows the time series of storm counts and minimum central pressures for the sample period.
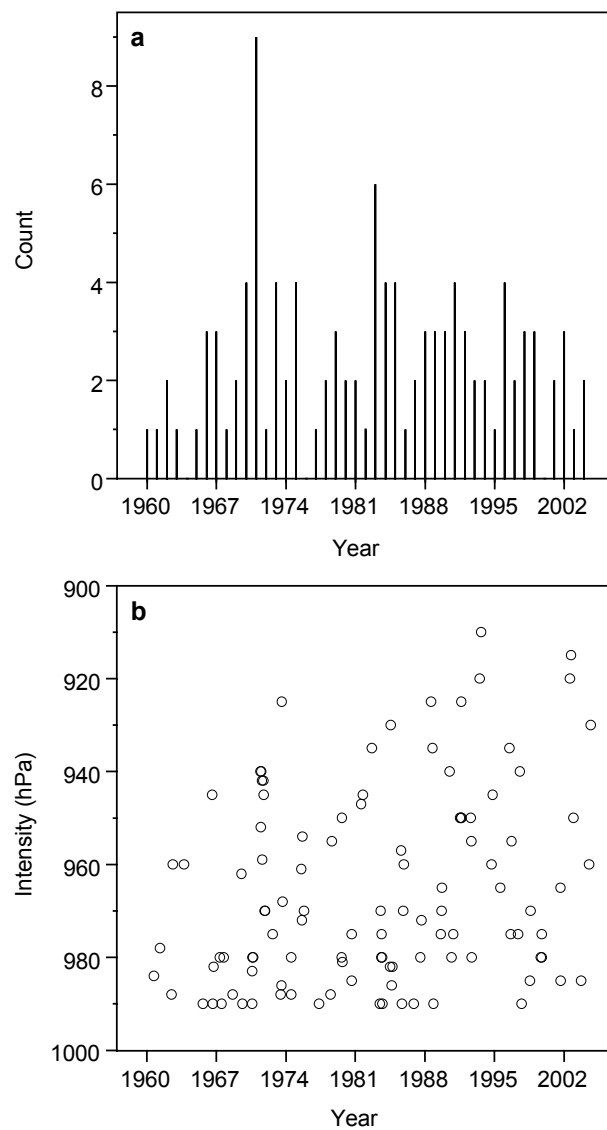
Figure 6.1 Time series of Coral Sea tropical cyclones over the period 1960/61-2004/05. (a) storm counts and, (b) minimum central pressures.

6.3 Trends and Climate

Before proceeding with the development of the regional simulation model, an investigation into trends and climate effects on the time series plotted in Figure 6.1 is firstly undertaken. This employs similar techniques used in Chapters 4 and 5 for the landfall record. Temporal dependence is firstly checked using autocorrelation plots. Linear and nonlinear time trends in the series are then investigated by fitting trend functions in the parameters of the adopted models for these variables. Lastly, the effect of ENSO on both seasonal activity and intensity is examined.

6.3.1 Counts

Over the 45 season instrumental era (1960/61-2004/05) a total of 108 regional tropical cyclone events were recorded, giving a mean rate of 2.4 events per season with a sample variance of 2.7. Application of the goodness-of-fit test for a Poisson process described in Chapter 4 indicated that the Poisson distribution was a suitable candidate for the series. Sample autocorrelation and partial autocorrelation plots for the series are graphed in Figure 6.2 against pointwise confidence limits for white noise. These demonstrate how much correlation is present between lagged observations with the confidence limits used to assess independence. Inspection of these plots indicates that storm counts are not serially correlated.

Under the assumption that counts follow a Poisson distribution, the possibility of a linear trend in the Poisson rate parameter over time, λ_t, was considered. The form of this model is given by equation 4.6 in which the mean rate is specified as a

function of time. The resulting fit obtained using the method of maximum likelihood is plotted in Figure 6.3.

Nonlinear trends were also investigated using the local likelihood estimation procedure described in Chapter 4. This is a semi-parametric regression technique for exploring any underlying trend in the process. This method basically supposes that the model parameters, in this case λ, can be approximated locally by fitting a low-order polynomial using data within the neighbourhood of each time point, t, with those values closest to t given greater weighting. Figure 6.3 plots the variation in the Poisson mean rate for nearest neighbourhood bandwidths of 0.25 and 0.40, which correspond to estimating λ_t at each time point in the series using 25% and 40% of the data respectively.

Inspection of Figure 6.3 suggests no evidence for a linear trend in the Poisson rate parameter. The plot shows a slight increase in the number of storms per year from 2.23 in 1960/61 to 2.58 at 2004/05, which based on a likelihood ratio test was not significant (p-value = 0.662). This implies tropical cyclone frequency has not substantially increased or decreased over time. The local likelihood fits plotted in Figure 6.3 show evidence of decadal variability with a peak in activity occurring during the early 1970s and again during the mid-1980s. The peak during the 1970s appears to be largely influenced by the active 1971/72 season in which nine tropical cyclones were recorded. Inactive periods are apparent during the 1960s and during the post-1995 period. During the 1960s the mean arrival rate was around 1.5 events per season, which is well below the mean arrival rate of 2.4 events per season for the entire series.
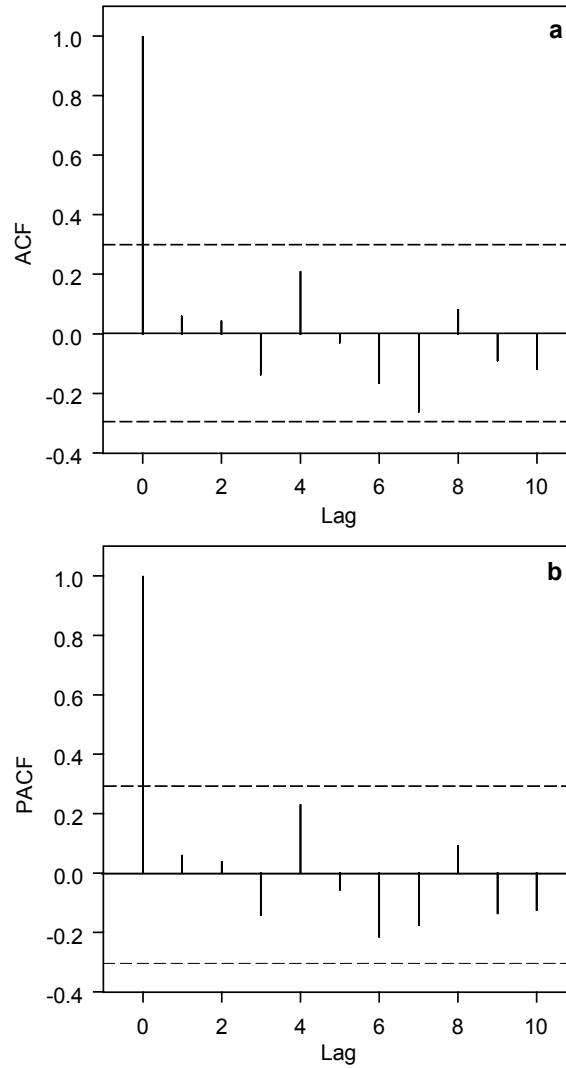
Figure 6.2 Serial correlation in Coral Sea storm counts. (a) Autocorrelation function (ACF) for seasonal counts, and (b) Partial autocorrelation function (PACF) for the series.

The effect of ENSO on Coral Sea activity was then examined by fitting a generalised linear model (GLM) of the form, $\ln(\lambda) = \beta_0 + \beta_1 \text{SOI}$, to seasonal counts. This model is similar to that presented in Chapter 4 for analysing the effect of ENSO on landfall counts. The index of ENSO is an average of the August-November monthly

values of the Southern Oscillation Index (SOI) as shown in Figure 4.3. Fitting of the

model is conducted using the method of maximum likelihood (McCullagh and

Nelder 1989) to estimate the parameter vector $\boldsymbol{\beta} = (\beta_0, \beta_1)$.
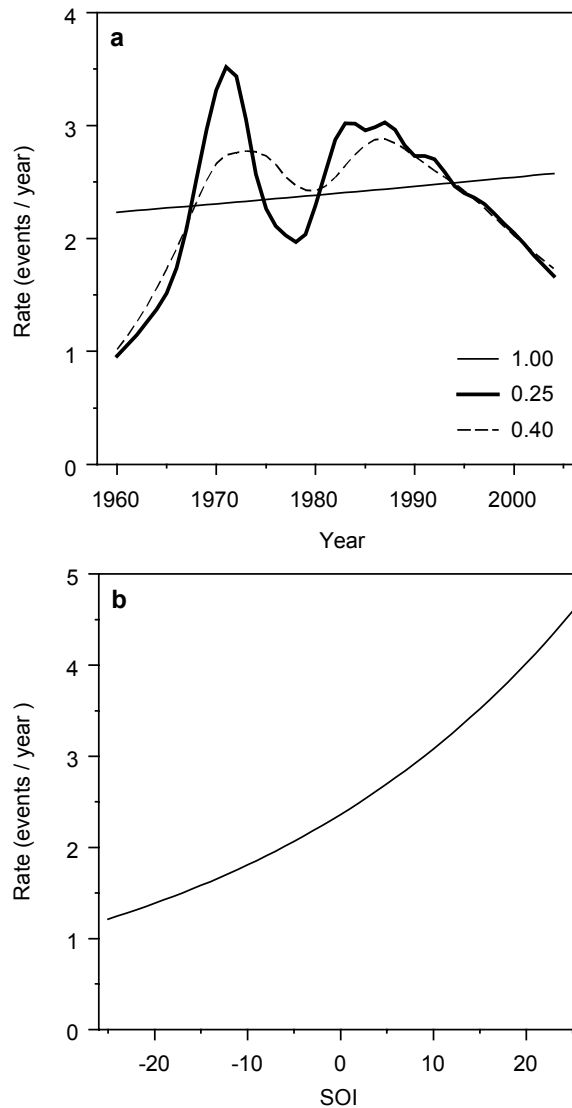
Figure 6.3 Variation in Poisson rate parameter for seasonal counts in the Coral Sea region. (a) temporal variability based on global linear fit and local likelihood fits, and (b) variation in relation to ENSO as measured by the SOI.

An analysis of deviance for this model shows that the SOI is a significant term in the model (p-value = 0.01), indicating that seasonal activity in the Coral Sea region is strongly influenced by ENSO. Figure 6.3 graphically illustrates how the Poisson rate parameter varies with the SOI. In particular, this demonstrates that during an extreme El Niño event (SOI = -20) the expected seasonal rate in the Coral Sea region is around 1.4 tropical cyclones per season, whilst during an extreme La Niña event (SOI = 20) the expected rate is about 4.0 events per season.

6.3.2 Intensities

Serial correlation in the time series of minimum central pressures was initially examined using autocorrelation plots similar to those presented in the previous section. These are graphed in Figure 6.4 against 95% confidence limits. Interestingly, these highlight a significant correlation for the lag-1 observation. Application of the Ljung–Box portmanteau test for independence (Ljung and Box 1978), further indicated that the lag-1 correlation was significant (p-value = 0.015). This suggests some evidence of dependence in the time series through the presence of clustering. A full understanding of this would require a more detailed investigation though, which is beyond the scope of the present study.

As described later in this chapter, the probability model adopted for the minimum central pressure of Coral Sea tropical cyclones is the Generalised Extreme Value (GEV) distribution. This model was introduced in Chapter 5 as an extreme value distribution for the maxima (or minima) of random variables. To test for a trend in minimum central pressures over time, the GEV distribution was fit to the observed

series allowing a linear trend for time in the GEV location parameter. This is similar to the approach used in Chapter 5 for assessing the significance of a trend in landfall intensities. This amounts to modeling variation over time in the time series by linearly relating the GEV location parameter to an index of time.
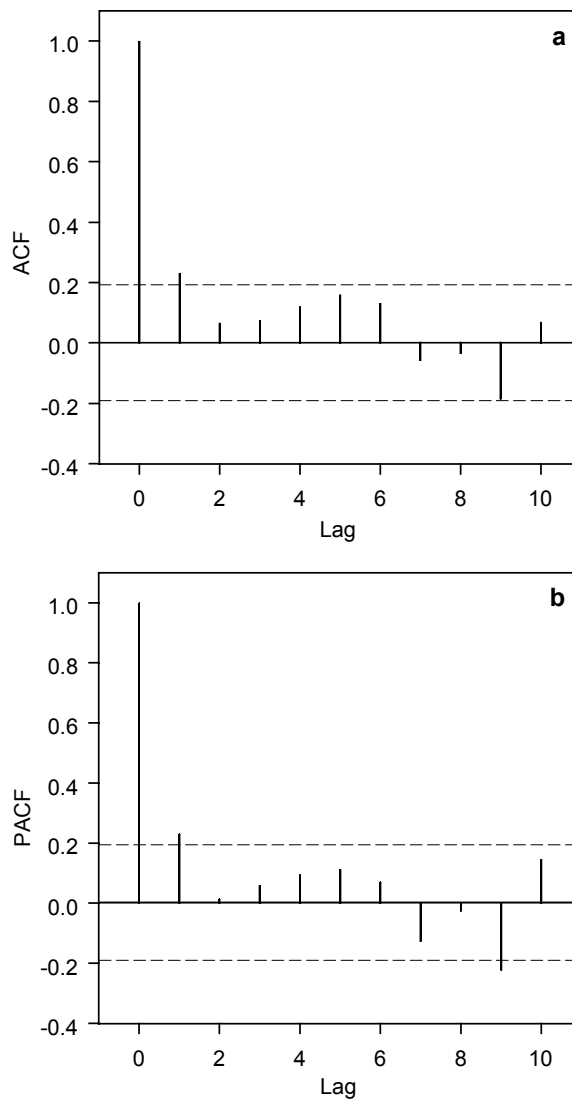
Figure 6.4   Serial correlation in Coral Sea storm intensities. (a) Autocorrelation function (ACF) for minimum central pressures, and (b) Partial autocorrelation function (PACF) for the series.
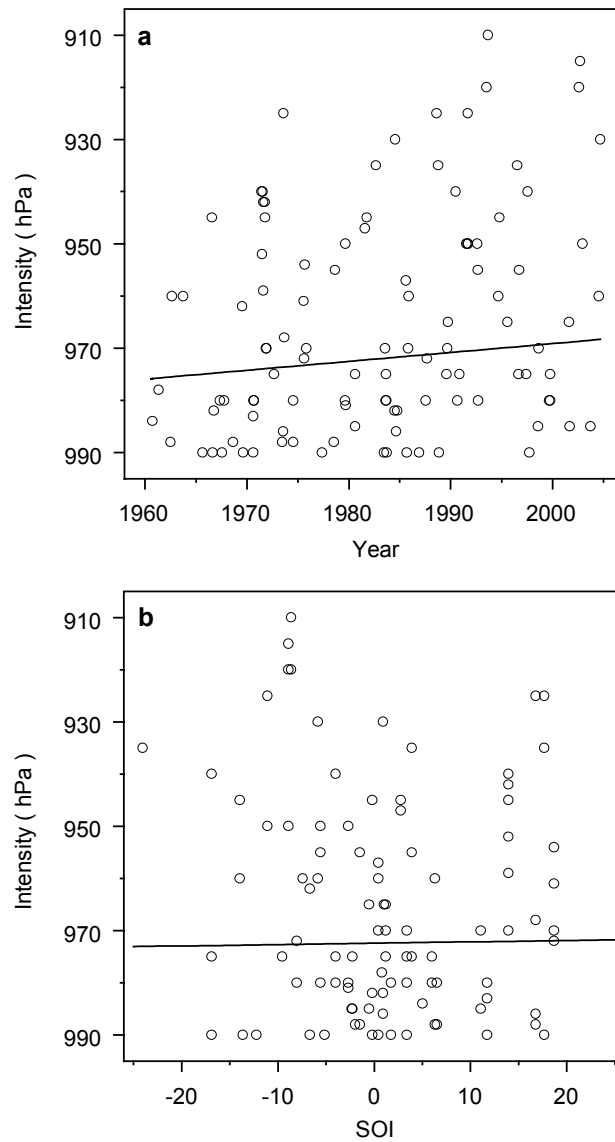
Figure 6.5 Estimate of median of the fitted GEV distribution for storm intensities incorporating a linear trend in location parameter for (a) time, and (b) the SOI.

Fitting of this model is undertaken using the method of maximum likelihood (see e.g. Coles 2001; Katz et al. 2002). The results are shown graphically in Figure 6.5 where the median of the GEV distribution is plotted against time. An assessment of the

significance of this time-dependent model using the likelihood ratio test described in Chapter 5 (equation 5.9), indicates that the trend is borderline significant (p-value = 0.073). The form of the trend highlights that minimum central pressures have apparently decreased over time, and thus storms have become more intense over the period of record. Specifically, median central pressures are seen to have increased from about 976 hPa at the beginning of the time series to 968 hPa at the end of the series.

The effect of ENSO on Coral Sea tropical cyclone intensities was investigated using a similar methodology. This involved fitting the GEV distribution with the location parameter linearly related to an index of ENSO (the SOI) instead of an index for time. The trend in the median of the fitted distribution is also plotted in Figure 6.5. The results of a likelihood ratio test indicate no dependence of storm intensity on the SOI (p-value = 0.842). For an SOI value of –20 (strong El Niño event) the median central pressure under this model is 972.9 hPa, while for an SOI value of 20 (strong La Niña event) the median value is 971.9 hPa. Hence, it can be assessed that ENSO has no significant effect on the intensity of tropical cyclones in the region.

6.4 Simulation Scheme

In this section the development of a model for simulating a landfall series of storm events from the Coral Sea regional dataset is outlined. As discussed in Chapter 3 there are several models described in the literature that make use of basin-wide data for similar purposes. One example is the approach of James and Mason (2005),

which aims to generate Coral Sea storm events on the basis of autoregressive models for storm tracks and intensities. This appears to be the only previous attempt to develop a basin-wide simulation model for the Coral Sea region.

The model employed here broadly follows the approach developed by Casson and Coles (2000) for simulating hurricanes in the North Atlantic region. The advantages of the Casson and Coles (2000) approach are twofold. First, it limits the number of assumptions made about the underlying process by making use of empirical relationships, derived from the observed sample, where practical. Second, it employs an extreme value modelling approach to simulate storm intensities, which provides a rational basis for quantifying the likelihood with which major events occur. The model described herein consists of two components, one governing the simulation of tropical cyclone tracks and another specifying the intensity of the simulated event.

6.4.1 Track Generation

Tropical cyclone motion is a complex process that depends on the storm's interaction with the surrounding environment in which it is embedded as well as various internal dynamics. Figure 6.6 shows the sample of Coral Sea tropical cyclone tracks from the period 1960/61-2004/05. As mentioned in Chapter 2, tropical cyclone motion in this region can be best summarised as erratic in nature. In the case of landfalling systems the general pattern is for storms to form north of about 15^0S and track southwestwards towards the Queensland coast. Overall, however, there is a strong tendency for many storms to follow an easterly trajectory, which directs their path

111

away from the coast. There is also a trend for some tropical cyclones to form relatively close to the coast and initially track offshore in an eastwards direction.
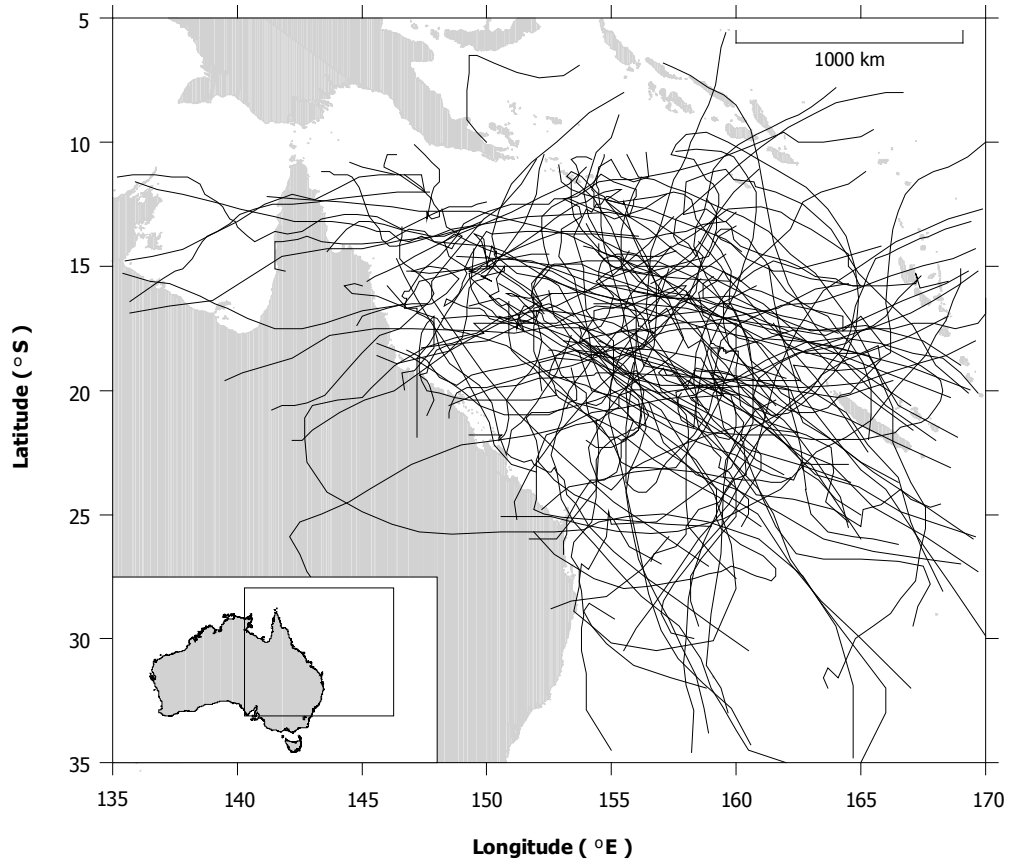
Figure 6.6 Coral Sea tropical cyclone tracks from the period 1960/61-2004/05.

Due to the highly variable and complex pattern of observed tropical cyclone tracks it is considered more appropriate to adopt a largely empirical approach to simulating track events. The strategy employed here follows that of Casson and Coles (2000) in

utilising the tracks of existing storms as a means to simulate new events. This involved randomly selecting an existing track from the 108 events recorded in the Coral Sea region over the period 1960/61-2004/05. These tracks, $\{(x_t, y_t): t = 1,...,T\}$, comprise a series of longitude (x_t) and latitude (y_t) fixes of the system's centre at time intervals ($t = 1,...,T$), typically six-hourly, over the lifetime of the event T.

Given the random selection of a track event, the process of generating new tracks involved simply applying a random shift uniformly to each fix (x_t, y_t) along the entire track ($t = 1,...,T$). Following Casson and Coles (2000) a normal distribution with a mean of zero and standard deviation σ is adopted to define the shift component. A value of σ equal to 1^0 (latitude and longitude) was initially selected on the basis that this represents a sufficiently small enough value for simulating tracks that are physically consistent with those observed historically (i.e. similar in terms of forward speeds and directional bearing), whilst large enough to allow for the simulation of the full spatial array of possible track events. This track generation process naturally defines the landfall point (or the closest point of approach to the coast for a nonlandfalling event), the track's directional bearing, as well as its forward speed.

In order to provide some verification for the adopted value for σ of 1^0, a comparison of observed track characteristics of landfalling storms over the period 1960/61-2004/05 with a simulated series of landfall tracks was undertaken. Figure 6.7 shows histograms of the forward speed and approach direction of the observed sample of landfalling tracks. These values were defined over the 12-hour period up to landfall.

113

These are plotted alongside histograms of the forward speed and approach direction of a 1,000 simulated events series obtained using the track generation procedure. The plots show relatively good agreement between observed and modelled track characteristics suggesting the value for σ of 1^0 is producing tracks that are reasonably consistent with the observed sample.
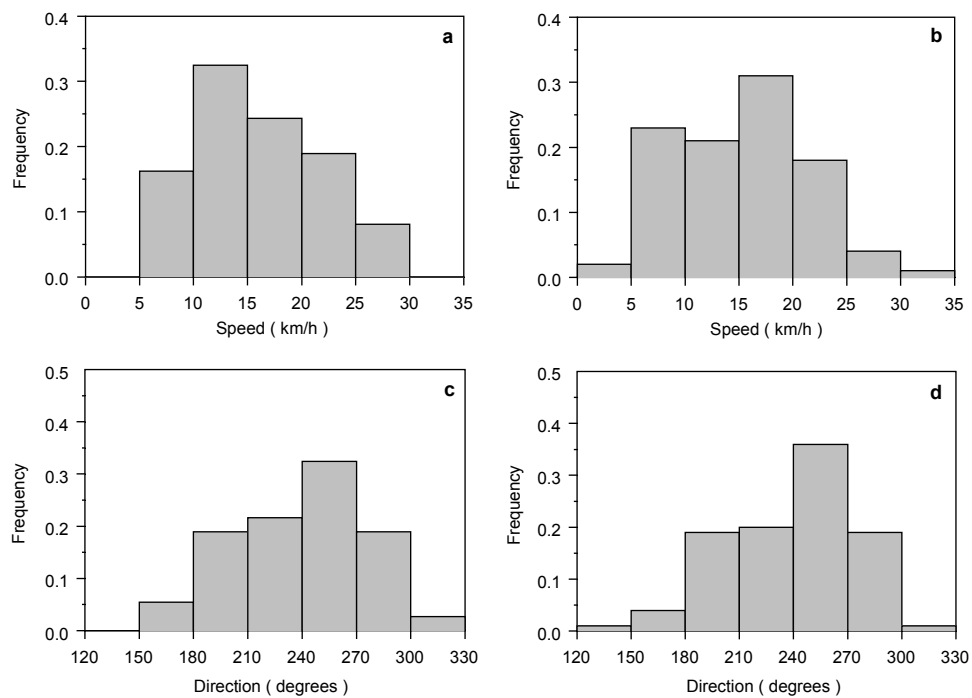
Figure 6.7 Histograms comparing observed landfall tropical cyclone tracks against simulated tracks. (a) Observed forward speed, (b) simulated forward speeds, (c) observed approach direction, and (d) simulated approach direction.

The process of track generation thus involved a random selection of an individual storm track from the 108 events recorded in the Coral Sea region. Each event was

assumed to have equal probability of occurrence and was therefore selected with probability 1/108. A new track event was then generated by randomly selecting a shift distance from a normal distribution with mean of zero and standard deviation of 1^0. This shift distance is then added to each fix along the original storm's track $\{(x_t, y_t): t = 1,...,T\}$ to define the new track event.

6.4.2 Simulated Intensities

The second part of the simulation scheme involved developing a strategy for generating the intensity of an event conditional on its simulated track. First, a model for simulating the minimum central pressure attained during the event is outlined. Second, the timing of the pressure minimum for simulated landfalling storms is modelled.

6.4.2.1 Pressure Minimum

Following Casson and Coles (2000) minimum central pressures are modelled using a Generalized Extreme Value (GEV) distribution. As shown in Chapter 5 this model has the distribution function:

$$F(x \mid \xi, \sigma, \kappa) = \exp\left\{-\left[1 + \kappa\left(\frac{x - \xi}{\sigma}\right)\right]^{-1/\kappa}\right\}, \tag{6.1}$$

where ξ, σ and κ are location, scale and shape parameters respectively. This distribution has support as a model for extremes on the basis of asymptotic argument. Fitting the GEV distribution given in equation 6.1 to sample minima requires a

115

transformation of the observed values to negatives. Casson and Coles (2000) considered separate models for landfalling and nonlandfalling events in fitting equation 6.1 to minimum central pressures for North Atlantic hurricanes. For this study, however, the sample is not of sufficient size to enable such a separation. Hence, the model is fit here to the combined record of landfalling and nonlandfalling events.

Figure 6.8 shows scatter plots of the minimum central pressure for each event against the longitude (x_t) and latitude (y_t) at which the minimum is reached. Also shown is a plot of the minimum central pressure versus the time to which the minimum is reached (t_p). Two main features stand out from these plots. First, there is an evident association between peak storm intensity and time taken to reach that peak, which indicates that more intense tropical cyclones generally take longer to reach their peak intensity. The second aspect likely to be of importance is the tendency for minimum central pressures to cluster between latitudes of about 12^0S and 23^0S. There is no apparent relationship between minimum central pressure and longitude of the pressure minimum.

The trend for few storms to reach peak intensity north of about 12^0S is likely to be a consequence of track behaviour. In general, few tropical cyclones are observed to form within 5^0 latitude of the equator and many initially follow polewards tracks (Emanuel 2003). Hence, by the time maximum intensity is reached few tropical cyclone tracks are observed at low latitudes. The scarcity of storms reaching peak intensity at latitudes south of 23^0S is likely to be a consequence of environmental conditions such as SSTs limiting tropical cyclone intensification in the southerly

116

region. It is well recognized that there exists an upper bound on tropical cyclone intensity, referred to as the maximum potential intensity (MPI), for the available energy in the ocean and atmosphere (Henderson-Sellers et al. 1998). Harper et al. (2001, Figure 3.6, p. 22) presents an MPI curve for the Queensland region showing latitudinal variations in MPI. This curve shows the MPI being constant at 895 hPa for latitudes north of about 21^{0}S. South of this latitude the MPI rises relatively sharply reaching a value of 940 hPa at about 27^{0}S.
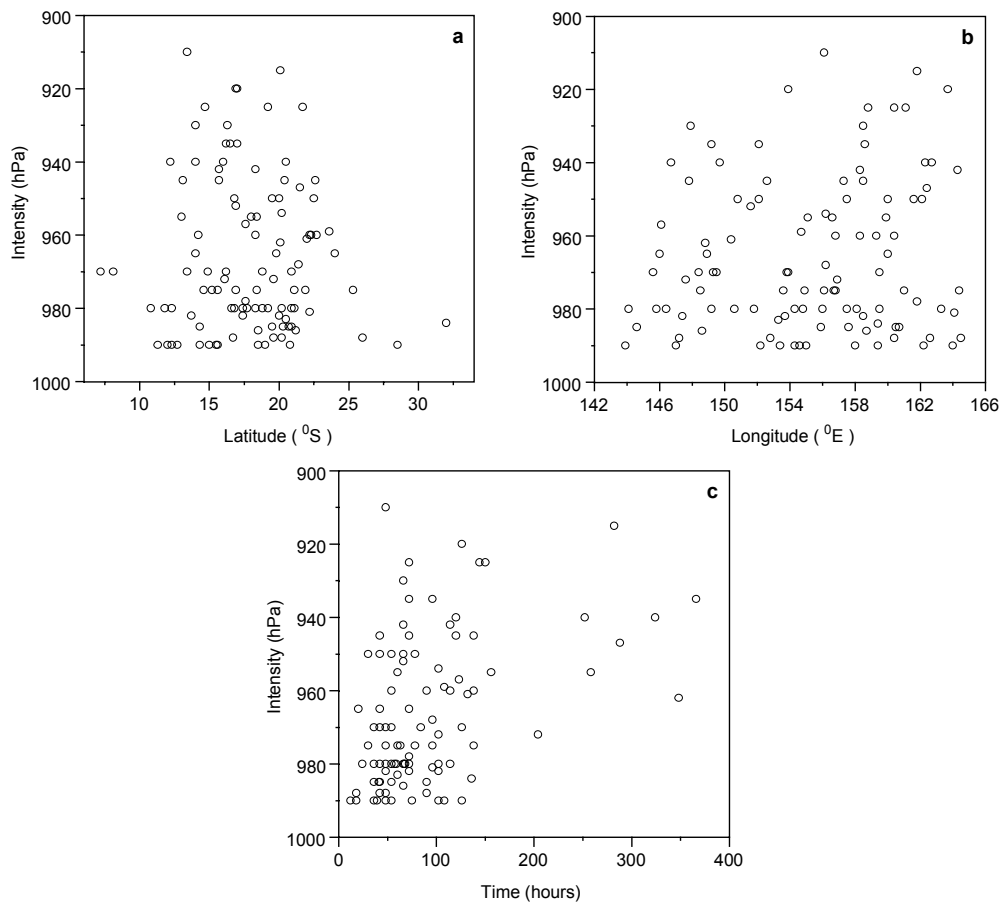
Figure 6.8 Spatial and temporal characteristics of minimum central pressures. (a) latitude, (b) longitude, and (c) time taken to reach peak intensity.

In order to account for the patterns observed in Figure 6.8 several models linearly

relating the GEV location parameter (ξ) to longitude (x_t), latitude (y_t) and time to

peak intensity (t_p) were considered. Given the size of the available sample, models

incorporating trends in the scale (σ) and shape (κ) parameters of the GEV

distribution were not considered due to an expected difficulty in estimating these

parameters with precision. The results of this analysis are summarised in Table 6.1

where the significance of each term's inclusion is assessed using a likelihood ratio

test (equation 5.9). In this case each model is tested against a base model where the

GEV location parameter is fixed (ξ_0). Of the models considered, only that

incorporating a linear trend in the GEV location parameter for time to peak intensity

(t_p) was found to be significant. Models incorporating linear specifications for

longitude and latitude were not found to explain significantly more of the variability

in the data than the base model with fixed-value parameters.

Table 6.1   Summary of models for minimum central pressures with covariates in
GEV location parameter (ξ) for longitude (x_t), latitude (y_t), and time to
peak intensity (t_p).

Base Model	Extended Model	*p*-value
$\xi = \xi_0$	$\xi = \beta_0 + \beta_1\ (x_t)$	0.939
$\xi = \xi_0$	$\xi = \beta_0 + \beta_1\ (y_t)$	0.879
$\xi = \xi_0$	$\xi = \beta_0 + \beta_1\ (t_p)$	<0.001
$\xi = \beta_0 + \beta_1 (t_p)$	$\xi = \beta_0 + \beta_1\ (t_p) + \beta_2 (y_t) + \beta_3 (y_t^2)$	0.217

Also shown in Table 6.1 are the results of a significance test for a model incorporating a quadratic term for latitude in the location parameter (y_t). This model is tested against a base model that includes the dependence on t_p. A likelihood ratio test indicated this offered no clear advantage over the model incorporating only the specification for time (*p*-value = 0.217). However, while statistical evidence for keeping the latitudinal dependence was not definitive, it was decided to retain this specification because it provides some way of limiting the intensity reached by events in the southerly regions.

Figure 6.9 shows trends in the median of the fitted GEV distribution incorporating the dependence of maximum intensities on time and latitude. The inclusion of time is seen to be quite strong with minimum central pressures lower for storms taking longer to reach maximum intensity. The specification incorporating a dependence on latitude is seen to have a less pronounced effect on the median curve, although it does impose a tendency for the distribution of minimum central pressures to be higher at the southern-most latitudes.

Given the range of specifications incorporated into the model for minimum central pressures it is necessary to assess the model's performance in representing the observed process. In Chapter 5 the application of probability and quantile plots were discussed as useful diagnostic techniques for evaluating the goodness-of-fit for an extreme value model of landfalling storm intensities. Because the fitted model here is non-standard, in that it incorporates covariates for time and space, model parameters are not fixed but vary according to the value of these covariates.
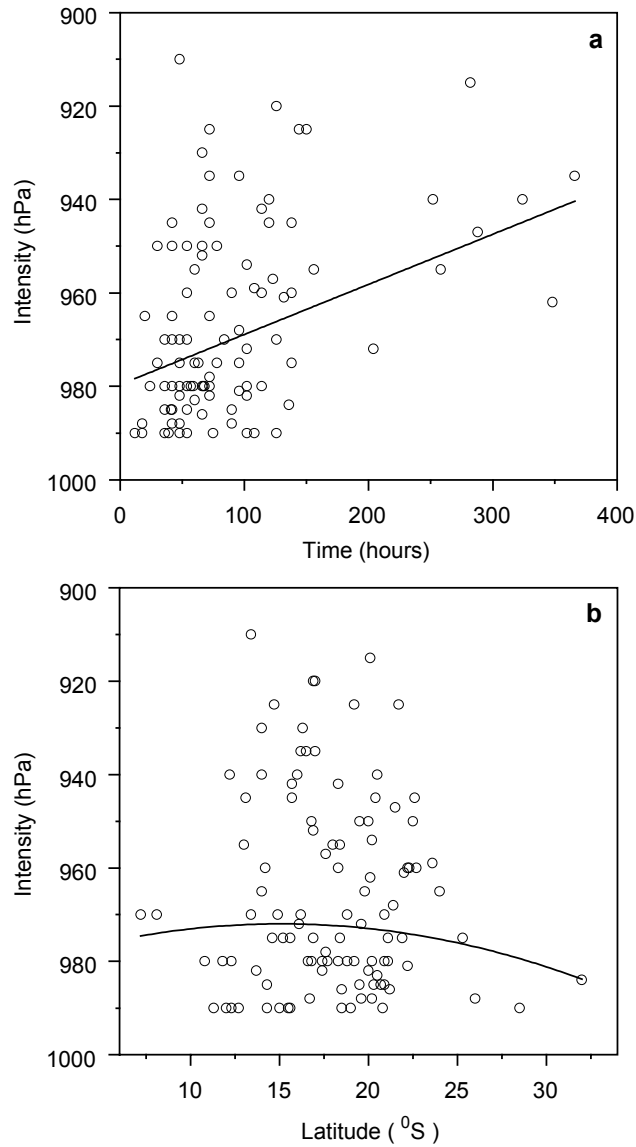
Figure 6.9   Trend in median of fitted GEV distribution incorporating covariates in location parameter for (a) time to peak intensity, and (b) latitude of peak intensity.

According to Coles (2001) in such cases a modification to the observed series is necessary to enable the use of such diagnostic checks. For data following a GEV distribution, this involves a transformation to the standardised variable:

$$z* = \frac{1}{\kappa *} \ln \left\{ 1 + \kappa * \left(\frac{x - \xi *}{\sigma *} \right) \right\} \tag{6.2}$$

which is identically distributed and follows a standard Gumbel distribution. In this formulation, $\xi*$, $\sigma*$ and $\kappa*$ denote GEV parameters that are functions of covariates. In the present case only the location parameter $\xi*$ was modelled with covariates (t_p and y_t), so $\sigma*$ and $\kappa*$ would be replaced by σ and κ in equation 6.2. Denoting the ordered values of $z*$ by $z^*_{(1)}, ..., z^*_{(m)}$, the probability and quantile plots of the transformed variables then respectively consists of the pairs (Coles 2001);

$$\left. \begin{array}{l} i/(m+1) \, , \, \exp(-\exp(-z^*_{(i)})) \\ \\ z^*_{(i)} \, , \, -\ln(-\ln(i/(m+1))) \end{array} \right\} \quad \text{for } i = 1, ..., m. \tag{6.3}$$

Figure 6.10 shows the resulting residual probability and quantile plots for the fitted GEV distribution. These highlight no immediate cause for concern with linearity of the plots suggesting the model is performing reasonably well for most of the data range. From examination of the quantile plot though, there is some evidence to suggest the model is overpredicting the most extreme events. The parameter estimate for the GEV shape parameter here is positive ($\hat{\kappa} = 0.156$), which is indicative of a distribution with an unbounded upper tail. This may partly explain the discrepancy of modelled and observed values at the upper-most portion of the quantile plot in Figure 6.10. A likelihood ratio test of this model against a base model in which $\kappa = 0$ (i.e. a reduction to a Gumbel form) gave a p-value of 0.048, indicating that the current model in which $\kappa \neq 0$ probably represents the preferred option.
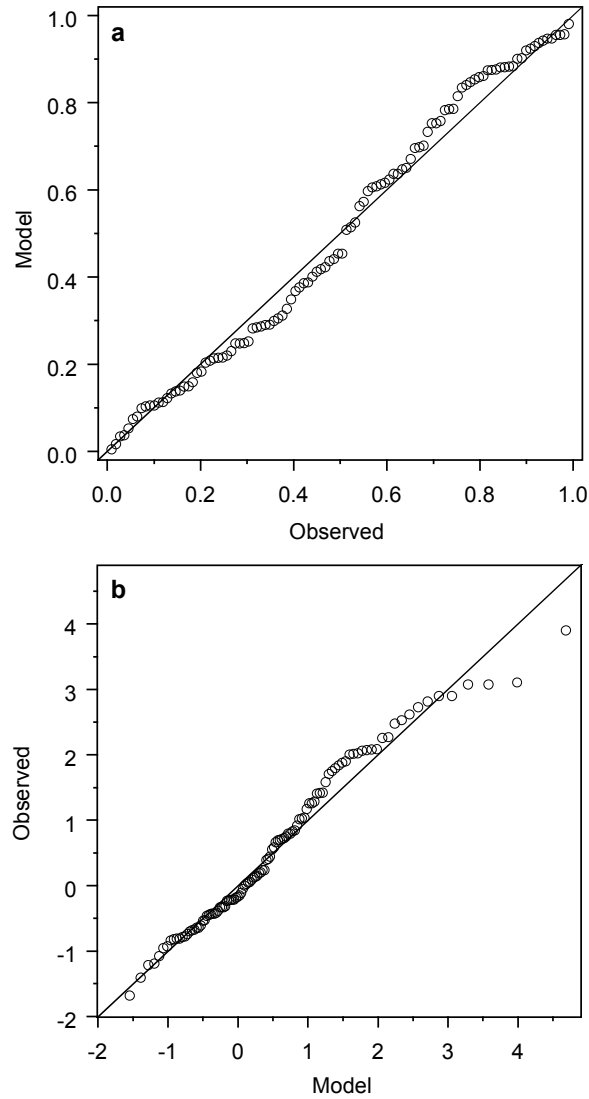
Figure 6.10 Model diagnostics for GEV distribution fit to minimum central pressures with covariates in the location parameter. (a) probability plot, and (b) quantile plot.

6.4.2.2 Timing of Pressure Minimum

Having derived a model for minimum central pressures that incorporates specifications for latitude and time, it is necessary to model the point where the

122

minimum occurs on the simulated track $\{(x_t, y_t): t = 1,\dots,T\}$. As the ultimate aim

is only in simulating landfall events, the modelling strategy used here is restricted to

defining this point for such events. The adopted approach again broadly follows that

developed by Casson and Coles (2000). Of the 37 landfalling tropical cyclones in

the dataset 12 storms attained their minimum central pressure exactly at landfall.

The remaining 25 tropical cyclones reached peak intensity at some stage prior to

landfall. For these 25 events, Figure 6.11 shows a density estimate of the ratio of

time to landfall (t_{lf}) against the time to minimum central pressure (t_p). The density

estimate is a smoothed approximation, obtained by applying a kernel density

estimation procedure using a standard normal kernel function with the Gaussian

reference bandwidth of Silverman (1986).
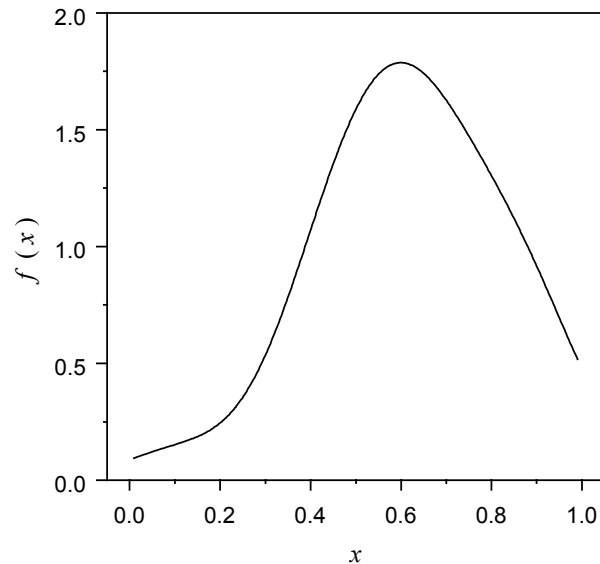
Figure 6.11 Empirical density estimate of t_{lf} / t_p; the proportion of time to landfall spent before Coral Sea landfalling tropical cyclones (1960/61-2004/05) reached their minimum central pressure.

The process of deriving the time point along the simulated track where the pressure minimum occurs is as follows. Given a simulated landfall track, the probability that the minimum central pressure is reached at landfall is taken to equal 12/37 (0.324). This represents an empirical estimate of the probability that Coral Sea landfalling tropical cyclones reach peak intensity at landfall. For these storms this completes their simulation by specifying both the time and location of the event's landfall intensity.

For events randomly sampled with a probability of 25/37 (0.676; the empirical probability that Coral Sea tropical cyclones reach peak intensity prior to landfall), a random selection from the empirical density shown in Figure 6.11 is used to obtain the point on the simulated track where the minimum occurs. The density in Figure 6.11 plots the proportion of time to landfall spent before a storm reaches its minimum central pressure (t_{lf} / t_p). Hence, by calculating the time to which a simulated storm track makes landfall (t_{lf}), combined with a randomly selected value of t_{lf} / t_p, allows the point on the simulated track where the pressure minimum is reached to be defined.

For these storms that do not reach peak intensity at landfall it is necessary to incorporate an additional step to complete the simulation of their landfall intensity. Specifically, this involved the modelling of a pressure series from t_p to t_{lf}. To accomplish this an empirical strategy is again preferred. This firstly involved a random selection from the 25 events that reached peak intensity prior to landfall to obtain a pressure series from t_p to t_{lf}, $\{ p_t : t = t_p, ..., t_{lf} \}$. This series serves as a template governing the rate of pressure change from the point at which the minimum

central pressure is attained to the point of landfall. The pressure series template $\{p_t : t = t_p, ..., t_{lf}\}$ is then simply transferred to the simulated event as a basis for defining its corresponding pressure series from peak intensity to landfall. In doing so it is necessary to rescale in time the randomly selected pressure series so that it matches that of the simulated event. This is because the time scale of the randomly selected series $(t = t_p, ..., t_{lf})$ is not necessarily equivalent to that of the simulated pressure series.

6.5 Summary

This chapter constituted an analysis of tropical cyclone events in the Coral Sea region, largely for the purposes of developing a simulation model capable of generating landfall events. A preliminary investigation into the presence of trends in the time series of Coral Sea storm counts showed no evidence of either an increase or decrease in activity over the period 1960/61-2004/05. There is, however, some suggestion of decadal variability in storm activity over this period, particularly given that an inactive period during the 1960s was followed by an active period during the 1970s. As with landfalling counts, ENSO plays a significant role in varying Coral Sea storm activity from season to season.

An examination of the time series of minimum central pressures reveals some evidence of temporal dependence as well as an upward trend in storm intensities over the period 1960/61-2004/05. Under the adopted probability distribution for this variable, median minimum central pressures were found to decrease over the period

of record, suggesting storms have generally become more intense. However, it should be noted that this apparent trend is only of borderline significance. There is no evident effect of ENSO on the minimum central pressures attained by Coral Sea tropical cyclones.

The simulation scheme developed in this chapter from the regional Coral Sea record can be summarised as follows:

1. A random selection from the observed tropical cyclone tracks in the region, followed by a random shift applied uniformly to each fix along its path $\{(x_t, y_t): t = 1,...,T\}$ to generate a new track event. Of the generated track events, only those that make landfall are retained.

2. Conditional on the landfalling storm's simulated track, the time (and thus location) of the pressure minima is identified using the empirical probabilities of the time to which peak intensity (t_p) and landfall (t_{lf}) occur.

3. A random selection of the minimum central pressure is obtained for each simulated event from a GEV distribution. Time (t_p) and latitude of the pressure minima (y_t) (defined by step 2) are used as inputs at each random selection, with the location parameter of the GEV distribution varying according to these values.

4. For storms not reaching maximum intensity at landfall, a random selection of a pressure series template from the observed landfall events (not including

those attaining minimum central pressure at landfall) is made. This is subsequently rescaled and used to derive a pressures series from the time of peak intensity to landfall $\{ p_t : t = t_p ,..., t_{lf} \}$.

The application of the simulation model presented in this chapter to the generation of a series of landfall events is addressed in Chapter 8. This includes a comparison against results obtained in Chapters 4 and 5 from the observed record of landfall tropical cyclones. Prior to this, a review of another major source of information on tropical cyclones in the Queensland region, the prehistorical record, is presented in the following chapter.

CHAPTER 7

GEOLOGICAL RECORDS OF PAST STORM

ACTIVITY

7.1 Introduction

The role of tropical cyclones as important agents in modifying coastal and reef environments is well established (e.g. Hopley 1974; Scoffin 1993). Furthermore, in certain settings distinct geological traces of these storms are preserved, which can allow for inferences on the nature of these events. Sedimentary deposits of particular relevance to the study of past tropical cyclones take the form of wave deposited features including washover fans and storm ridges. At several locations along the Queensland coast the presence of coral shingle ridges has been inferred to be a product of elevated water levels associated with severe tropical cyclones (Nott and Hayne 2001). At a number of these sites, ridge sequences have gradually prograded over the late Holocene (i.e. approximately the last 5,000 years), thus documenting the passage of multiple depositional events.

In this chapter methods to extract a long-term history of storm events from this record are assessed. The chapter initially reviews some recent developments in the study of past tropical cyclones from geological records. Then follows a description of several sites in the Queensland region where such evidence, namely in the form of

storm ridge deposits, has been documented. A brief introduction to the methodology for reconstructing palaeostorm intensity from storm ridge features is subsequently provided. An evaluation of the robustness of this methodology is then undertaken. The chapter ends with a discussion on the merits and limitations of this prehistoric record.

7.2 Palaeotempestology

An emerging field of research, recently termed palaeotempestology (Liu and Fearn 2000; Nott 2004), whereby past unobserved storm events are reconstructed on the basis of evidence preserved in the geological record, has offered a means to gain an insight into the long-term behaviour of tropical cyclones. A variety of sedimentary and erosional forms have archived this unique record within the coastal landscape. To date though, few studies have offered a reliable means to estimate the magnitude of depositional storms. Some success has, however, been recently reported with reconstructions based on overwash deposits found in coastal lake sediments of the United States (e.g. Liu and Fearn 1993) and storm ridges located in the Great Barrier Reef (GBR) region of Queensland (e.g. Nott and Hayne 2001).

7.2.1 Overwash Deposits

Overwash deposition occurs when the height of tropical cyclone forced water levels overtops a shoreward sand barrier. The wave activity erodes and transports coarse sand from the barrier and deposits it in adjacent inland areas in the form of a

washover fan (Liu and Fearn 1993; 2000). Common depositional sites, where sand layers can be preserved, are across sheltered coastal lakes as well as back barrier marshes. These layers are often interbedded with muddy, organic or fine-grained sediments that normally accumulate in these environments. Assuming the geomorphic setting at a particular site to remain relatively stable, Liu and Fearn (1993) first hypothesised that the lateral extent and thickness of an overwash layer is a proxy for the intensity of the depositional hurricane. Thus, individual events can potentially be reconstructed on the basis that storms of greater magnitude are likely to deposit more extensive sand layers at a particular site.

Several recent studies have compiled a history of major United States hurricanes by examining the stratigraphy and chronology of these sand layers. Liu and Fearn (1993; 2000) sampled overwash layers in non-tidal coastal lakes of Alabama and Florida. Donnelly et al. (2001a; 2001b) identified sand layers from cores in the backbarrier marshes of New England and New Jersey. More recently, Scott et al. (2003) used offshore foraminifera as a tracer for overwash deposits when examining marsh sediments along the South Carolina coast.

In each of these studies the magnitude of depositional events was estimated by a comparison to recent storms that also deposited layers in the sampled area. For instance, Liu and Fearn (2000) utilised the sedimentary layer of Hurricane *Opal* as a base event to reconstruct a history of major hurricane landfalls in northwest Florida from sediment cores taken in Western Lake. Deposited layers corresponding to prehistoric events were inferred to be from storms of greater severity than *Opal*, a

category 3 system at landfall, on the basis of their layers exhibiting greater spatial extent and thickness.

Nott (2004) recently raised some concerns regarding the veracity of extending this approach over long time periods. These concerns were based on the absence of a detailed chronostratigraphy of the overwashed barriers to establish that their height and position had remained relatively stable over time. Nott (2004) cited field evidence of several major tropical cyclones impacting the Western Australian coast in recent years where overtopping of coastal dunes had resulted in their complete removal. Consequently, it can be inferred that any significant erosion to barrier dunes during a storm event would increase the vulnerability of the site to overwash deposition by subsequent storms of lesser intensity. Furthermore, the susceptibility of a site to overwash deposition can also be influenced by the formation of tidal inlets in the barrier dunes, which would also promote the transportation of sediment during events of lesser intensity.

Liu and Fearn (2000) argued that the similarity of long-term washover records reconstructed from multiple sites, located some distance apart and fronted by different barrier dune systems, demonstrates that inferences on major United States hurricane activity made from these sites are legitimate. However, lacking knowledge of both the temporal and structural changes associated with erosion and rebuilding phases of the regularly overwashed barrier dunes, the credibility of this approach has yet to be fully shown.

7.2.2 Storm Ridge Deposits

Storm ridges form when tropical cyclone wind-waves superimposed on the storm tide entrain and transport coarse marine sediment onshore and deposit it, as a ridge, at sites beyond the range of regular wave and tidal action (Hayne and Chappell 2001; Nott and Hayne 2001; Nott 2004). Along the east Queensland coast such features are preferentially located on the inner continental shelf at island sites in the Great Barrier Reef (GBR). Shore-parallel sequences of these ridges often form when new ridges are emplaced on the shoreward side of older deposits. As a result, where a sequence of ridges occurs at a particular location the ages of individual ridges are often found to progressively increase inland (Hayne 1997; Nott and Hayne 2001). In many cases individual ridges represent a distinct unit, although it is possible for two or more deposits to be reworked into a composite unit. In this case a careful examination of the stratigraphy of each unit combined with radiocarbon dating of multiple samples is necessary to identify whether a particular ridge can be assigned to a single depositional event (Hayne 1997).

The storm ridge sequences identified in this region have not been observed to form under normal meteorological conditions, but are episodically emplaced by high wave action associated with tropical cyclones. This is supported by contemporary observations of ridge development during tropical cyclone events in other regions (e.g. Maragos et al. 1973; Bayliss-Smith 1988; Scoffin 1993). While the formation of these features is known to occur under stormy conditions, the actual processes involved in their formation are less clear. Maragos et al. (1973) suggested that the deposition of the near-continuous 19km long storm ridge on Funafuti Atoll during

tropical cyclone *Bebe* in 1972 was in parts indicative of a single depositional event, but in other areas may also have formed by the progressive accretion of a series of sediment units.

Hayne and Chappell (2001) describe several elements as indicative of storm ridge deposits. Beachface and berm facies are porous, clast-supported, shingle deposits that are usually structureless and generally show little or no clastic imbrication, but occasionally dip seawards. Crest facies are horizontally bedded, matrix-supported, finer-grained shingle. Washover facies are bedded, typically dip landwards, and sometimes contain imbricated clasts. The bulk of their material is usually coral fragments derived from the reef crest and reef front between depths of 0 and 20 m (Hopley 1982; Scoffin 1993). Although, depending on their location, shell or other material may dominate their composition. The coarse nature of the material comprising these ridges is indicative of the high-energy conditions associated with their formation.

The development of storm ridge sequences is dependent on the availability of a sufficient sediment supply. If the period of time taken for source material to replenish were overly long, then it may be that insufficient sediment is available for each tropical cyclone event to deposit a ridge. The effects of storms on coral reefs are variable at both spatial and temporal scales and thus reefs have time scales of recovery that reflect such variability. In many cases it would appear that there is sufficient coral regrowth in the surrounding reef to provide enough sediment for each successive event to deposit a ridge. Hayne and Chappell (2001) estimated that the fringing reef at Curacoa Island supplying coral material for its ridges had a

regeneration time that was much less than the average time between ridge forming events. Furthermore, the similar frequency of ridge forming events at multiple sites in the GBR region (Nott and Hayne 2001) suggests that the availability of source material is not a limiting factor.

7.3 Regional Sequences

Storm ridge deposits have been identified at several sites along the east Queensland coast (Figure 7.1). At many of these sites, however, vulnerability to wave action reworking unconsolidated material post-depositionally limits the preservation of extensive ridge sequences. Storm ridges at such sites are often gradually reworked into more protected locations to form a more stable landform. Only those locations that are afforded a relatively high degree of shelter from such processes (e.g. sites on the leeside of islands) favour the formation of extensive ridge sequences. Cementation of the initial unconsolidated deposits occurs more readily at these sites and thus allows ridge features to stabilise.

The distribution of sites where storm ridges have been documented is fairly dense in the northern and central regions of the Great Barrier Reef (see Figure 7.1). In some cases it would also appear that sites located in close proximity are likely to record the impact of the same events. Nott (2003) identified several sites in the vicinity of Cairns that record the passage of several intense tropical cyclones over the century prior to European settlement in the region. This includes Fitzroy and Double Islands, which each contain a series of storm ridges of coral shingle along their northern

shorelines. Red Cliff Point comprises a uniquely different feature in that it consists of 4 terraces eroded into a raised gravel beach deposit. Nott (2003) hypothesised that tropical cyclone generated waves were responsible for the formation of these terraces, rather than other potential triggers such as sea-level oscillations or tsunamis.
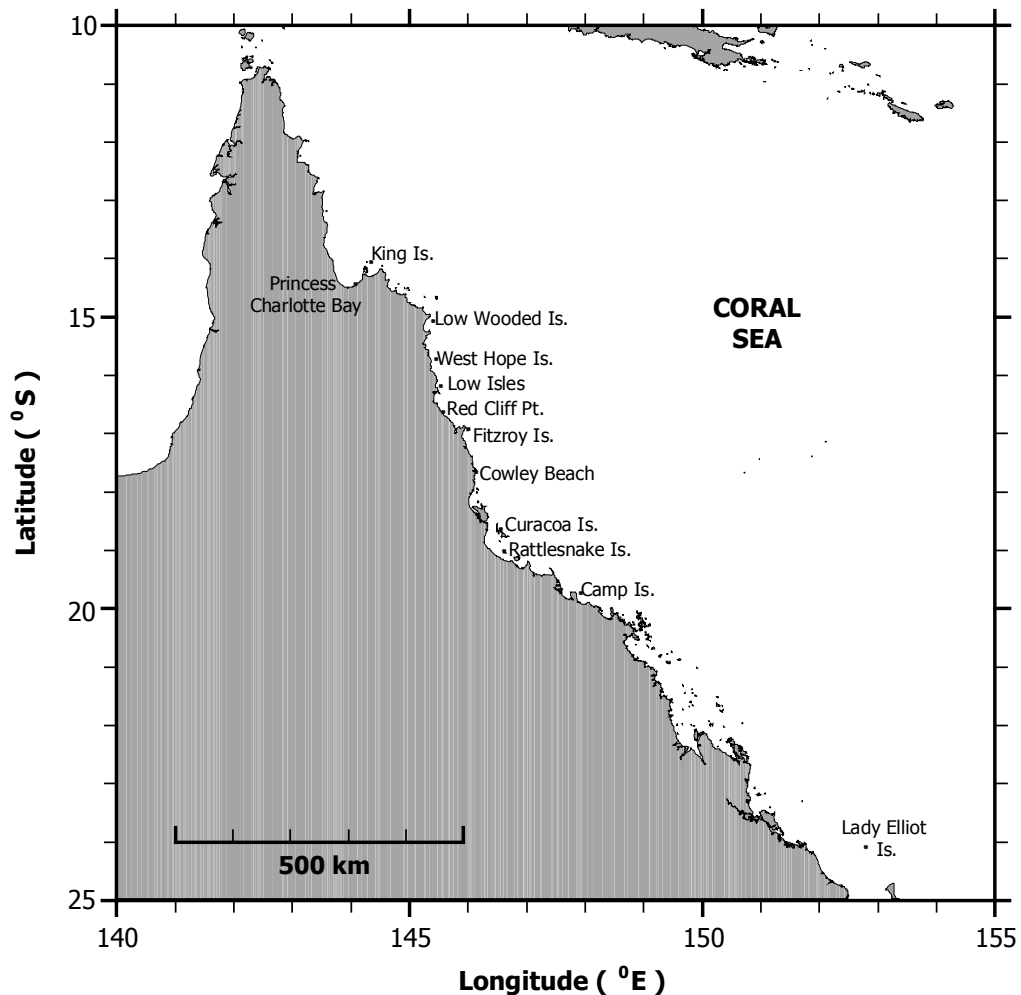
Figure 7.1 Some locations where geological indicators of past tropical activity have been identified along the east Queensland coast.

135

Chappell et al. (1983) describes several low reef islands in the northern GBR including Low Wooded and West Hope Islands, which each contain several storm built ridges. These sites are typical of many of the low wooded islands on platform reefs in the northern GBR, which according to Scoffin (1993) have characteristic ridges of coral shingle with steep, landward-facing slopes and gentle seaward-facing slopes that have planar or convex profiles. The ridges at these sites are often located on the island's windward side where the lack of any high-standing protection results in the continual redistribution of shingle and modification to the initial units by wave activity. Ridge heights and ages at many of these sites are thus generally quite variable (Chappell et al. 1983).

Hopley (1971) describes several additional sites in the central GBR region including the high continental islands of Curacoa, Rattlesnake, and Camp. These sites are characterised by the presence of spits on their leeward sides that are often infilled with a series of coral shingle ridges. Some prominent regional examples where ridge sequences have been extensively studied include Lady Elliot Island, Curacoa Island, and Princess Charlotte Bay.

7.3.1 Lady Elliot Island

Lady Elliot Island is a 0.54 km^2 shingle cay located on a platform reef at the southernmost end of the GBR. As described by Chivas et al. (1986) the cay is constructed largely from a series coral and shell shingle ridges. According to Flood et al. (1979), dating of the older ridges indicates that the island formed over a shallow reef platform some 3,200 years ago following a slight drop in sea levels.

The ridges form a unique, near-concentric arrangement with the lower portions of the inner ridges being cemented through phosphatisation. The ridges are elevated up to about 2.5 m above highest astronomical tide (HAT) and have prograded at fairly uniform rates on both leeward and windward sides of the island. Based on this observation, Chivas et al. (1986) inferred that the frequency of ridge forming events showed no significant variation over time.

7.3.2 Curacoa Island

Curacoa is a high continental island located on the innershelf of the central GBR in the Great Palm Island Group north of Townsville. It contains a series of storm ridges that lie on a cuspate spit between the shoreline and the leeside of a large, protective boulder embankment that extends from the northwest corner of the island (Hopley 1971; Hayne and Chappell 2001). The ridges are composed of coarse sediment, mainly coral shingle with variable amounts of beach gravel, and are elevated up to 3 m above HAT.

Hayne and Chappell (2001) found that 'groundsurfaces' separated many of the Curacoa storm ridges. These comprise lenses of pebble-sized pumice and a weak earthy palaesol that developed when the ridge surface had originally been exposed. Furthermore, because ridge heights and sediments become progressively smaller towards the eastern end of the spit, this indicates longshore transport of ridge material from the western tip of the spit. A comprehensive stratigraphic and dating analysis reported by Hayne and Chappell (2001) identified 22 separate ridges in the

sequence (Figure 7.2). They also inferred that the frequency of ridge formation had

remained statistically constant at this site over the last 5,000 years.
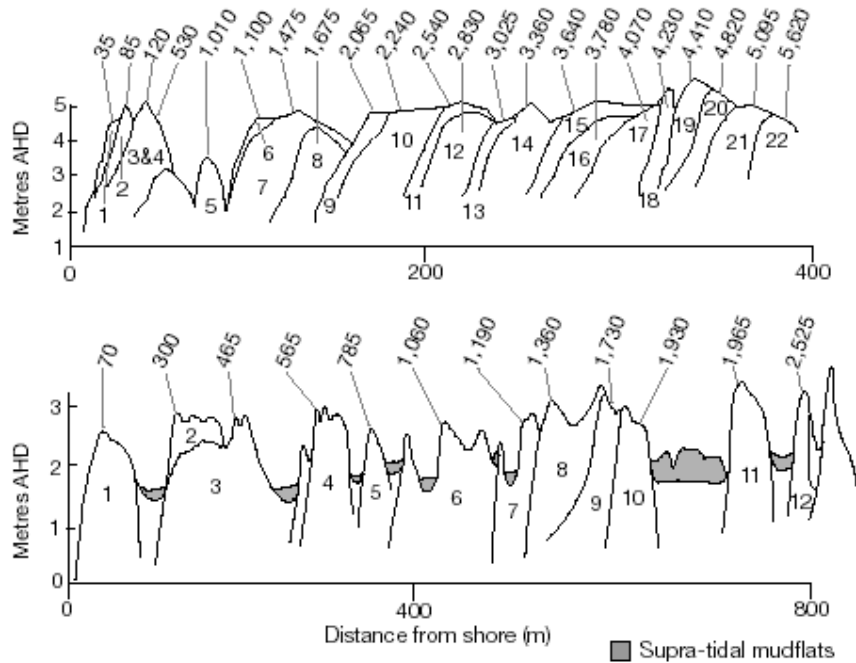
Figure 7.2 Storm ridge sequences at Curacoa Island (top) and Princess Charlotte Bay (bottom) (Source: Nott and Hayne, 2001, p. 509). Mean reservoir-corrected, uncalibrated, radiocarbon ages are labelled for each ridge.

7.3.3 Princess Charlotte Bay

Princess Charlotte Bay is a shallow, northward facing embayment situated towards

the northern end of the GBR. The bay is partly protected by several reefs and islands

to the north and northeast. Its coastal plain is fronted by a narrow tract of mangrove

forest behind which rests a series of long, shore-parallel chenier ridges that overlay a broad supratidal mud-flat (Chappell and Grindrod, 1984). To the northeast of this plain, the chenier ridge system passes into what Chappell and Grindrod (1984) describe as a separate beach ridge system. These beach ridges sit on a similar substrate as the cheniers but differ in that that have been deposited at greater frequency over the late Holocene and coalesce with no intervening muddy swales. The site is analogous to Curacoa and Lady Elliot Islands in that coarse marine sediment has been deposited as a series of ridges with crests that are elevated well above HAT. Recent surveys and sampling conducted by Hayne (1997) identified a series of 12 storm ridges forming over about the last 2,500 years at this site (Figure 7.2).

7.4 Reconstructing Palaeostorm Intensity

According to Nott and Hayne (2001) storm ridge sequences at sites such as Lady Elliot Island, Curacoa Island and Princess Charlotte Bay form to an elevation that is governed by the level of tropical cyclone marine inundation. These levels are determined by the combined height of the storm surge, astronomical tide as well as wave set-up and run-up levels. In a pioneering study, Nott and Hayne (2001) adopted an at-site relationship between water level height and tropical cyclone intensity to reconstruct the magnitude of ridge forming events at several sites in the GBR. This methodology rests on the assumption that the height of a particular ridge is a direct function of the height of water levels generated by the depositional storm.

As the prevailing meteorological and tidal conditions are unknown at the time when a particular ridge was emplaced, the methodology of Nott and Hayne (2001) actually seeks to obtain a lower bound on the intensity of ridge building storms. That is, by effectively considering a 'worst case scenario' in terms of the storm's path, speed of movement and size, a lower bound on the intensity of a storm capable of depositing a ridge is estimated. More specifically, by assuming values for these parameters that maximise the at-site water level response, the lowest possible storm intensity (i.e. highest central pressure) necessary to build a ridge is obtained. Uncertainty margins can also be incorporated within this process and thus allow for the uncertainty associated with unknown tidal conditions to be quantified (Nott and Hayne, 2001; Nott 2003). In this study an investigation into the site response to tropical cyclone forcing at one particular ridge sequence location, Lady Elliot Island, was undertaken in order to evaluate the robustness of this methodology.

7.4.1 Site Description

Lady Elliot Island is an exposed reef system located in deep water near the edge of the continental shelf at the southernmost end of the GBR. As shown in Figure 7.3 the island comprises a near-concentric system of storm built ridges composed mainly of coral shingle, *Tridacna* clam shells, and bioclastic sand bound together with a guano-derived phosphate cement (Chivas et al. 1986). The unique arrangement of these ridges is largely governed by the shape and size of the surrounding reef and its role in influencing local wave conditions. According to Hopley (1982) shingle cays like Lady Elliot develop from the coalescence of several coral shingle ridges, with the initial focal point being a hammerhead spit or tongue of shingle in the rubble

zone of the reef flat. The ridges at Lady Elliot are fairly uniform in height and range from approximately 1.5 m to 2.5 m above HAT with ages that indicate they become younger closer to the shore (Chivas et al. 1986).
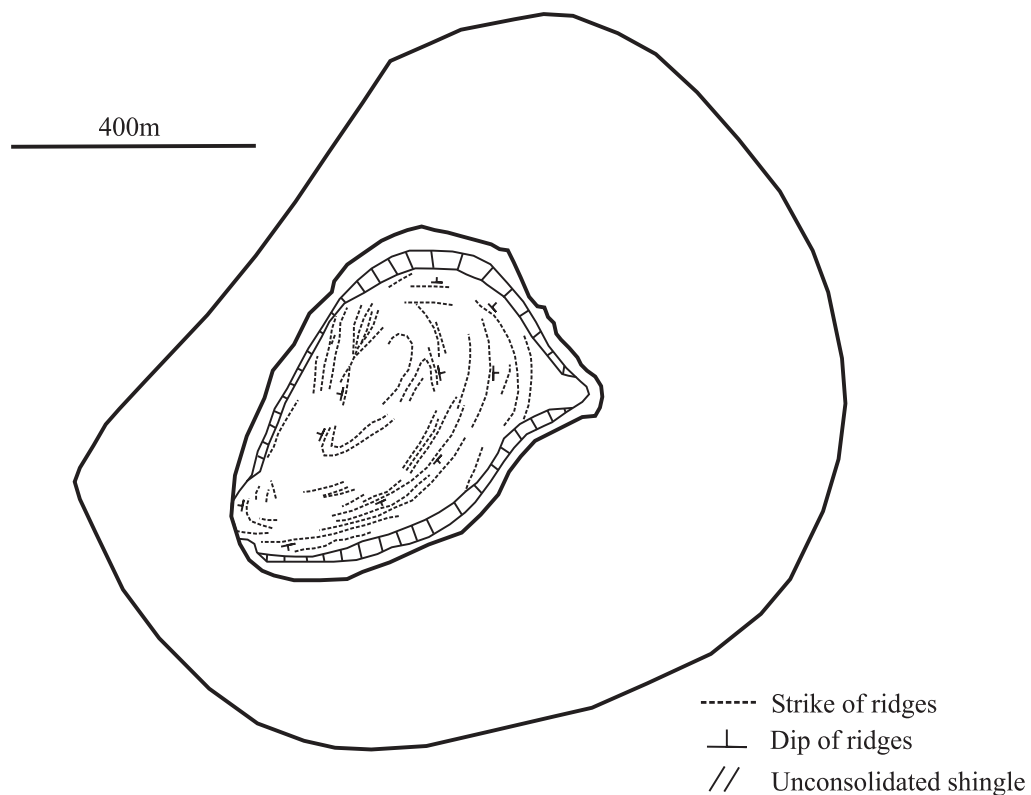
Figure 7.3 Lady Elliot Island and edge of surrounding platform reef (adapted from Flood et al. 1979).

The Lady Elliot cay is situated towards the leeward margin of a platform reef (Figure 7.3). The windward reef is relatively wide and extends out continuously to 500 m at points on the eastern side. The leeward reef is much narrower, extending out

continuously to less than 70 m at some points. A wide, gently seaward sloping reef rim adjoins the reef flat on the windward side. The reef crest is elevated slightly above the level of the reef flat. The reef rim separates the reef flat from a steep subtidal reef slope on the windward side. On the leeward side the reef flat directly adjoins the reef slope. A large portion of both the reef flat and reef rim is exposed for several hours during the daily low tide.

According to Chivas et al. (1986) there are from one to four uncemented shingle ridges between the beach and the older cemented ridges on Lady Elliot. The most seaward cemented ridge dated by Chivas et al. (1986) was found to be about 770 years of age. In the more recent, and unconsolidated foreshore deposits, several samples collected and radiocarbon dated by Chivas et al. (1986) were found to be post-bomb in age. This indicates that material had recently accumulated at elevation on the cay at sometime between the mid-1950s and early 1980s. During this period there were several tropical cyclone events to affect the southern GBR region.

Here the water level response at Lady Elliot to two of these tropical cyclones, *Dinah* (1967) and *David* (1976), was investigated. Severe tropical cyclone *Dinah* in particular is known to have caused extensive flooding at Lady Elliot Island in late January 1967. During this event heavy swells persisted for several days at Lady Elliot and as *Dinah* tracked close to the site on the 29th January, the combined effects of a high tide, storm surge and extreme waves temporarily inundated the cay. The effect of tropical cyclone *David* at Lady Elliot is less well documented, although it is known that this event generated high water levels that were responsible for inundating other coral cays in the region (see e.g. Gourlay and McMonagle 1989).

Because no direct measurements of water-level heights at the site are available, an attempt to reconstruct these levels is undertaken using a modelling approach.

7.4.2 Tropical Cyclones Dinah and David

Tropical cyclone *Dinah* developed near the Solomon Islands late on the 22nd January 1967 and moved southwestwards towards the Queensland coast. It continually intensified over this time and later recurved eastwards (Figure 7.4). The centre of the system passed just to the west of Lady Elliot Island at approximately 0330 UTC on the 29th January. The eye made landfall over Fraser Island where its peak central pressure of 945 hPa was recorded at Sandy Cape at about 0700 UTC. Between 2300 UTC on the 27th and 2300 UTC on the 29th satellite imagery showed that *Dinah* had a circular eye about 40 km in diameter. *Dinah* was an unusual event in that it maintained high intensity at subtropical latitudes. This combined with its relatively large circulation contributed to the generation of heavy seas, which caused extensive coastal impacts over a large swathe to the south of its path. Figure 7.5 shows a synoptic map of the storm near landfall. During the event a strong pressure gradient developed between the cyclone and a high-pressure system located to the south.

Tropical cyclone *David* (Figure 7.4) originated near Vanuatu early on the 14th January 1976 and tracked in a general west-southwesterly direction towards the Queensland coast. The storm was intensifying right up to the time of landfall, which occurred at about 1200 UTC on the 19th January south of Mackay. Its lowest central pressure was estimated to be 961 hPa just prior to landfall, before it decayed relatively slowly overland. The radius of maximum winds was estimated to be

143

between 60 and 70 km at landfall (Gourlay and McMonagle 1989). While tropical cyclone *David* passed some distance to the north of Lady Elliot Island, a feature of this storm was its large circulation with gale force winds produced over an extensive area. Figure 7.5 shows a synoptic map of the system just prior to landfall. As with tropical cyclone *Dinah*, the presence of a strong pressure gradient between the cyclone and a high-pressure system to its south contributed to strong winds and large waves being generated during the storm's approach.
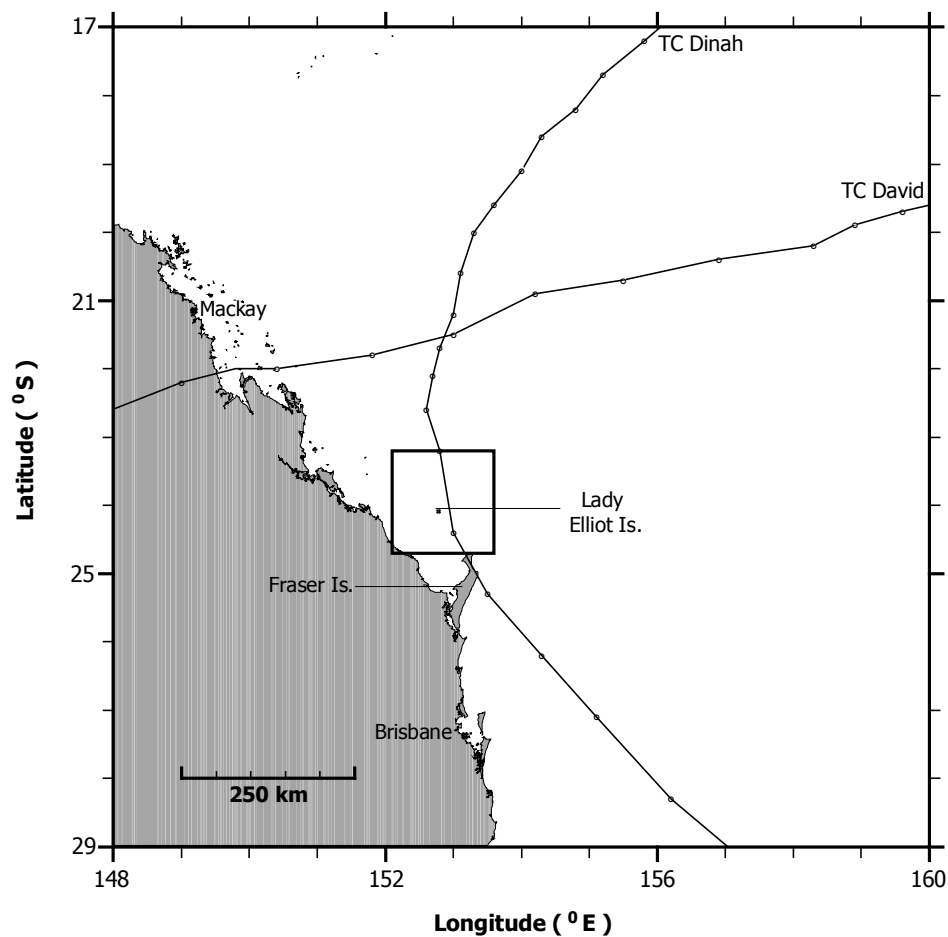
Figure 7.4 Tracks of tropical cyclone's *Dinah* and *David*. Boundaries of coarse and fine grid model domains are also shown.
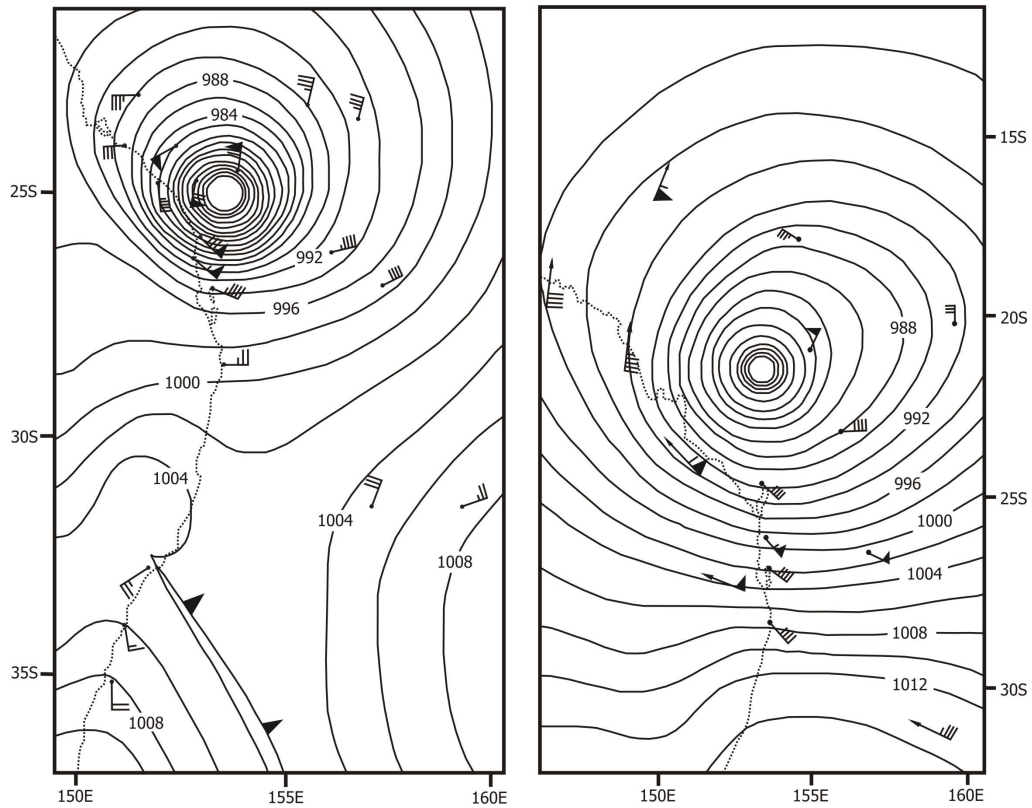
Figure 7.5 Synoptic features of severe tropical cyclone *Dinah* (left) at 1100 UTC on 29th January 1967 and *David* (right) at 2300 UTC on 18th January 1976.

Other than using positional and intensity estimates of these storms from the best-track recordings, as well as an estimate of their radius of maximum winds, no attempt has been made to extensively reconstruct the wind fields of tropical cyclones *Dinah* and *David*. This is due, in part, to the limited amount of direct observations for these events, but more so because the adopted methodology for palaeostorm reconstruction uses a relatively simple parametric model of the tropical cyclone wind field. This is a necessary consequence of unknown meteorological conditions at the

time of storm ridge deposition. As such, it is more relevant in this case to assess the methodology on a similar basis.

7.4.3 Modelling Water Levels

A series of storm simulations were conducted to determine the height of water levels generated by these tropical cyclones at Lady Elliot Island. Several models were employed to simulate this response. This included the two-dimensional storm tide model *GCOM2D* (Hubbert and McInnes 1999), and the third generation spectral wind-wave model *SWAN* (Booij et al. 1999). Tropical cyclone forcing was provided from the parametric model of Holland (1980), with surface wind and pressure fields derived in the manner described by Hubbert et al. (1991). These are interpolated both spatially and temporally to the numerical surge and wave model grids.

Inputs to cyclone model are the time history of the parameters specifying the storm's position (i.e. latitude, longitude), central and peripheral pressures, radius to maximum winds and radial profile shape. The basic form of the Holland (1980) model has been extensively utilised in tropical cyclone wind, storm surge and wave modelling in the Queensland region (e.g. Hubbert et al. 1991; McInnes et al. 2000). With adequate tuning of the radial wind profile parameters, this model is generally capable of reproducing the peak conditions during tropical cyclones quite well. One potential limitation is that the model only considers the influence of the vortex winds, while the winds resulting from the background synoptic flow are not taken into account.

Both the *SWAN* and *GCOM2D* ocean models are run over an outer coarse grid and a nested fine grid with a higher spatial resolution. The spatial extents of these grids are shown in Figure 7.4. The water level elevations from the coarse grid simulations are transferred to the boundaries of the fine grid. The *SWAN* model is an arbitrary scale model that simulates wind-wave growth, propagation and dissipation for specified wind forcing, bathymetry and currents. It can be applied in both deep and shallow water environments. A spatial resolution of 0.05^0 (~5.6 km) was used for the *SWAN* coarse grid with a total of 48 directional bins and 25 frequencies. A spatial resolution of 0.005^0 and a similar spectral resolution were used for fine grid simulations.

The storm tide model *GCOM2D* solves the depth-averaged hydrodynamic equations for specified atmospheric forcing and tides over an arbitrary region defined by bathymetric and topographic information to provide water-level heights, currents, and coastal inundation levels. An advantage of the model is that it can be applied in most settings with little calibration. Here a spatial resolution of 5 km was employed for the coarse grid simulations and a resolution of 0.5 km for the fine grid. Tidal forcing is implemented in this model as a change in water levels at the open water boundaries of the coarse grid from the amplitudes and phases of the dominant constituents (M_2, N_2, K_2, S_2, O_1, P_1, and K_1).

Lady Elliot Island is located in relatively deep water so any wind setup of the storm surge is likely to be negligible. Hence, the contribution of the storm surge to total water level at this site is likely to be relatively small. The location of this site at the southernmost end of the GBR also means that there is little sheltering effect as Lady

Elliot is isolated from neighbouring islands and reefs. The abrupt transition from relatively deep to shallow water at the platform reef results in significant modification to off-reef wave conditions. Waves break on the seaward reef margin, dissipating much of their energy and generating a set-up of the mean water level. Following initial breaking any residual energy is transferred into a breaking 'surge' that reforms into stable oscillatory waves, which lose further energy propagating over the shallow reef top due to surface roughness.

Wave set-up levels are modulated by the storm surge and tide levels, with set-up generally larger at lower levels of submergence as well as for higher off-reef wave heights (Gourlay 1996). A semi-empirical model is applied here to estimate the magnitude of wave-generated water levels on the Lady Elliot Island reef for off-reef wave and water level conditions obtained from the ocean models. Figure 7.6 highlights the processes involved with wave transformations on coral reefs.
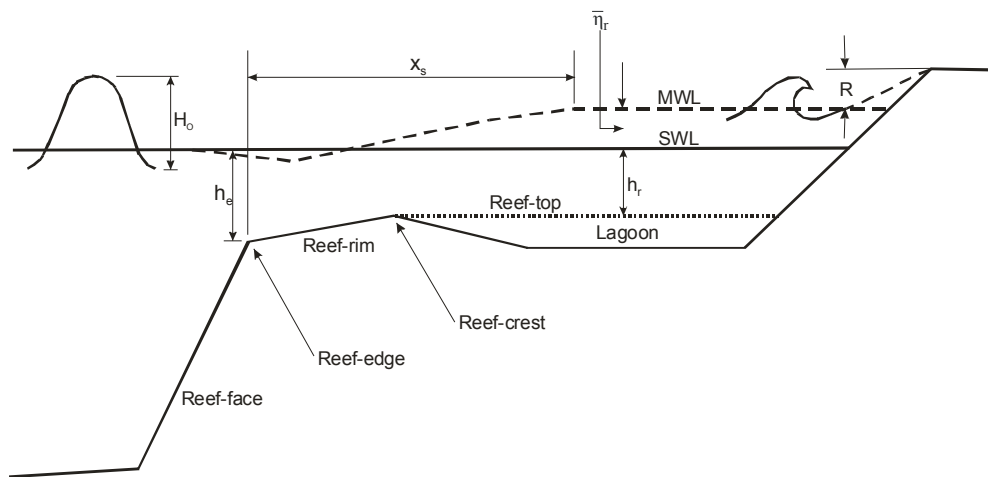
Figure 7.6 Outline of wave process on coral reefs (adapted from Gourlay 1997, p.959).

148

On the basis of laboratory and field experiments Gourlay (1996; 1997) derived the following formulation for wave setup on a reef-top ($\overline{\eta}_r$) as a function of offreef wave conditions and reef characteristics:

$$\overline{\eta}_r = \frac{3}{64\pi} K_P \frac{\sqrt{g} \, H_o^2 \, T_0}{(\overline{\eta}_r + h_r)^{3/2}} \left\{ 1 - 0.16 \left[\frac{(\overline{\eta}_r + h_r)}{H_o} \right]^2 \right\}, \tag{7.1}$$

where H_o and T_o are the off-reef wave height and period, h_r is the still water depth on the reef, and K_P is a reef profile coefficient.

The coefficient K_P depends largely on the slope and roughness of the reef at the breaking point. Gourlay (1997, Figure 2, p. 961) gives values for K_P as a function of the slope of the reef face. Given the extreme wave heights likely to accompany tropical cyclones it is apparent that waves would break at the seaward reef edge for the modelling scenarios considered here. This is because Lady Elliot Island is situated near the edge of the continental shelf in relatively deep water and the contribution of the storm surge to the reef top water level is relatively minor, while the off-reef wave heights comparatively larger. It is thus apparent that $H_o \gg 0.4 h_r$, where $H_o \sim 0.4 h_r$ is approximately the point below which waves pass over a horizontal reef top without breaking (Gourlay 1996).

In order to account for the irregular nature of storm waves, H_o is taken as the off-reef root mean square wave height (H_{rms}). A value for the reef top water level (h_r) is obtained from the contribution of the storm surge and tide. Assuming the wave

height on a horizontal reef top is depth-limited and taking a reef top wave height-to-depth ratio of $\gamma_r = 0.4$, the maximum significant wave height is given by $H_r = 0.4(\overline{\eta}_r + h_r)$ (Gourlay 1996). The reduction in wave height with bottom friction is then given as:

$$\frac{dH_r}{dx} = -\frac{f_w}{3\pi} \frac{H_r^2}{(\overline{\eta}_r + h_r)^2} \; , \tag{7.2}$$

where x is the distance from the end of the surf zone to the shore, and f_w is a friction factor. A representative value of f_w on coral reefs is around 0.1-0.2 (Gourlay 1997). The maximum value for the surf zone width (x_s), which represents the furthest distance travelled by the breaking surge, is (Gourlay 1997):

$$x_s = (2 + 1.1 H_o / h_e) T \sqrt{g h_e} \; , \tag{7.3}$$

where h_e is the water depth at the reef edge. Finally, run-up of the reformed waves reaching the shore of the cay is estimated with the following:

$$R_{2\%} = 0.64 \tan\alpha_B \; T_r \sqrt{gH_r} \tag{7.4}$$

where $R_{2\%}$ is the run-up height exceeded by 2% of the incoming waves, $\tan\alpha_B$ is the beach slope, and T_r is the reef top wave period, which is generally shorter than the corresponding off-reef value.

7.4.4 Results

Given that relatively reliable meteorological information regarding the intensity and track of these tropical cyclones is available, and providing that the adopted models for reconstructing water levels are reasonably accurate, the validity of some of the assumptions underlying the reconstruction methodology of Nott and Hayne (2001) can be more closely examined. One important assumption is that the depositional events were intense tropical cyclones that tracked nearby the site. On this basis, tropical cyclones *Dinah* and *David* represent suitable candidates for testing this assumption given that they were both severe tropical cyclones that tracked across the southern GBR region.

Figure 7.7 gives the results of employing the series of models to predict the height of water levels at Lady Elliot Island associated with tropical cyclones *Dinah* and *David*. The plots give a time series of the maximum water levels and the estimated wave set-up levels for a 36-hour period during the storm's passage in the southern GBR region. The hindcast for *Dinah* indicates that water levels would, at most, reach about 2.3 m above HAT. The maximum water level generated by *David* was estimated to be around 1.0 m above HAT.

The major contributor to the total water level is the wave set-up component, which is a consequence of the exposed nature of the site favouring the generation of large off-reef waves as well as the influence of the reef on local wave conditions. It is also apparent that wave set-up is larger at lower levels of reef submergence during the tidal low. The hindcasts indicate that during the peak of these events, extreme

conditions at Lady Elliot persisted for some time, such that similar off-reef wave conditions were experienced across the tidal cycle. This resulted in the larger total water levels being experienced during the tidal high.
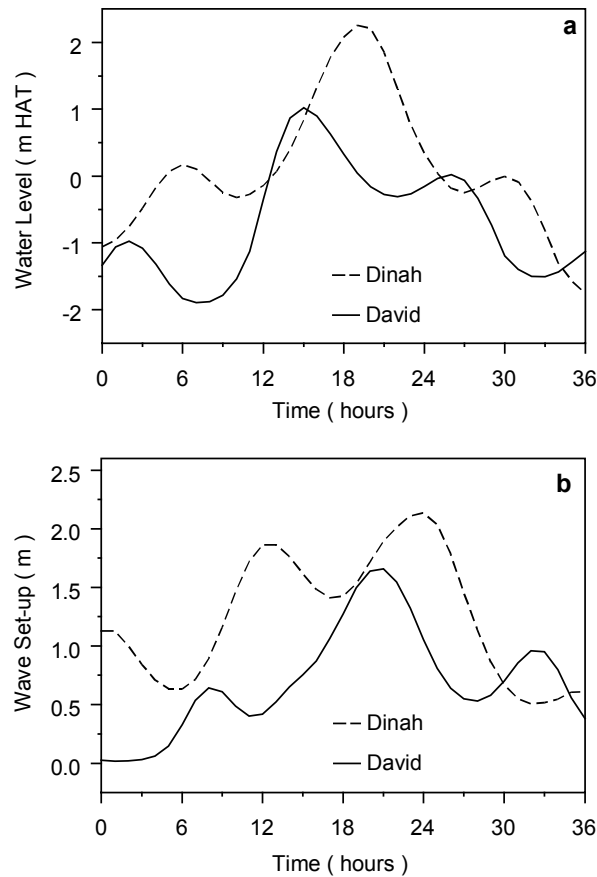
Figure 7.7 Modelled water levels at Lady Elliot Island for tropical cyclones *Dinah* and *David*, (a) total water levels, and (b) wave set-up levels. For *Dinah* the time series commences at 0600 UTC on 28th January 1967 and for *David* at 0900 UTC on 18th January 1976.

The modelled water levels are likely be an underestimation of the maximum achieved level, as the instantaneous value of η_r would likely reach levels higher

than the mean value ($\overline{\eta}_r$) due to the presence of wave groups (Gourlay 1996). Larger reformed waves and consequently a higher level of wave run-up would likely accompany a temporarily higher level of wave set-up.

The results indicate a tropical cyclone similar to *Dinah's* severity and path are likely necessary to generate water levels comparable to the height of storm ridges at Lady Elliot. Tropical cyclone *David*, which tracked a greater distance from the site, appears unlikely to have produced water levels sufficiently high enough to be comparable to the ridge heights. This suggests that the methodology of Nott and Hayne (2001) is relatively robust with respect to its assumptions on reconstructing palaeostorm intensities, despite the level of simplification involved with simulating a complex series of processes.

The height of water levels generated at Lady Elliot from tropical cyclone *Dinah* indicates a tendency towards lower intensity estimates than were reconstructed by Nott and Hayne (2001, Table 2). The results here show a lower intensity storm, indicative of a weak category 4 system, may be a more representative estimate at this site. It is apparent, though, that this difference can largely be explained by knowledge of the tidal conditions during tropical cyclone *Dinah*. Inspection of the uncertainty margins for unknown tidal conditions given by Nott and Hayne (2001, Table 2) indicates a similar intensity would be reconstructed under the assumption that ridges are emplaced during high tide conditions.

At this stage it remains difficult to further assess the methodology in the absence of direct observations of storm ridge formation under tropical cyclone conditions. In

this case it is not known whether tropical cyclone *Dinah* deposited a storm ridge at Lady Elliot. Although, it is likely that some coarse sediment was deposited at elevation with the storm-generated inundation of the cay. This is consistent with observations that indicate the elevated water levels during *Dinah* initiated the onshore transport of coral fragments including existing sedimentary units that rested above high water.

7.5 Summary and Discussion

It is apparent that a unique set of rarely occurring conditions, most likely triggered by severe tropical cyclones, was responsible for the formation of storm ridge sequences found throughout the Queensland region. At several of these sites storm ridges are permanent features in the landscape having formed stable landforms over time. Individual ridge heights at these sites are therefore likely to act as a reliable indicator for the minimum level of site inundation generated by the depositional storms. The approach to reconstructing the intensity of ridge forming events though, is necessarily simplistic and conservative given the complex nature of the unknown meteorological conditions associated with the depositional storms.

The simulations conducted in this study for tropical cyclones *Dinah* and *David* at Lady Elliot Island substantiate the methodological framework for reconstructing palaeostorm intensities developed by Nott and Hayne (2001). Moreover, other studies have shown that water level responses under known tropical cyclone conditions can be reconstructed and compared to sedimentary traces of their

occurrence (e.g. Fletcher et al. 1995; Nott 2004). Given that the geomorphic response of these environments to wave action is a complex process, however, there are limitations associated with the reconstruction methodology, such as the role of wave run-up, that warrant further investigation. A potentially important limitation of the modelling process presented here is the extent to which the unaccounted effects of wave refraction and diffraction at Lady Elliot reef would influence water level calculations.

One important aspect that underlies the interpretation of past storm events using this methodology is the assumption of a relatively stable geomorphic setting over the period in which a particular sequence has been constructed. Most important is the relationship of modern sea levels to those when the ridges were actually emplaced. Hayne (1997) suggests the reduction in ridge heights by about 50 cm over Curacoa ridge sequence (Figure 7.2) reflects the influence of a fall in sea levels over the late Holocene. On the basis of intertidal coral micro-atolls found on fringing reef flats across the region, Chappell (1983) reconstructed a peak at about 1 m in postglacial sea-level rise at around 5,500-6,000 years BP and thereafter a smooth linear fall to its present level. More recently, Baker and Haworth (2000) suggested a possible alternative statistical interpretation of Chappell's micro-atoll data, opting to fit a high-order polynomial curve to the data in view of an oscillatory rather than smooth decline in sea levels.

Any potential mis-interpretation introduced by the lack of an accurate understanding of late-Holocene sea-levels may be minimised by concentrating on only the more recent prehistoric record. In the case of Lady Elliot Island, it is apparent that the

progradation of storm ridges over the last 3,000 years has taken place at sea-levels more or less at present levels. While smaller amplitude changes that are not resolved in the available palaeo-sea level indicators may have occurred over this period, it is unlikely that they would affect the general results. Moreover, one factor that potentially offsets the need to adjust ridge heights in accordance with sea-level changes is the degree to which progressive compaction and settling has reduced their original standing (Nott 2004).

One further aspect regards the precision with which a reliable chronology can be obtained from the record. A high temporal resolution record of past tropical cyclone activity is not obtainable from the ridges sequences, instead being limited to the recording of only the most extreme events at a few sites. Furthermore, radiocarbon dating of individual ridges can only provide ages for depositional events that fall within a range, which complicates the identification of trends in the chronology. In addition, a possible sampling bias exists in the dating process due to the fact that samples may not have been alive at transport, but had been reworked from existing accumulations of rubble on the reef (Nott 2004), or had been reworked between ridges. Due to this potential delay in transport of ridge material, ages given for ridge formation actually represent an average maximum age for the deposit.

This bias can be minimised to some extent by examining surface features on corals or mollusc shells, such as abrasion or boring, to indicate whether a sample was alive at the time of transport (Hayne 1997). Chivas et al. (1986) also selected shell samples, which would be more resistant to reworking due to their large size. Nott (2004) also points out that the narrow fringing reef at Curacoa Island is not

conducive to accumulating a significant amount of coral rubble at shallow depths to be subsequently entrained by storm waves. Hence, most coral fragments found in ridges at this site were likely to have been alive at transport.

In any case, given that the time period for when individual ridges were deposited can be suitably bracketed, an understanding of the regional frequency of severe tropical cyclones can be obtained by collating multiple site records. Having a greater understanding of such limitations then allows for an improved discrimination of the merits of this record. This is particularly important to facilitate comparisons with the modern record, which is addressed in the following chapter.

CHAPTER 8

COMPARITIVE ANALYSIS OF INSTRUMENTAL, HISTORICAL AND PREHISTORICAL RECORDS

8.1 Introduction

The purpose of this chapter is to provide a comparison of the landfall climatologies presented in previous chapters. The main emphasis is placed on assessing how predictions on the frequency of extreme events differ for each component. The chapter begins by comparing a series of landfall events generated from the Coral Sea regional simulation model developed in Chapter 6 against the observed landfall record based on historical and instrumental eras that was presented in Chapter 5. This initially involved the application of the regional simulation model to generate a series of landfall events and a subsequent analysis of that series to determine extreme event probabilities.

As with any statistical analysis, predictions of event probabilities are sensitive to the size of the available sample, and hence the quantification of uncertainty plays an important role. This is particularly relevant to the practical application of simulation-based approaches, because the objective of this method is the generation of a series of events that exceeds in size the observed series. For this reason a detailed investigation is undertaken to assess the level of uncertainty associated with

predictions from the regional simulation model. These results are subsequently compared against uncertainty levels for the observed landfall record. Finally, a comparison of simulated and observed records against the prehistorical record that was discussed in the previous chapter is outlined.

8.2 Comparison of Simulated and Observed Records

Chapter 6 described the development of a simulation model for generating tropical cyclone tracks and intensities in the Coral Sea region based on data from the instrumental era (1960/61-2004/05). This model is employed here to simulate a series of landfall events with which to compare against the observed record. Vickery et al. (2000) used a similar comparative technique to evaluate their simulation model for Atlantic Basin hurricanes. The observed record here comprises tropical cyclone landfalls along the Queensland coast over the historical and instrumental eras encompassing the period 1898/99-2004/05.

8.2.1 Analysis of Simulated Series

In total, 3,077 Coral Sea storms were generated using the regional simulation model. Each simulated event consisted of the track's location at 6-hourly intervals along with a corresponding minimum central pressure. With a mean arrival rate of 2.4 storms per year, the 3,077 event series is equivalent to a simulation period of approximately 1,282 seasons. Of the 3,077 regional storms generated, 1,000 were classified as landfall events. This gives a landfall arrival rate of approximately 0.8

storms per year. The central pressure at landfall was extracted for each simulated event and the resulting series is plotted in Figure 8.1.

The analysis undertaken here seeks to compare this simulated dataset against the observed landfall record in terms of its capacity to produce similar predictions of extreme event occurrences. To accomplish this, the simulated series shown in Figure 8.1 was subject to an extreme value analysis consistent with the methodology employed in Chapter 5 for the observed record. Specifically, this involved the fitting of a Generalised Pareto Distribution (GPD) (equation 5.2) to the simulated landfall central pressures. When combined with a Poisson distribution for seasonal event occurrences, this gives return period levels for landfalling tropical cyclone intensities on an annual scale.
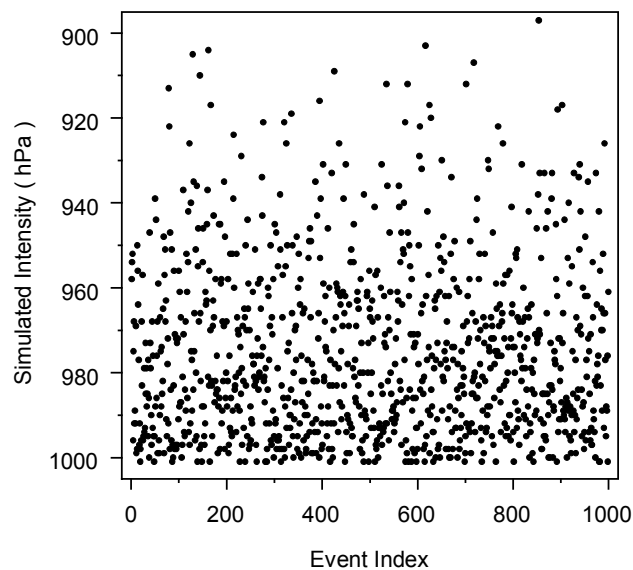
Figure 8.1 Series of landfall central pressures (hPa) generated from Coral Sea simulation model.

Figure 8.2 shows a mean excess plot for the simulated central pressure series. As described in Chapter 5 the mean excess plot is a useful diagnostic tool to aid in the selection of an appropriate threshold for fitting the GPD to data. Examination of the mean excess plot for linearity above a particular threshold indicates the point where the GPD provides a valid approximation to the distribution of excesses. Confidence intervals are also given on the plot, which are derived under the assumption that sample means are approximately normally distributed. Inspection of Figure 8.2 indicates that the mean excess curve is more or less linear across the threshold range. To be consistent with the analysis in Chapter 5, the GPD was fit to the simulated series with a threshold of 1002 hPa. Parameter estimates for the model were obtained using the maximum likelihood method, which was outlined in Chapter 5.

In order to provide further confirmation that the adopted threshold is reasonable, a threshold stability plot of the GPD shape parameter (κ) is given in Figure 8.3. As explained by Coles (2001) this comprises estimates of the shape parameter (κ), together with confidence intervals, for a range of thresholds. The plot provides a way to graphically examine variation in κ across the threshold range, which can aid threshold selection by signaling the point where parameter estimates remain relatively stable. Confidence intervals for the maximum likelihood estimate of $\hat{\kappa}$ at each threshold are obtained using the standard delta method, which assumes asymptotic normality of parameter estimates. The threshold stability plot in Figure 8.3 highlights some variability across the threshold range, although the selected threshold of 1002 hPa appears reasonable when confidence intervals are taken into account.
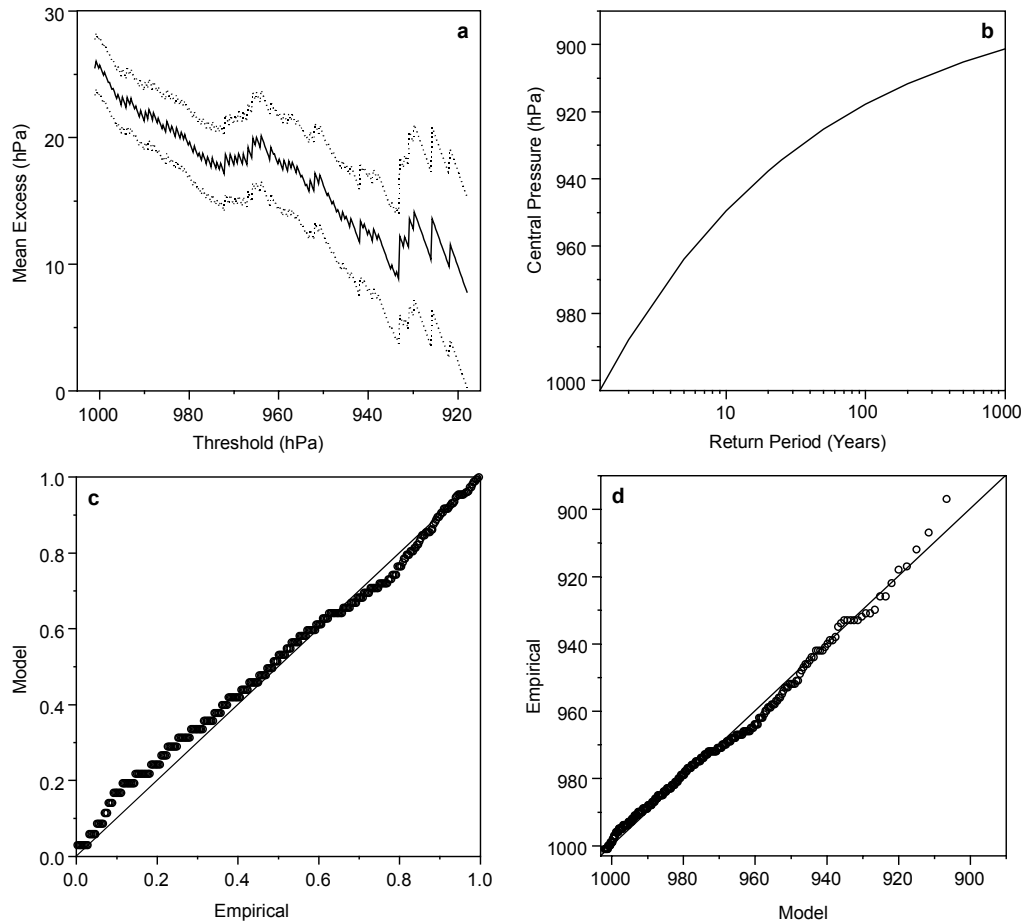
Figure 8.2 GPD fit to simulated landfall central pressures. (a) Mean excess plot, (b) return period curve, (c) probability plot, and (d) quantile plot.

The return period curve based on maximum likelihood fitting of the GPD to simulated landfall intensities is displayed in Figure 8.2. Also plotted in Figure 8.2 are probability and quantile plots of the fitted model to assess goodness-of-fit. These indicate that relatively good agreement is obtained between the simulated data and the model fit. Maximum likelihood estimates of the GPD parameters are $\hat{\sigma} = 33.8$ and $\hat{\kappa} = -0.286$.
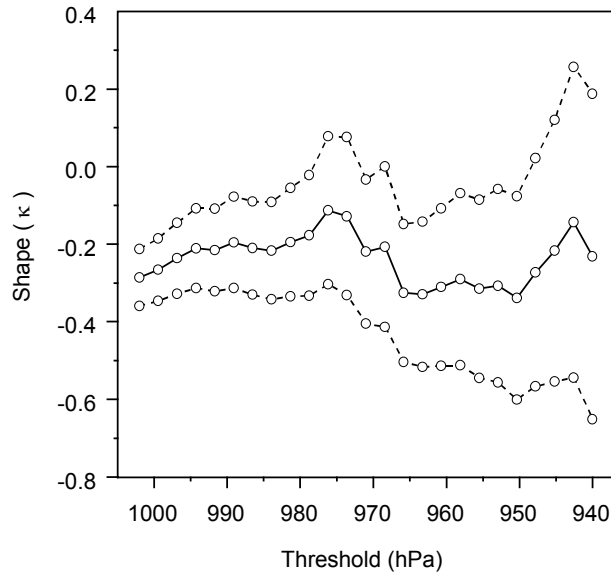
Figure 8.3 Threshold stability plot of GPD shape parameter (κ) for simulated landfall central pressures.

8.2.2 Quantile Comparisons

Figure 8.4 graphs the respective return period curves based on simulated and observed records. The return period curve labeled 'Instrumental+Historical' is that plotted in Figure 5.7 of Chapter 5. This corresponds to the Bayesian predictive distribution for the GPD fit to the combined historical and instrumental records of landfall central pressures. The curve labeled 'Simulated' corresponds to that plotted in Figure 8.2, which represents the GPD fit to simulated landfall central pressures. Also graphed is the return period curve based on the GPD fit to the instrumental record (labeled 'Instrumental'). This corresponds to that plotted in Figure 5.2 of

Chapter 5, which involved fitting the model to observed landfall intensities over the period 1960/61-2004/05.
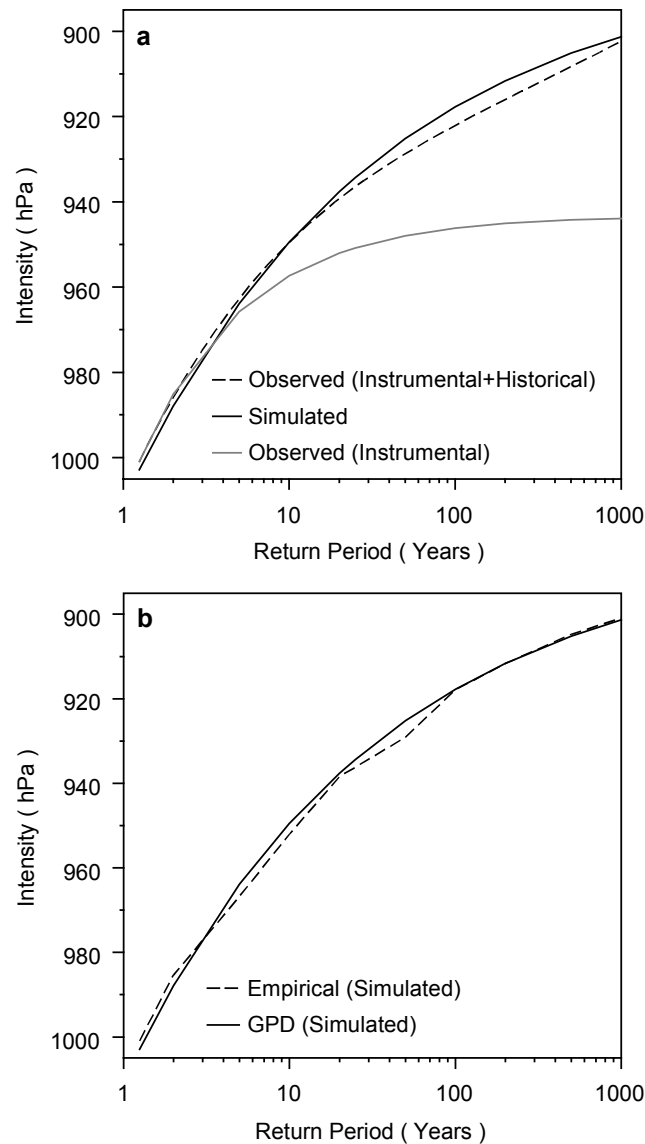
Figure 8.4 Comparison of return period curves for simulated and observed records. (a) Plots based on a GPD fit to observed landfall central pressures (instrumental era, combined historical and instrumental eras), as well as the simulated series, and (b) Plots based on GPD fit to simulated series and corresponding empirical estimate for the simulated series.

Also shown in Figure 8.4 is a nonparametric estimate of the return period curve for the simulated output series. These return period estimates were calculated from the empirical percentiles of the output simulated series. Comparison of the empirical quantile curve with that based on the GPD fit to the output series shows close agreement. This suggests that adopting the parametric model for the simulated output series, so as to be consistent with techniques used for the observed record, should not overly bias subsequent comparisons with the observed record.

Comparison of the return period curves in Figure 8.4 indicates that quantile predictions derived from the simulated series are fairly consistent with those from the observed record combining instrumental and historical data. This implies both approaches lead to similar predictions regarding the frequency of major landfall events in the Queensland region. The return period curve based on only the instrumental record of observed landfall events is seen to give comparatively lower estimates, indicative of a shorter-tailed distribution. As an example comparison, Figure 8.4 shows the 100-year return level from the simulated series is 918 hPa, from the observed (combined historical and instrumental) record it is 922 hPa, while from the observed instrumental series it is 946 hPa. The corresponding empirical estimate of the 100-year return level (Figure 8.4b) from the simulated series is 918 hPa.

8.3 Uncertainty Analysis

Coles and Simiu (2003) differentiate between two sources of uncertainty that arise in the application of simulation models to the generation of a series of tropical cyclone events. Namely;

1. That related to the length of the generated series, which typically comprises 1,000 or even 10,000 simulated events, and;

2. That related to sampling variability associated with parameter estimates of the different components that constitute the regional simulation model.

As mentioned in Chapter 3, while it is common to assess statistical uncertainty based only on the simulated output series, this component characterises only a small fraction of the level of uncertainty in the overall process. This is because the simulated series comprises a very large dataset of events, such that sampling uncertainty is artificially small.

As noted by Coles and Simiu (2003) a potentially greater level of uncertainty arises from inference on the observed tropical cyclone events, which form the basis of the simulation model. This is naturally subject to greater sampling variability because the size of the observed sample of tropical cyclones is limited. For this reason it is also important to assess uncertainty in terms of this available record. A relatively simple approach proposed by Coles and Simiu (2003) to perform this involves the use of bootstrap resampling techniques on the simulated series.

8.3.1 Bootstrap Confidence Intervals

Given a sequence of observations $(x_1,...,x_m)$, conventional bootstrap techniques amount to repeatedly drawing a sample of size m, with replacement, from the original sequence to generate B bootstrap replicate series. In this process each

observation is resampled with equal probability. For each of the *B* bootstrap samples an estimate of the statistic of interest is obtained, which then allows a reliable sampling distribution of the statistic to be constructed (providing the number of bootstrap samples is sufficiently high). The basic premise of the approach presented by Coles and Simiu (2003) is to apply a bootstrap resampling scheme on the simulated series as a means to assess uncertainty in return period estimates. A variant on the conventional nonparametric bootstrap technique is actually used by Coles and Simiu (2003), whereby the fitted model for the simulated series is used to generate bootstrap samples. This procedure is referred to as a parametric bootstrap.

A similar approach is applied here to estimate the uncertainty margins in return levels that arise separately from the simulated output and from the simulation model itself. The critical distinction between the two components centres on the length (*m*) of each bootstrap sample generated. For the output component, the size of each bootstrap sample is taken to be equivalent to the number of observations used to fit the GPD model to the simulated series. In this case a total of 1,000 landfall events were generated from the Coral Sea regional simulation model. For the simulation component, the size (*m*) of each bootstrap sample is selected to correspond to the number of tropical cyclone observations originally used in developing the model. As mentioned in Chapter 6 this was based on a total of 108 tropical cyclone events recorded in the Coral Sea region over the period 1960/61-2004/05.

Uncertainty measures are typically expressed in the form of confidence intervals for high quantile estimates. The bootstrapping procedure applied here to obtain these intervals can be summarised as follows:

- $B = 999$ samples of size m are randomly generated from a Poisson distribution with an arrival rate equivalent to the threshold exceedance rate for the Poisson-GPD fit to the simulated series (i.e. ~0.8 events per season),

- For each of the 999 generated samples, a mean arrival rate $\hat{\lambda}^*$ is then calculated,

- For each $\hat{\lambda}^*$ in the replicated series $\hat{\lambda}_1^*,...,\hat{\lambda}_{999}^*$, $B = 999$ samples of size $\hat{\lambda}^* m$ are then generated from a GPD distribution with parameters (σ, κ). The parameter estimates used here are $\hat{\sigma} = 33.8$ and $\hat{\kappa} = $ -0.286, with the threshold (u) fixed at 1002 hPa,

- For each of the 999 generated samples, the GPD parameters $(\hat{\sigma}^*, \hat{\kappa}^*)$ are estimated by the method of maximum likelihood,

- T-year quantiles (z_T, $T = 1.25, 2, 5, ..., 1000$) are then calculated using each set of parameter estimates, $(\hat{\theta}_1^*,...,\hat{\theta}_{999}^*; \hat{\theta}^* = \hat{\lambda}^*, \hat{\sigma}^*, \hat{\kappa}^*)$, again with the threshold (u) fixed at 1002 hPa

- From this series of bootstrap replicates $(z_{T(1)}^*,...,z_{T(999)}^*)$, the $100(1-\alpha)\%$ confidence intervals are obtained as the $\alpha/2(B+1)$ and $(1-\alpha/2)(B+1)$ values in the order sequence of replicates.

This procedure was implemented to estimate two separate sets of uncertainty margins for quantiles of the fitted GPD model. For both the output and simulation model components the approach was essentially identical, except that the number of observations (m) generated for each of the 999 bootstrap samples was smaller for the

simulation model component to reflect the shorter length of the tropical cyclone record. This can therefore be viewed as obtaining a smaller subset of the output series (Figure 8.1) to assess uncertainty.
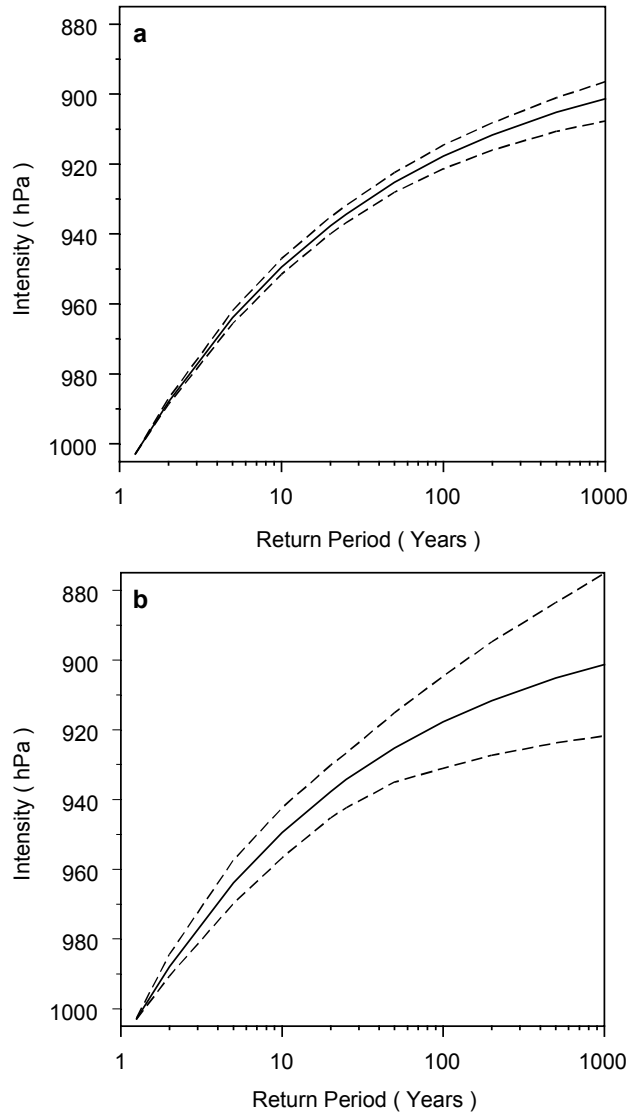
Figure 8.5 Uncertainty margins (95% confidence intervals) for simulated series of landfall central pressures. (a) uncertainty based on 1,000 event simulated series, and (b) uncertainty based on a subset of the series that is representative of the size of the observed tropical cyclone record.

169

Following Coles and Simiu (2003) it was also necessary to apply a bias-correction to the bootstrap estimates of (σ, κ) because of the tendency for bootstrap methods to produce samples with shorter tails than the true sampling distribution. Figure 8.5 shows 95% confidence intervals (i.e. $\alpha = 0.05$) for the return period curve estimated by the application of this procedure. This highlights that uncertainty margins are much broader for the simulation model component than for the output component. As expected, variability in quantile estimates also increases at higher return periods. Importantly, this effect becomes more pronounced for the confidence intervals based on the simulation model component.

8.3.2 Simulated versus Observed

As a further comparison of simulated and observed records, Figure 8.6 plots histograms of the GPD shape and scale parameter estimates against posterior densities of these parameters. The histograms represent sampling distributions derived from the bootstrap procedure described previously and applied to estimate confidence intervals for the simulation model (Figure 8.5b). The posterior densities shown in Figure 8.6 (smoothed curves) are derived from the Bayesian analysis applied to combined historical and instrumental records of landfall central pressures (see Figure 5.4).

Most notably, the plots demonstrate a similar spread in these quantities, suggesting both approaches lead to similar levels of variability in parameter estimates. This level of agreement is to be expected in some respects because the Bayesian approach made use of more data through the inclusion of historical information, while the

simulation-based approach incorporated additional data by considering a wider geographical region to develop a model.
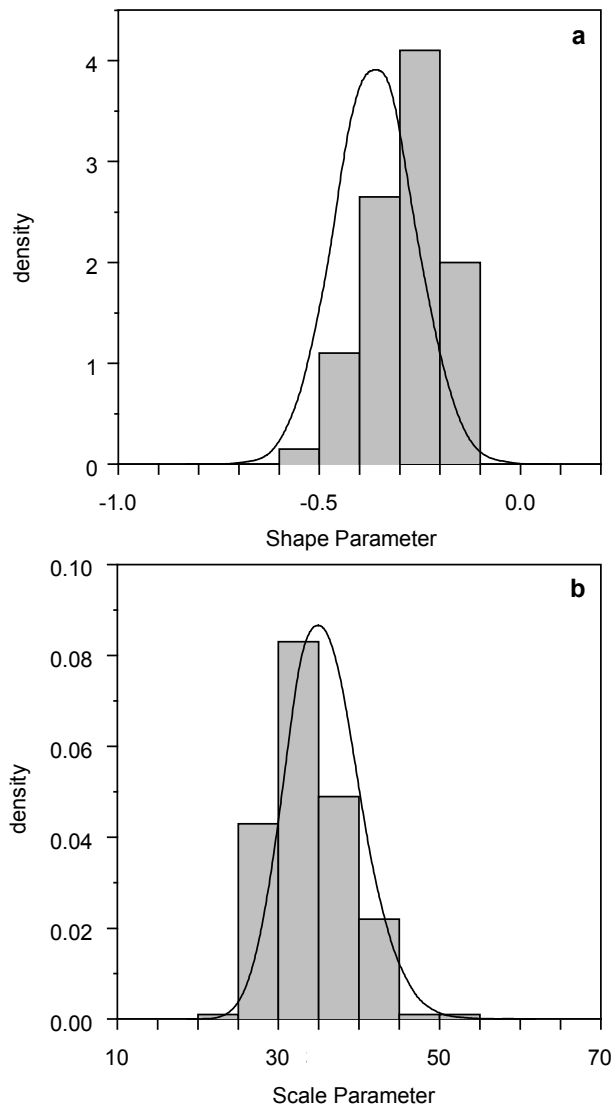
Figure 8.6 Comparison of uncertainty measures in parameter estimates of simulated series and observed record. (a) GPD shape parameter, and (b) GPD scale parameter. Histograms represent sampling distributions of the simulated output series of landfall central pressures. The smoothed curves represent Bayesian posterior distributions estimated from the combined historical and instrumental record of landfall central pressures.

8.4 Comparisons with Prehistorical Record

The previous uncertainty analysis showed that predictions of extreme quantiles exhibit a large degree of variability, which is a consequence of the short length of the available tropical cyclone record. Moreover, while the adoption of asymptotic models for extremes, the use of regional simulation techniques, and the incorporation of historical data provide an improved means to derive a landfall climatology, it remains difficult to verify the adequacy of subsequent predictions. As discussed in Chapter 7 though, there exists a long-term geological record of extremes that can be used for comparative purposes.

A direct comparison is, however, problematical because the chronology of events comprising the geological record is limited by both spatial and temporal incompleteness. This is because the storm ridge sequences preserve a record of only the most extreme events at only a few sites along the Queensland coast. Reconstructing event magnitudes from this record is also subject to some inherent limitations. As discussed in Chapter 7 these are largely associated with the inability to reconstruct the tidal conditions at the time of ridge formation. While the phasing of the tide is unrelated to the magnitude of the depositional storm, it does however, contribute to total height of water levels associated with the depositional storm. The $\pm 1\sigma$ and $\pm 2\sigma$ uncertainty margins reported by Nott and Hayne (2001, Table 2, p. 510) reflect the influence of these unknown tidal conditions.

Due to the spatially incomplete nature of the geological record, only an at-site estimate of ridge forming events can be obtained from sites where ridge sequences

have been preserved. For instance, over about the last 2,500 years the average at-site frequency of these events (i.e. the average time interval between ridge deposition) was 231-years (11 ridges in 2,540 years) and 210-years (12 ridges in last 2,525 year) for the Curacoa Island and Princess Charlotte Bay sites respectively. It has been hypothesised that the frequency of ridge forming events has remained relatively stable for the past several thousand years in this region (Hayne and Chappell 2001). The last 2,500 years captures a period of storm activity recorded by several sites. It is also a period when boundary conditions in the region, especially palaeosea levels, were unlikely to have been significantly different than present.

The analysis conducted in this study has been largely focused on the frequency and intensity characteristics of landfall events along the entire Queensland coast. In order to facilitate a direct comparison with the geological record requires a transformation of these regional models to the at-site level. This was undertaken by firstly estimating separate occurrence rates governing at-site frequencies for a particular ridge site.

Here it is assumed that a 100 km sampling radius around a ridge site is a representative zone of influence for at-site frequencies. Thus, an assumption is made that an intense storm tracking within this 100 km sampling radius would be likely to deposit a ridge. There is a degree of arbitrariness in adopting this scheme for comparison, however, based on the sensitivity analysis of Nott (2003, Figure 2) this is seen as a conservative representation. In reconstructing a history of past major storm events in the Cairns region, Nott (2003) also found that two sites located in

close proximity to each other, were both likely to have recorded the impact of the same events.

Recall that the Poisson-GPD model fit to landfall intensities incorporated two components, one governing the occurrence rate as a Poisson process (λ) and another specifying event magnitudes as following a GPD model (σ, κ). Then, having obtained an estimate of the 'at-site' occurrence rate of events (λ_S), this replaces λ in the Poisson-GPD model for landfall intensities. Thus, combining this at-site occurrence rate estimate (λ_S) with the GPD model for event magnitudes (σ, κ) completes the specification of the 'at-site' distribution of landfall intensities.

Figure 8.7 shows the results of comparing the prehistorical record with the at-site distributions of storm intensity. The comparison is restricted here to only Princess Charlotte Bay and Curacoa Island, as these are the only sites where comprehensive sampling of storm ridges has been conducted (Hayne 1997). The reconstructed intensity estimates of Nott and Hayne (2001) for these sites are plotted as a single value for all ridges in the sequence along with associated uncertainty margins. The return period for the reconstructed intensity estimates are assigned based on the average time interval between radiocarbon dates for the ridge sequence.

The return period curve for model fit to observed data (historical and instrumental records), and adjusted to the at-site level, is shown to produce estimates that fall below the empirical estimates at both the Princess Charlotte Bay and Curacoa Island sites. Similarly, the return period curve for the simulated series of landfall intensities,

when adjusted to the at-site level, also falls below the empirical estimates from the storm ridge sites.
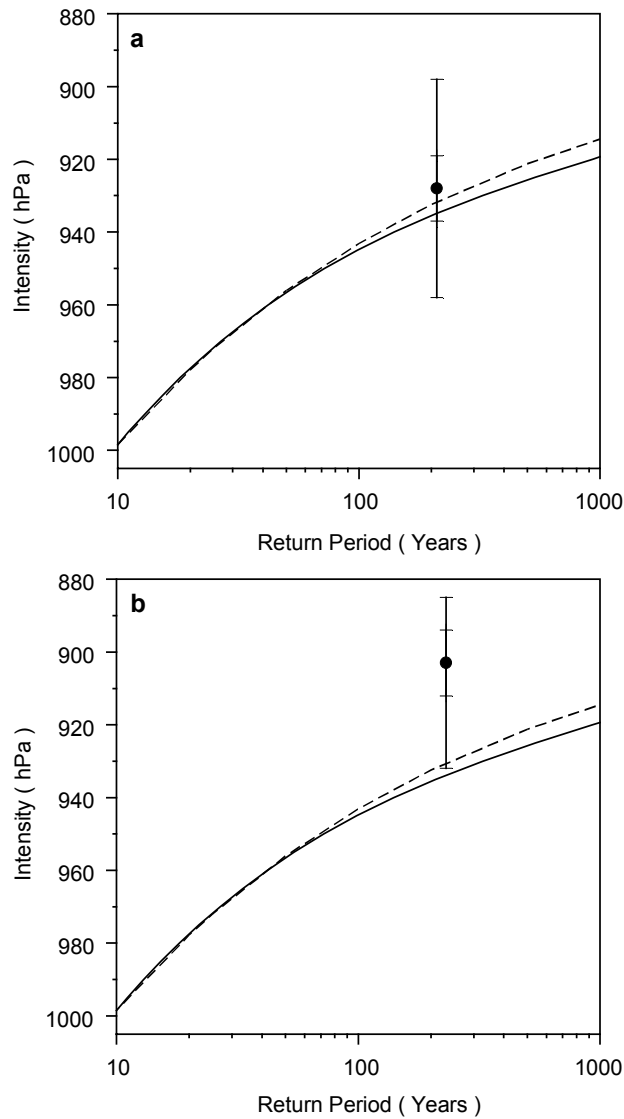
Figure 8.7 Comparison of return period curves for observed (solid curve) and simulated (dashed curve) landfall intensities adjusted to the at-site level, and plotted against empirical estimates of ridge forming events. (a) Princess Charlotte Bay site, and (b) Curacoa Island site. Reconstructed intensity estimates are obtained from Nott and Hayne (2001, Table 2, p. 510) and show $\pm 1\sigma$ and $\pm 2\sigma$ uncertainty margins around mean estimated represented by filled circle.

One feature that is apparent from Figure 8.7, and was mentioned in Chapter 7, is the substantial range of uncertainty associated with reconstructed intensity estimates from the storm ridge record. The uncertainty margins plotted in Figure 8.7 are due to variability associated with unknown tidal conditions. Their relatively wide range reflects the fact that storm ridges are actually emplaced by tropical cyclones of various intensities depending on the prevailing tidal conditions at the time of deposition. In the case of the Princess Charlotte Bay site, the return period curves based on both the observed and simulated records are seen to fall just below the mean estimate, although within the plotted $\pm 1\sigma$ uncertainty margins. For the Curacoa Island site, the return period curves are seen to fall well below the mean estimate and at the lower end of the $\pm 2\sigma$ uncertainty margins.

8.5 Summary

This chapter has comprised a comparative analysis of the major sources of tropical cyclone information for Queensland landfalling tropical cyclones. The evaluation has been primarily aimed towards comparing predictions of extremes from each of these data sources. Results demonstrate that relatively good agreement in predicted quantiles is found from simulated and observed records that include historical data. Predictions derived solely from the observed instrumental record are substantially different to those obtained from the Coral Sea region simulation model. This is despite both being derived from data covering the same post-1960 time period. This implies that the record of landfalling storm intensities over recent decades is

inconsistent not only with that observed during the historical era, as was established in Chapter 5, but also with that in the Coral Sea region over recent decades.

Statistical uncertainty that arises from the application of the regional simulation to the generation of an event series is shown to be small, and can be made arbitrarily negligible by simulating a large enough event series. The uncertainty associated with these predictions is shown to be more substantial, however, when it is quantified in terms of the length of the tropical cyclone record used to develop the simulation model. A subsequent comparison of uncertainty margins for observed and simulated records shows similar levels of variability in parameter estimates of the assumed probability model for landfall intensities.

Comparisons of simulated and observed model predictions with prehistorical data provide an independent means to assess their capability to predict major events. In this case there is evidence to suggest models based on the entire landfall record as well as that derived from the regional simulation model are tending to underestimate the frequency of major events in the region. When uncertainties inherent in reconstructing storm intensities from geological evidence are taken into account though, the differences apparent from the comparison are less straightforward.

CHAPTER 9

SUMMARY, DISCUSSION AND CONCLUSIONS

9.1 Introduction

The principal objective of this thesis has been to examine ways to maximise use of available information in developing an improved statistical description of Queensland landfalling tropical cyclones. This was approached in three main ways. First, through the incorporation of historical information to improve understanding of the frequency and intensity of landfall events. Second, through the use of regionalisation techniques as a means to make use of additional data from which a landfall event series can then be simulated. Third, through the use of prehistorical information to provide an independent basis for comparing predictions from instrumental, historical and regional records.

This study represents the first meaningful attempt to obtain a comprehensive landfall climatology of Queensland tropical cyclones. Previous studies have tended to examine only isolated aspects of the process such as the effect of ENSO on Coral Sea storm activity. By design, this study has been more holistic in aiming to research not only the frequency and intensity of landfall events, but also in investigating temporal trends and climate factors. In addition, the incorporation of historical and prehistorical information represents a novel approach in the Queensland context,

where such data has largely been ignored in recent studies. To facilitate the incorporation of past data sources various statistical techniques, previously applied in other tropical cyclone basins as well as in other fields of natural hazards research, have been employed. This chapter summarises key findings from this research, discusses important implications, including those relevant to risk assessment in Queensland, and presents several avenues for extensions to the analysis.

9.2 Summary of Findings

Modelling of the statistical properties of Queensland landfalling tropical cyclones has been based on best-track records compiling observations over the last century. Any analysis of this record is complicated by the less reliable nature of observations sampled prior to the introduction of satellite monitoring and analysis techniques in the 1960s. In order to address these sampling limitations a separation of the best-track record into an historical era (pre-1960/61) and an instrumental era (post-1959/60) was first implemented.

Bayesian statistical techniques were subsequently employed to provide a rational means to incorporate less precise historical information by using it to specify informative priors for models of seasonal activity and intensity. In constructing these prior distributions, bootstrapping techniques were used to allocate a credible range of uncertainty to estimates of model parameters obtained from historical observations. This follows a similar approach outlined by Elsner and Bossak (2001) and Elsner and Jagger (2004) who examined time series of United States hurricanes. In the

Queensland context, use of the Bayesian approach to combine historical and instrumental samples represents a unique contribution.

The results of Chapter's 4 and 5 demonstrate that the two main advantages of the approach are increased model certainty and improved predictions of the frequency of extremes. An inherited outcome of adopting a Bayesian modelling strategy is predictive distributions showing the probability of future events reaching specific levels. Bayesian predictive distributions have the advantage of implicitly accounting for uncertainty due to randomness and parameter variability. Example predictive distributions for seasonal landfall activity and intensity are given in Figures 4.2, 4.5 and 5.6. Furthermore, as more data becomes available posterior and predictive distributions presented here can readily be updated. Likewise, the same applies to the specification of informative prior distributions in the event that greater quantitative data becomes available from historical and prehistorical sources.

An extreme value analysis applied to records of landfall central pressures indicated that a higher frequency of major landfall events is expected under a model that incorporates historical information. This was largely a consequence of the largest magnitude events in the series occurring prior to the 1920s, and due to few weak major systems being recorded during the instrumental era. These extreme event predictions were subsequently confirmed through a censoring-based procedure that incorporated only the largest events recorded during the historical era. Comparison of the results of this approach against those of the Bayesian model highlighted similar estimates of the frequency of major landfall events.

A regional simulation model was next derived from the Coral Sea record using events from the period 1960/61-2004/05. This model was subsequently applied to generate a series of landfall events. When this simulated series was analysed using similar techniques as were employed for the observed series, predictions of extreme levels were comparable to those based on the landfall record combining historical and instrumental eras. An analysis conducted to assess and compare uncertainty levels in the simulation model with those based on the observed record demonstrated that both approaches produce a similar range of variability in parameter estimates.

A trend analysis conducted on landfall central pressures recorded over the last century identified the presence of a significant downward trend, largely a consequence of the early series peak in the incidence of major storms. It is this early series peak that is responsible for the higher predictions of landfall extremes obtained when historical information is incorporated in the analysis. Hence, this demonstrates the importance of using pre-satellite records for developing a statistically robust landfall climatology.

When similar trend detection techniques were applied to the regional Coral Sea record, an upward trend in storm intensities was identified over the period 1960/61-2004/05, which is in contrast to the downward trend detected in the landfall record. The fact that the increase in tropical cyclone intensity in the Coral Sea region over the instrumental period is not reflected in the landfall record over this period remains to be explained. One possible explanation is that this may be related to some background mechanism, perhaps linked to ENSO, controlling tropical cyclone track patterns in the region.

For both landfall storm counts and Coral Sea counts the trend analysis highlighted no evidence of either a consistent downward or upward trend in storm activity over time. There is, however, some evidence to suggest the presence of multi-decadal variability in both series.

The results of a regression analysis on seasonal counts demonstrates that the El Niño Southern Oscillation (ENSO) plays a significant role in influencing tropical cyclone activity from season to season for both landfall and Coral Sea records, consistent with the results of previous studies (e.g. Grant and Walsh 2001). Predictive distributions showing the probability of seasonal tropical cyclone activity conditional on the value of the SOI are given in Chapter 4. A trend analysis investigating the strength of the relationship between ENSO and landfalling storm activity over time, highlighting a distinct pattern of multi-decadal variability.

A review of geological records of past tropical cyclones in the Queensland region focused on recent work aimed at reconstructing the frequency of major events from storm ridge sequences throughout the region. An analysis into the veracity of the reconstruction methodology developed by Nott and Hayne (2001) indicates that the assumptions upon which it is based are reasonable. Limitations to this methodology are, however, apparent due to the uncertainties inherent in reconstructing past unobserved events from geological evidence. These stem largely from an inability to reconstruct tidal levels associated with ridge forming events, the spatially and temporally incomplete nature of the record, and the difficulties associated with assigning precise ages to individual ridges.

A comparison of return level predictions for observed and simulated landfalling storm intensities with prehistoric records from two storm ridge sites (Curacoa Island and Princess Charlotte Bay) showed a degree of discrepancy. In particular, there was a tendency for return level estimates to fall well below empirical estimates of the frequency of ridge forming events at these sites.

9.3 Discussion

One of the principle uses of the tropical cyclone climatology is that it often serves as a basis for simulating event responses, which are subsequently employed to assess risk levels. This is most commonly in the form of design levels that guide planning and emergency management policy. Hence, it is instructive to examine the implications of the results obtained from this study for the assessment of risk in Queensland. Furthermore, it is of interest to evaluate how results obtained here directly compare with those of previous studies. Also of relevance, are the results of the trend analyses previously summarised, which have implication for the assessment of risk, but must also be placed in the context of the less reliable nature of the historical record.

9.3.1 Comparison with Previous Studies

A direct comparison of the results derived from this research with those of other studies conducted in the Queensland region is problematical due to the wide range of sampling strategies previously employed. As discussed in Chapter 3, these have

largely been based on the use of fixed subregional approaches examining the process on small spatial scales around specific target sites. Ideally, it would be advantageous to employ the simulation model developed in Chapter 6 to generate a response series of either tropical cyclone wind speeds or sea levels for such sites. This generated response series could then be used to make comparisons with the results from recent simulation-based studies such as those reported by Harper (1999) and McInnes et al. (2000).

Some limited comparisons are possible with simulation model of James and Mason (2005) who utilised observations over the post-1968 period to develop an approach for generating tropical cyclone tracks and intensities in the Coral Sea region. Most notably, James and Mason (2005) reported that the application of this model gave a probability of observing a landfall event, similar in magnitude to tropical cyclone *Mahina* (914 hPa) (the largest in the observed series), of 6% over a 105-year period. Based on the methodology applied in this study to the record of landfall events (including historical information), the corresponding result indicates that there is around a 26% chance of this level being reached in a 105-year period.

In fact, results here suggest that the length of time associated with a 6% probability of the 914 hPa level being equalled or exceeded is actually closer to 17 years. This estimate was arrived at using the Bayesian predictive approach described in Chapter 5, which implicitly allows for uncertainty in parameter estimates. When estimates of the probability of other major event levels being equalled or exceeded in a future 105 year period were compared with those given by James and Mason (2005), results here consistently indicate a considerably higher frequency of extremes. This

conclusion applies not only to the analysis of the observed record, but also for the simulated series generated from the regional simulation model described in Chapter 6. Given that both this model and that of James and Mason (2005) was based on a similar dataset of tropical cyclone events, it appears likely that simulated event characteristics are highly sensitive to the mathematical form of the regional simulation model.

As discussed in Chapter 3, the comparison of model predictions with observed data represents an integral component of verifying a simulation model developed from a basin-wide record. Typically, this is conducted by comparing a simulated landfall event series with the observed record of such events (e.g. Vickery et al. 2000; Casson and Coles 2000). In the Queensland context, James and Mason (2005) present comparisons of simulated event characteristics from their Coral Sea simulation model with observed values for three subregions of the Queensland coast.

A similar approach was taken in Chapter 8, wherein predictions of the frequency of landfall extremes obtained from the observed record were compared against a simulated event series. The advantage of the approach taken here, in contrast to that presented by James and Mason (2005) whose comparison was limited to the instrumental record, is that the observed dataset here incorporated historical information. This fundamentally represents an improved method of verifying simulated event characteristics from a Coral Sea regional simulation model, because the historical record contains a number of landfall events more extreme than was recorded during the satellite era.

9.3.2 Implications for Risk Modelling

Nott (2004) recently argued that because the prehistorical record appears to register events larger than that seen in the modern record, this calls for a reappraisal of tropical cyclone risk in the Queensland region. Results reported in Chapter 8 where both simulated and observed records were compared with prehistorical evidence lend some support this assertion. This is further supported by the previous discussion comparing results obtained from this research with those given by James and Mason (2005). As the models developed here produce estimates of extreme landfall events that suggest a much higher frequency, the simulation model developed by James and Mason (2005) may in fact be producing conservative estimates of risk. This is especially important when it is considered that the model of James and Mason (2005) forms the basis of the most recent attempts to estimate design levels for storm tides and wind-waves in the Queensland region (Hardy et al. 2003; 2004).

In Chapter 2 two components of the tropical cyclone hazard, extremes winds and coastal flooding, were briefly reviewed from the perspective of their potential for impact in Queensland. To highlight the importance of obtaining accurate design level estimates of such variables, it is useful to consider the sensitivity of measures of vulnerability to these estimates. For instance, Zerger (1999) investigated the vulnerability of two sites in Queensland to the storm tide inundation hazard. According to Zerger (1999) the critical level for storm tides at one of these sites, Cairns, occurs at about the 2.2 m AHD level. Above this level Zerger (1999) found a dramatic increase in the number of buildings susceptible to inundation, including around 15% of structures in Cairns at the 2.8 m AHD level. This is a consequence of

Cairns having a large number of buildings located at relatively low elevations on a low-lying and flat coastal plain.

When these results are placed in the context of typical design levels estimates for storm tides in the Cairns region, a clear indication of this sensitivity is highlighted. Specifically, estimates of the 100-year design level for Cairns, based on the application of simulation-based approaches, generally fall between about 2.0-2.5 m AHD (e.g. Hardy et al. 1987; McInnes et al. 2000; Hardy et al. 2004). While this range of estimates is seemingly narrow (largely as a consequence of the small tidal range at Cairns), in light of the results obtained by Zerger (1999) it is apparent that any variation in the 100-year design level estimate would be accompanied by a significantly different quantification of the extent of building vulnerability.

The accuracy of such design level estimates is largely a function of simulation model used for generating events as well as the physical models used to simulate wind field and water level responses. Previous comparisons demonstrated that simulated event characteristics are highly sensitive to functional form of this model. Furthermore, when the uncertainties due to the limited amount of observed tropical cyclone data are taken into account (see e.g. Figure 8.5), it is easy to see how obtaining reliable design level predictions represents a difficult task. When this is combined with uncertainties resulting from simulating event responses using parametric and numerical models, this further exacerbates the difficulty of this task.

Recently, Harper (1999) advocated the use of observed wind speed from AWS (Automatic Weather Station) sites in Queensland to verify wind speed predictions

derived from a simulation-based modelling approach. While such an approach has merit as a diagnostic tool, aside from issues of independence, the available data on extreme tropical cyclone wind speeds in the Australian region is scarce and thus sampling variability likely to be high. In fact, the extent of this variability is readily apparent for several of the comparison presented by Harper (1999).

9.3.3 Trends

An important aspect regarding the assessment of temporal trends in tropical cyclone time series is the issue of record accuracy. Ultimately, this dilemma necessitates using limited temporal records in most analyses. This is readily apparent from recent studies examining global trends in tropical cyclone frequency and intensities (e.g. Emanuel 2005; Webster et al. 2005). For this reason, the results of the trend analyses presented in this thesis, particularly those including historical data, must be treated with some caution. In particular, no general strategy was taken to address the reliability of historical observations in these analyses. This was because of the need to preserve the temporal structure of the observed series. In this case, techniques such as those proposed by Solow and Nicholls (1990) and Solow and Moore (2000) for reconstructing incomplete historical records may offer a more practical approach to assess trends.

The upward trend in storm intensities found for the Coral Sea region over the period 1960/61-2004/05 is broadly consistent with what Nicholls et al. (1998) found for Australian region tropical cyclones. Nicholls et al. (1998) found that the number of severe tropical cyclones (central pressures ≤ 970 hPa) had increased slightly over the

period 1966/67-1994/95. It is apparent that part of the regional trend found here might be the result of an inactive period for major storms at the beginning of the instrumental series. Over the first decade (1960/61-1969/70) there were just four tropical cyclones that reached severe intensity (≤ 970 hPa). This is in contrast to 16 storms during the 1970s (1970/71-1979/80), 12 during the 1980s (1980/81-1989/90), and 16 during the 1990s (1990/91-1999/00). Thus, whether the upward trend in storm intensities represents an actual positive trend or is indicative of multi-decadal variability is difficult to establish from the short period of record. There also remains the possibility that the trend partly reflects improvements in the observational network.

One interesting feature uncovered during analysis was the possibility of decadal variations in the relationship between ENSO and storm landfalls over time. As a physical explanation for such a trend, there is some evidence with other climate variables to suggest that their association with ENSO varies over decadal time scales. For instance, a significant weakening in the relationship between ENSO and northeast Australian rainfall was observed during the 1931 to 1945 period (Cai et al. 2001). Furthermore, Hendy et al. (2003) using luminescent banding in Porites coral in the central GBR as a proxy for Burdekin river runoff and Queensland summer rainfall, found that these variable ENSO teleconnections have been prevalent in the region over at least the last 400 years.

While the mechanisms behind this are yet to be fully explored, Power et al. (1999) recently showed that the strength of ENSO teleconnections with the eastern Australian climate are dependent on low-frequency Pacific SST anomalies associated

189

with the Interdecadal Pacific Oscillation (IPO).   The IPO time series is shown in Figure 9.1, which is that derived by Power et al. (1999) from Empirical Orthogonal Function (EOF) analyses of 13-year low-pass filtered global SST anomalies.
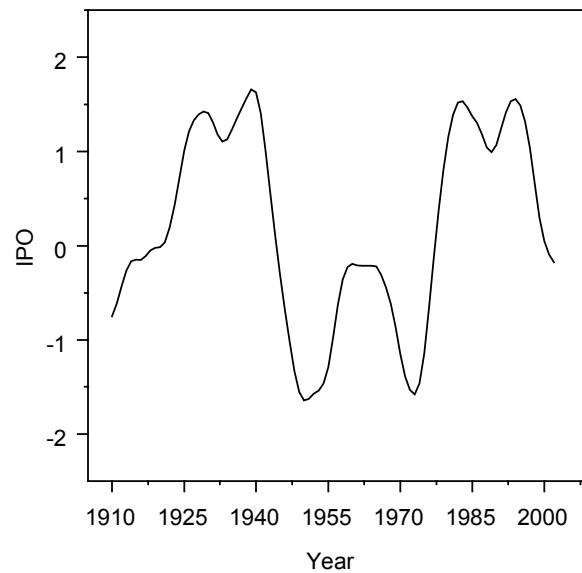
Figure 9.1   IPO time series for the period 1910/11-2004/05.

The IPO time series is seen to be broadly consistent with the trend pattern exhibited in Figure 4.8, whereby the weakening of the relationship between ENSO and Queensland landfalls tends to occur during the IPO positive phase.   This is most notable for the IPO positive phase of 1924/25-43/44, although less so for the IPO positive phase of 1979/80-97/98. This trend implicates the IPO as a possible factor

in modulating the strength of the ENSO relationship with tropical cyclone landfalls, although to confirm this link more research is required.

This feature may also partly explain why Nicholls (1992) observed a lower correlation between Australian region tropical cyclone activity over the IPO positive period 1979/80-1990/91, than over the non-IPO positive period 1959/60-1978/79. One additional feature of the IPO effect on ENSO teleconnections is that it influences not only the frequency of ENSO events, but also their magnitude (Kiem et al. 2003). It would be advantageous to examine whether this trend in the landfall record is also reflected in the Coral Sea record, although the historical record of tropical cyclone activity is unlikely be of sufficient accuracy to repeat the analysis on the basin-wide scale. Interestingly though, Elsner et al. (2001) also found a pattern of variable strength in the relationship between ENSO and United States hurricanes.

9.4 Future Research

There exist several avenues for extension to the analysis presented in this thesis. One general area that offers obvious potential for broadening the scope of the study's objectives is through the use of improved statistical techniques. Another approach that warrants some discussion are ways to better incorporate prehistorical data.

9.4.1 Statistical Approaches

Because of the relatively high number of zero counts (i.e. seasons in which no landfall was observed), a zero-inflated Poisson (ZIP) model (Wikle and Anderson

2003) may offer a better fit to the available record of storm counts. This model assumes that there is a probability (p) that a count is zero, and a probability (1-p) that a count is drawn from a Poisson distribution. This model could also be extended for use in a regression situation incorporating ENSO as a predictor of seasonal activity. Moreover, use of a suitable cross-validation procedure would be advantageous to assess the predictive performance of the regression model presented in Chapter 4 for seasonal activity conditioned on the SOI.

With respect to a trend analysis, it may be that changes in storm frequency occur abruptly, in which the record shifts between periods of lower and higher activity. Chu and Zhao (2004) describe the application of a hierarchical Bayesian change-point model to central North Pacific tropical cyclone counts aimed at detecting such shifts. This may prove a useful statistical tool when applied to assessing trends in Queensland landfalling and regional storm activity. For storm intensities, the trend analysis could also be extended to incorporate semi-parametric regression techniques such as local likelihood estimation. Although, the availability and reliability of data may in practice not permit the use of such an approach.

A further application of the Bayesian approach utilised in this analysis is the ability to incorporate systematic error in the recording of storm intensities. Even with the advent of improved observational capabilities through remote sensing technologies, their still exists a margin for error in the estimation of tropical cyclone central pressures due to the indirect manner in which most storms are sampled. As mentioned in Chapter 2, there is a well-recognised potential for considerable error in satellite-based estimates of storm intensity. In this case it could be assumed that

measurement error is centred at the observed value, but has random noise about this observation. This general approach is widely used in the field of flood frequency analysis to account for systematic errors in stage-discharge rating curves (e.g. Kuczera 1999).

To properly address the issue of representativeness it is apparent that the development of a tropical cyclone climatology must encompass a lengthy enough time period to capture the substantial range of variability exhibited in the climate system. A comprehensive investigation into the existence and causes of variability in tropical cyclone activity in the Australian region, particularly on decadal time scales, has been lacking in comparison to other basins. It is clear from the trend analyses presented for Queensland landfalling and regional Coral Sea tropical cyclones that a more detailed investigation into aspects such as dependence and stationarity properties is also required.

One aspect of the tropical cyclone climatology that has not been considered here is the role of anthropogenic climate change. McInnes et al. (2000) investigated the effects of projected increases in cyclone intensity and mean sea-level rise at one site in Queensland, and found substantial increases in design level estimates for storm tides. Henderson-Sellers et al. (1998) provide a comprehensive summary of the expected effects of global climate change on tropical cyclones. The main conclusions from their study suggests that there is little evidence to indicate a change in the frequency of events globally, although the maximum potential intensity (MPI) of tropical cyclones may undergo at most a modest increase of about 10-20% for a doubled CO_2 climate.

Recent studies also provide evidence of increases in the frequency of intense tropical cyclones over the last few decades (Webster et al 2005; Emanuel 2005). Although, it remains difficult to directly attribute such trends to global warming due to the limited time span of reliable data and because of the dependence of storm intensities on a range of factors. The full picture is further complicated because of the strong dependence of tropical cyclone activity in the Queensland region on ENSO, whose behaviour in a warmer world is not yet fully understood.

9.4.2 Incorporation of Prehistorical Records

The lack of a high-resolution chronology of tropical cyclone activity represents an obstacle to a greater understanding of tropical cyclone risk in the Queensland region. The study of prehistoric tropical cyclones, referred to as palaeotempestology, is an emerging field of research that may eventually offer a solution to this predicament. As yet there remains much scope for future research into reconstructing past storm events from geological evidence. Nevertheless, the reconstructed record of past extremes from a number of storm ridge sites across the region does offer a valuable contribution to resolving the issue of representativeness discussed in Chapter 3.

Future research is necessary though, to reduce uncertainties inherent in reconstructing palaeostorm intensities from the storm ridge record. This would require a combination of both modelling-based simulations of site responses to tropical cyclone forcing accompanied by further geomorphological analyses of sediment transport during storm events, including its relationship to ridge stratigraphy. In contrast to the study of other hazards like floods and earthquakes, studies of prehistoric tropical cyclones have been rather limited.

There are several approaches that may offer an improve means to achieve a better comparison with prehistorical data than was attempted in this study. One way to facilitate such a comparison would be to use a regional simulation model of the type described in Chapter 6 to generate a series of events to affect a particular ridge location. This simulated record could then be directly compared with the prehistoric record of reconstructed intensities to examine more closely how predictions of extremes correspond.

An extension to this approach based on a comparative analysis of storm ridge elevations, rather than reconstructed intensities, offers perhaps a more sound approach. This is because the elevation of storm ridges is a direct indicator of the height of water levels generated by the depositional storms (Nott and Hayne 2001). Thus, while ridge height acts only as a proxy for palaeostorm intensity, it is a direct indicator of water levels generated by major tropical cyclones. Thus, a strategy in which the regional simulation model is first used to simulate a series of water level responses at a particular site, and then compared against return periods of ridge forming events, may offer a better basis for evaluation. The advantage of using this methodology is that it avoids much of the uncertainty in reconstructing storm intensities from ridge elevations.

9.5 Conclusions

The increases in population and development along the Queensland coastal margin that have taken place over recent decades highlight the importance of mitigating the risks from tropical cyclones so as to reduce future loses. Tropical cyclones are,

however, complex phenomena whose dynamics are not fully understood. The ability to reduce such risks is therefore heavily dependent on analysing past records of these events to gain an indication of the likelihood of future impacts.

This can best be achieved by maximising the use of all sources of information available on tropical cyclones, including historical, prehistorical and regional records. Furthermore, uncovering forms of variability that directly or indirectly act to modulate tropical cyclone frequency and intensity over time is a necessary component of the risk prediction process. Clearly, must progress is needed in this direction before reliable design level estimates, and hence comprehensive assessments of vulnerability, can be acquired.

Finally, based on the results of Nott and Hayne (2001) and of this research, further improvement in the landfall climatology is likely to be obtained through the direct use of information reconstructed from the geological record. While there may remain some scepticism as to the veracity of event reconstructions from such evidence, the opportunity for improvement such data provides far outweighs its limitations.

REFERENCES

Baker, V.R. 1994. Geomorphological understanding of floods. *Geomorphology*, 10: 139-156.

Baker, R.G.V. and Haworth, R.J. 2000. Smooth or oscillating late Holocene sea-level curve? Evidence from cross-regional statistical regressions of fixed biological indicators. *Marine Geology*, 163: 353-365.

Basher, R.E. and Zheng, X. 1995. Tropical cyclones in the southwest Pacific: Spatial patterns and relationships to Southern Oscillation and sea surface temperature. *Journal of Climate*, 8: 1,249-1,260.

Bayliss-Smith, T.P. 1988. The role of hurricanes in the development of reef islands, Ontong Java Atoll, Solomon Islands. *The Geographical Journal*, 154: 377-391.

Blong, R. 2004. Residential building damage and natural perils: Australian examples and issues. *Building Research and Information*, 32: 379-390.

Booij, N., Ris, R.C. and Holthuijsen, L.H. 1999. A third-generation wave model for coastal regions. 1. Model description and validation. *Journal of Geophysical Research*, 104: 7,649-7,666.

Buckley, B.W., Leslie, L.M. and Speer, M.S. 2003. The impact of observational technology on climate database quality: Tropical cyclones in the Tasman Sea. *Journal of Climate*, 16: 2,640-2,645.

Bureau of Meteorology. 1978. *Australian tropical cyclone forecasting manual*, Bureau of Meteorology, Melbourne, 274pp.

Cai, W., Whetton, P.H. and Pittock, A.B. 2001. Fluctuations of the relationship between ENSO and northeast Australian rainfall. *Climate Dynamics*, 17: 421-432.

Callaghan, J. 1996. Tropical cyclones – Analyses of the destructive wind zone. *Proceedings of Conference on Natural Disaster Reduction*, Institute of Engineers Australia, ACT, pp. 341-345.

Callaghan, J. and Smith, R.K. 1998. The relationship between maximum surface wind speeds and central pressure in tropical cyclones. *Australian Meteorological Magazine*, 47: 191-202.

Callaghan, J. 2004. *Tropical cyclone impacts along the Australian east coast from November to April 1858 to 2004*. Bureau of Meteorology Working Paper, Brisbane, 35 pp.

Casson, E. and Coles, S. 2000. Simulation and extremal analysis of hurricane events. *Applied Statistics*, 49: 227-245.

Chappell, J. 1983. Evidence for smoothly falling sea level relative to north Queensland, Australia, during the past 6,000 yr. *Nature*, 302: 406-408.

Chappell, J., Chivas, A., Wallensky, E., Polach, H.A. and Aharon, P. 1983. Holocene palaeo-environmental changes, central to north Great Barrier Reef inner zone. *BMR Journal of Australian Geology and Geophysics*, 8: 223-235.

Chappell, J. and Grindrod, J. 1984. Chenier plain formation in northern Australia. In Thom B.G. (ed.) *Coastal Geomorphology in Australia*. Academic Press, Sydney, pp. 197-231.

Chivas, A., Chappell, J., Polach, H., Pillans, B. and Flood, P. 1986. Radiocarbon evidence for the timing and rate of island development, beach-rock formation and phosphatization at Lady Elliot Island, Queensland, Australia. *Marine Geology*, 69: 273-287.

Chu, P-S. and Wang, J. 1998. Modeling return periods of tropical cyclone intensities in the vicinity of Hawaii. *Journal of Applied Meteorology*, 37: 951-960.

Chu, P-S. and Zhao, X. 2004. Bayesian change-point analysis of tropical cyclone activity: The central North Pacific case. *Journal of Climate*, 17: 4,893-4,901.

Coles, S.G. and Powell, E.A. 1996. Bayesian methods in extreme value modelling: A review and new developments. *International Statistical Review*, 64: 119-136.

Coles, S.G. and Tawn, J.A. 1996. A Bayesian analysis of extreme rainfall data. *Applied Statistics*, 45: 463-478.

Coles, S. 2001. *An introduction to statistical modeling of extreme values*. Springer, London, 208 pp.

Coles, S. and Simiu, E. 2003. Estimating uncertainty in the extreme value analysis of data generated by a hurricane simulation model. *Journal of Engineering Mechanics*, 129: 1,288-1,294.

Dare, R.A. and Davidson, N.E. 2004. Characteristics of tropical cyclones in the Australian region. *Monthly Weather Review*, 132: 3,049-3,065.

Davidson, J.T., Hubbert, G.D., Woodcock, F. Bergin, M. and Morison, R. 1993. Modelling storm surge in the Mackay region. *Proceedings of the 11th Australian Conference on Coastal and Ocean Engineering*, Institute of Engineers Australia, ACT, pp. 351-356.

Davidson, J. and Dargie, S. 1996. Improving our knowledge of the cyclone hazard in Queensland. *Proceedings of Conference on Natural Disaster Reduction*, Institute of Engineers Australia, ACT, pp. 347-350.

Davison, A.C. and Smith, R.L. 1990. Models for exceedances over high thresholds. *Journal of the Royal Statistical Society - Series B*, 52: 393-442.

Donnelly, J.P., Bryant, S.S., Butler, J., Dowling, J., Fan, L., Hausmann, N., Newby, P., Shuman, B., Stern, J., Westover, K. and Webb, T. 2001a. 700 yr sedimentary record of intense hurricane landfalls in southern New England. *Geological Society of America Bulletin*, 113: 714-727.

Donnelly, J.P., Roll, S., Wengren, M., Butler, J., Lederer, R. and Webb, T. 2001b. Sedimentary evidence of intense hurricane strikes from New Jersey. *Geology*, 29: 615-618.

Efron, B. and Tibshirani, R.J. 1993. *An introduction to the bootstrap*. Chapman and Hall, New York, 436pp.

Elsner, J.B. and Bossak, B.H. 2001. Bayesian analysis of U.S. hurricane climate. *Journal of Climate*, 14: 4,341-4,350.

Elsner, J.B., Bossak, B.H., and Niu, X. 2001. Secular changes to the ENSO-U.S. hurricane relationship. *Geophysical Research Letters*, 28: 4,123-4,126.

Elsner, J.B. and Jagger, T.H. 2004. A hierarchical Bayesian approach to seasonal hurricane modeling. *Journal of Climate*, 17: 2,813-2,827.

Emanuel, K. 2003. Tropical Cyclones. *Annual Review of Earth and Planetary Science*, 31: 75-104.

Emanuel, K. 2005. Increasing destructiveness of tropical cyclones over the past 30 years. *Nature*, 436: 686-688.

Fletcher, C.H., Richmond, B.M., Barnes, G.M. and Schroeder, T.A. 1995. Marine flooding on the coast of Kaua'i during Hurricane Iniki: Hindcasting inundation components and delineating washover. *Journal of Coastal Research*, 11: 188-204.

Flood, P.G., Harjanto, S. and Orme, G.R. 1979. Carbon-14 dates, Lady Elliot Reef, Great Barrier Reef. *Queensland Government Mining Journal*, 80: 444-447.

Gelfand, A.E. and Smith, A.F.M. 1990. Sampling-based approaches to calculating marginal densities. *Journal of the American Statistical Association*, 85: 398-409.

Goldenberg, S.B., Landsea, C.W., Mestas-Nunez, A.M. and Gray, W.M. 2001. The recent increase in Atlantic hurricane activity: Causes and implications. *Science*, 293: 474-479.

Gourlay, M.R. and McMonagle, C.J. 1989. Cyclonic wave prediction in the Capricornia Region, Great Barrier Reef. *Proceedings of the 9th Australian Conference on Coastal and Ocean Engineering*, Institute of Engineers Australia, ACT, pp. 112-116.

Gourlay, M.R. 1996. Wave set-up on coral reefs. 2. Set-up on reefs with various profiles. *Coastal Engineering*, 28: 17-55.

Gourlay, M.R. 1997. Wave set-up on coral reefs: Some practical applications. *Proceedings of the 13th Australian Coastal and Ocean Engineering Conference*, Institute of Engineers Australia, ACT, pp. 959-964.

Granger, K., Jones, T., Leiba, M. and Scott, G. 1999. *Community risk in Cairns: A multi-hazard risk assessment*. Australian Geological Survey Organisation, Canberra.

Grant, A.P. and Walsh, K.J.E. 2001. Interdecadal variability in north-east Australian tropical cyclone formation. *Atmospheric Science Letters*, 2: 9-17.

Gray, W.M. 1990. Strong association between west African rainfall and U.S. landfall of intense hurricanes. *Science*, 249: 1,251-1,256.

Hardy, T.A., Mason, L.B., Young, I.R., bin Mat, H. and Stark, K.P. 1987. *Frequency of cyclone-induced water levels including the effect of mean sea level rise: Trinity Point*. Department of Civil and Systems Engineering, James Cook University, Townsville.

Hardy, T.A., McConochie, J.D. and Mason, L.B. 2003. Modeling tropical cyclone wave population of the Great Barrier Reef. *Journal of Waterway, Port, Coastal, and Ocean Engineering*, 129: 104-113.

Hardy, T., Mason, L. and Astorquia, A. 2004. *Queensland climate change and community vulnerability to tropical cyclones: Ocean hazards assessment – Stage 3*. Department of Natural Resources and Mines, Queensland Government, Brisbane, 56pp.

Harper, B.A. 1999. Numerical modelling of extreme tropical cyclone winds. *Journal of Wind Engineering and Industrial Aerodynamics*, 83: 35-47.

Harper, B., Hardy, T., Mason, L., Bode, L., Young, I. and Nielsen, P. 2001. *Queensland climate change and community vulnerability to tropical cyclones: Ocean hazards assessment – Stage 1*. Department of Natural Resources and Mines, Queensland Government, Brisbane, 318pp.

Hayne, M.C. 1997. *Cyclonic frequency during the Holocene in northeastern Australia*. Ph.D. Thesis, Australian National University (unpublished).

Hayne, M. and Chappell, J. 2001. Cyclone frequency during the last 5000 years at Curacoa Island, north Queensland, Australia. *Palaeogeography, Palaeoclimatology, Palaeoecology*, 168: 207-219.

Henderson-Sellers, A. Zhang, H., Berz, G., Emanuel, K., Gray, W., Landsea, C., Holland, G., Lighthill, J., Shieh, S-L., Webster, P. and McGuffie, K. 1998. Tropical cyclones and global climate change: A post-IPCC assessment. *Bulletin of the American Meteorological Society*, 79: 19-38.

Hendy, E.J., Gagan, M.K. and Lough, J.M. 2003. Chronological control of coral records using luminescent lines and evidence for non-stationary ENSO teleconnections in northeast Australia. *The Holocene*, 13: 187-99.

Holland, G.J. 1980. An analytical model of the wind and pressure profiles in hurricanes. *Monthly Weather Review*, 108: 1,212-1,218.

Holland, G.J. 1981. On the quality of the Australian tropical cyclone database. *Australian Meteorological Magazine*, 29: 169-181.

Holland, G.J. 1984. On the climatology and structure of tropical cyclones in the Australian/southwest Pacific region. I: Data and tropical storms; II: Hurricanes; III: Major hurricanes. *Australian Meteorological Magazine*, 32: 1-46.

Hopley, D. 1971. The origin and significance of north Queensland island spits. *Zeitschrift für Geomorphologie*, 15: 371-389.

Hopley, D. 1974. Coastal changes produced by tropical cyclone Althea in Queensland; December 1971. *The Australian Geographer*, 12: 445-456.

Hopley, D. 1982. *The geomorphology of the Great Barrier Reef: Quaternary development of coral reefs*. John Wiley and Sons, New York, 453 pp.

Hosking, J.R.M. and Wallis, J.R. 1997. *Regional frequency analysis: An approach based on L-moments*. Cambridge University Press, Cambridge, UK, 224 pp.

Huang, Z., Rosowsky, D.V. and Sparks, P.R. 2001. Hurricane simulation techniques for the evaluation of wind-speeds and expected insurance losses. *Journal of Wind Engineering and Industrial Aerodynamics*, 89: 605-617.

Hubbert, G.D., Holland, G.J. Leslie, L.M. and Manton, M.J. 1991. A real-time system for forecasting tropical cyclone storm surges. *Weather and Forecasting*, 6: 86-97.

Hubbert, G.D. and McInnes, K.L. 1999. A storm surge inundation model for coastal planning and impact studies. *Journal of Coastal Research*, 15: 168-185.

Jagger, T., Elsner, J.B. and Niu, X. 2001. A dynamic probability model of hurricane winds in coastal counties of the United States. *Journal of Applied Meteorology*, 40: 853-863.

James, M.K. and Mason, L.B. 2005. Synthetic tropical cyclone database. *Journal of Waterway, Port, Coastal, and Ocean Engineering*, 131: 181-192.

Katz, R.W., Parlange, M.B. and Naveau, P. 2002. Statistics of extremes in hydrology. *Advances in Water Resources*, 25: 1,287-1,304.

Keim, B.D. and Cruise, J.F. 1998. A technique to measure trends in the frequency of discrete random events. *Journal of Climate*, 11: 848-855.

Kiem, A.S., Franks, S.W. and Kuczera, G. 2003. Multi-decadal variability of flood risk. *Geophysical Research Letters*, 30, 1035, doi:10.1029/2002/GL015992.

Krayer, W.R. and Marshall, R.D. 1992. Gust factors applied to hurricane winds. *Bulletin of the American Meteorological Society*, 73: 613-617.

Kuczera, G. 1999. Comprehensive at-site flood frequency analysis using Monte Carlo Bayesian inference. *Water Resources Research*, 35: 1,551-1,557.

Liu, K-B. and Fearn, M.L. 1993. Lake-sediment record of late Holocene hurricane activities from coastal Alabama. *Geology*, 21: 793-796.

Liu, K-B. and Fearn, M.L. 2000. Reconstruction of prehistoric landfall frequencies of catastrophic hurricanes in northwestern Florida from lake sediment records. *Quaternary Research*, 54: 238-245.

Ljung, G.M. and Box, G.E.P. 1978. On a measure of lack of fit in time series models. *Biometrika*, 65: 297-303.

McBride, J. and Keenan, T.D. 1982. Climatology of tropical cyclone genesis in the Australian region. *Journal of Climatology*, 2: 13-33.

McConochie, J.D., Mason, L.B. and Hardy, T.A. 1999. A Coral Sea cyclone wind model intended for wave modelling. *Proceedings of the 14th Australian Coastal & Ocean Engineering Conference*, Institute of Engineers Australia, ACT, pp. 413-418.

McCullagh, P. and Nelder, J.A. 1989. *Generalized Linear Models, 2nd Edition*. Chapman and Hall, 511pp.

McDonnell, K.A. and Holbrook, N.J. 2004. A Poisson regression model approach to predicting tropical cyclogenesis in the Australian/southwest Pacific Ocean region using the SOI and saturated equivalent potential temperature gradient as predictors. *Geophysical Research Letters*, 31, L20110, doi:10.1029/2004GL020843.

McInnes, K.L., Walsh, K.J.E. and Pittock, A.B. 2000. *Impact of sea-level rise and storm surges on coastal resorts*. CSIRO Division of Atmospheric Research, Aspendale, Victoria, 17pp.

Maragos, J.E., Baines, G.B.K. and Beveridge, P.J. 1973. Tropical Cyclone Bebe creates a new land formation on Funafuti Atoll. *Science*, 181: 1,161-1,164.

Martin, J.D. and Gray, W.M. 1993. Tropical cyclone observation and forecasting with and without aircraft reconnaissance. *Weather and Forecasting*, 8: 519-532.

Martins, E.S. and Stedinger, J.R. 2001. Historical information in a generalized maximum likelihood framework with partial duration and annual maximum series. *Water Resources Research*, 37: 2,559-2,567.

Murnane, R.J., Barton, C., Collins, E., Donnelly, J., Elsner, J., Emanuel, K., Ginis, I., Howard, S., Landsea, C., Liu, K-B., Malmquist, D., McKay, M., Michaels, A., Nelson, N., O'Brien, J., Scott, D. and Webb, T. 2000. Model estimates Hurricane wind speed probabilities. *EOS, Transactions of the American Geophysical Union*, 81: 433, 438.

Nicholls, N. 1984. The Southern Oscillation, sea-surface temperature, and interannual fluctuations in Australian tropical cyclone activity. *Journal of Climatology* 4: 661-670.

Nicholls, N. 1992. Recent performance of a method for forecasting Australian seasonal tropical cyclone activity. *Australian Meteorological Magazine*, 40: 105-110.

Nicholls, N., Landsea, C. and Gill, J. 1998. Recent trends in Australian region tropical cyclone activity. *Meteorology and Atmospheric Physics*, 65: 197-205.

Nott, J.F. 2003. Intensity of prehistoric tropical cyclones. *Journal of Geophysical Research*, 108, 4212, doi:10.1029/2002JD002726.

Nott, J. 2004. Palaeotempestology: The study of prehistoric tropical cyclones – A review and implications for hazard assessment. *Environment International*, 30: 433-447.

Nott, J. and Hayne, M. 2001. High frequency of 'super-cyclones' along the Great Barrier Reef over the past 5,000 years. *Nature*, 413: 508-512.

Parisi, F. and Lund, R. 2000. Seasonality and return periods of landfalling Atlantic Basin hurricanes. *Australian and New Zealand Journal of Statistics*, 42: 271-282.

Power, S., Casey, T., Folland, C., Colman, A. and Mehta, V. 1999. Inter-decadal modulation of the impact of ENSO on Australia. *Climate Dynamics*, 15: 319-324.

Scoffin, T.P. 1993. The geological effects of hurricanes on coral reefs and the interpretation of storm deposits. *Coral Reefs*, 12: 203-221.

Scott, D.B., Collins, E.S., Gayes, P.T. and Wright, E. 2003. Records of prehistoric hurricanes on the South Carolina coast based on micropaleontological and sedimentological evidence, with comparison to other Atlantic Coast records. *Geological Society of America Bulletin*, 115: 1,027-1,039.

Silverman, B.W. 1986. *Density estimation for statistics and data analysis*. Chapman and Hall, London, 175 pp.

Smith, D. I. and Greenaway, M.A. 1994. *Tropical storm surge, damage assessment and emergency planning: A pilot study for Mackay, Queensland*. Centre for Resources and Environmental Studies, Australian National University, Canberra, 59 pp.

Solow, A. R. 1989. Statistical modeling of storm counts. *Journal of Climate*, 2: 131-136.

Solow, A. and Nicholls, N. 1990. The relationship between the Southern Oscillation and tropical cyclone frequency in the Australian region. *Journal of Climate*, 3: 1,097-1,101.

Solow, A.R. and Moore, L. 2000. Testing for a trend in a partially incomplete hurricane record. *Journal of Climate*, 13: 3,696 –3,699.

Stewart, M.G. 2003. Cyclone damage and temporal changes to building vulnerability and economic risks for residential construction. *Journal of Wind Engineering and Industrial Aerodynamics*, 91: 671-691.

Trenberth, K.E. 1997. The definition of El Niño. *Bulletin of the American Meteorological Society*, 78: 2,771-2,777.

Vickery, P.J. and Twisdale, L.A. 1995. Prediction of hurricane wind speeds in the United States. *Journal of Structural Engineering*, 121: 1,691-1,699

Vickery, P.J., Skerlj, P.F. and Twisdale, L.A. 2000. Simulation of hurricane risk in the U.S. using empirical track model. *Journal of Structural Engineering*, 126: 1,222-1,237.

Walker, G.R. and Reardon, G.F. 1986. Wind speeds in the Great Barrier Reef region from cyclone Winifred and their effects on buildings. *Proceedings of Workshop on Offshore Effects of Cyclone Winifred*, Great Barrier Reef Marine Park Authority, Townsville, pp. 28-40.

Walsh, K.J.E. and Ryan, B.F. 2000. Tropical cyclone intensity increase near Australia as a result of climate change. *Journal of Climate*, 13: 3,029-3,036.

Webster, P.J., Holland, G.J., Curry, J.A. and Chang, H-R. 2005. Changes in tropical cyclone number, duration, and intensity in a warming environment. *Science*, 309: 1,844-1,846.

Wikle, C.K. and Anderson, C.J. 2003. Climatological analysis of tornado report counts using a hierarchical Bayesian spatio-temporal model. *Journal of Geophysical Research*, 108, 9005, doi:10.1029/2002JD002806.

Zerger, A.Z. 1999. *Cyclone inundation risk mapping*. Ph.D. Thesis, Australian National University (unpublished).